

# Graph Kernels

## State-of-the-Art and Future Challenges

**Karsten Borgwardt**  
**Elisabetta Ghisu**  
**Felipe Llinares-López**  
**Leslie O’Bray**  
**Bastian Rieck**

Machine Learning and Computational Biology Lab  
Department of Biosystems Science and Engineering  
ETH Zurich  
Basel, Switzerland

Swiss Institute of Bioinformatics

December 13, 2021

### Abstract

Graph-structured data are an integral part of many application domains, including chemoinformatics, computational biology, neuroimaging, and social network analysis. Over the last two decades, numerous *graph kernels*, *i.e.* kernel functions between graphs, have been proposed to solve the problem of assessing the similarity between graphs, thereby making it possible to perform predictions in both classification and regression settings. This manuscript provides a review of existing graph kernels, their applications, software plus data resources, and an empirical comparison of state-of-the-art graph kernels.

# Contents

<b>1</b>	<b>Introduction</b>	<b>3</b>
<b>2</b>	<b>Background on graph comparison and kernel methods</b>	<b>6</b>
2.1	A primer in graph theory . . . . .	6
2.2	Classical approaches for graph comparison . . . . .	10
2.3	A brief introduction to kernel methods . . . . .	13
<b>3</b>	<b>Kernels for graph-structured data</b>	<b>19</b>
3.1	Bag of structures . . . . .	25
3.2	Information propagation . . . . .	39
3.3	Extensions of common graph kernels . . . . .	65
3.4	Conclusion . . . . .	78
<b>4</b>	<b>Experimental evaluation of graph kernels</b>	<b>80</b>
4.1	Data sets . . . . .	80
4.2	Experimental setup . . . . .	82
4.3	Classification performance . . . . .	90
4.4	Analysing the difficulty of data sets . . . . .	107
4.5	Grouping graph kernels . . . . .	118
4.6	Choosing a graph kernel . . . . .	122
4.7	Conclusion . . . . .	125
<b>5</b>	<b>Discussion &amp; future directions</b>	<b>126</b>
5.1	Current limitations in graph kernels research . . . . .	126
5.2	Emerging topics and future challenges . . . . .	131
5.3	Conclusion . . . . .	139
	<b>References</b>	<b>140</b>

# 1 Introduction

Among the data structures commonly used in machine learning, graphs are arguably one of the most general. Graphs allow modelling complex objects as a collection of entities (nodes) and of relationships between such entities (edges), each of which can be annotated by metadata such as categorical or vectorial node and edge features. Many ubiquitous data types can be understood as particular cases of graphs, including unstructured vectorial data as well as structured data types such as time series, images, volumetric data, point clouds or bags of entities, to name a few. Most importantly, numerous applications benefit from the extra flexibility that graph-based representations provide.

In *chemoinformatics*, graphs have been used extensively to represent molecular compounds (Trinajstić, 2018), with nodes corresponding to atoms, edges to chemical bonds, and node and edge features encoding known chemical properties of each atom and bond in the molecule. Machine learning approaches operating on such graph-based representations of molecules are becoming increasingly successful in learning to predict complex molecular properties from large annotated data sets (Duvenaud *et al.*, 2015; Gilmer *et al.*, 2017; Wu *et al.*, 2018), offering a promising set of tools for drug discovery (Vamathevan *et al.*, 2019). In *computational biology*, graphs have likewise risen to prominence due to their ability to describe multi-faceted interactions between (biological) entities. Examples of crucial importance include, but are not limited to, protein-protein interaction networks (Szklarczyk *et al.*, 2018), co-expression networks (Zhang and Horvath, 2005; Lonsdale *et al.*, 2013), metabolic pathways (Kanehisa and Goto, 2000), gene regulatory networks (Karlebach and Shamir, 2008), gene-phenotype association networks (Goh *et al.*, 2007), protein structures (Borgwardt *et al.*, 2005) and phylogenetic networks (Huson and Bryant, 2005). Graphs also play a key role in other application domains in the life sciences, such as *neuroscience*, where they are commonly used to concisely represent the brain connectivity patterns of different individuals (He and Evans, 2010), or *clinical machine learning*, where they have been employed to describe and exploit relationships between medical concepts by means of ontologies (Choi *et al.*, 2017) and knowledge graphs (Rotmensch *et al.*, 2017). In recent years, social network analysis has become a research field on its own, generating ever-larger graph data sets (Scott, 2011; Wasserman and Faust, 1994) and spanning a wide range of applications such as viral marketing (Leskovec *et al.*, 2007), community detection (Du *et al.*, 2007), influence estimation (Du *et al.*, 2013) or fake news detection (Tschitschek *et al.*, 2018).

The great representational power of graph-structured data is however a source of important challenges for method development. Graphs are intrinsically discrete objects, containing a combinatorial number of substructures. As a result, even seemingly simple questions, such as determining whether two graphs are identical (*graph isomorphism*) or

whether one graph is contained in another graph (*subgraph isomorphism*), are remarkably hard to solve in practice. In particular, no polynomial time algorithm is known for the former question, while the latter question is known to be NP-complete. Machine learning methods operating on graphs must therefore grapple with the need to balance computational tractability with the ability to leverage as much of the information conveyed by each graph as possible.

To this end, a popular family of early approaches, many of which were motivated by chemoinformatics (Todeschini and Consonni, 2008), aim to embed graphs into fixed-dimensional vectorial representations by computing a set of hand-engineered features (also known as *topological descriptors*). However, designing these features often proved to be a daunting task, requiring substantial application-specific prior knowledge and potentially depending on which statistical learning algorithm was to be subsequently used to learn from the resulting vectorial representations. Moreover, the amount of topological information captured by these representations was not only limited by the need to maintain computational tractability, but also often in practice by the desire to obtain a parsimonious representation of low-to-moderate dimensionality.

Crucially, the popularisation of *kernel methods* in machine learning (Schölkopf and Smola, 2002) provided a principled way to ameliorate all of the aforementioned limitations. Put briefly, kernel methods represent objects by implicitly embedding them as elements of a reproducing kernel Hilbert space by means of a *positive definite kernel*, which explicitly quantifies the similarity between any pair of objects and is mathematically equivalent to the inner product between the corresponding embeddings. This allows kernel methods to lift the wealth of existing statistical approaches based on linear models for vectorial data to other settings, such as non-linear modelling of vectorial data or, as is the case for graphs, modelling of structured data for which a vectorial representation might not be available or might be too high-dimensional to use explicitly. Moreover, they accomplish this while allowing to control the capacity of the underlying model via regularisation (Hofmann *et al.*, 2008).

These aspects make kernel methods a great fit for machine learning on graph-structured data, as evidenced by the almost two decades of fruitful research on *graph kernels*<sup>1</sup> which we review in this manuscript. Existing graph kernels mainly differ in (i) the type of substructures they use to define the positive definitive kernel function that measures the similarity between two graphs, and (ii) the underlying algorithm used to efficiently evaluate this function. In this quest to construct increasingly informative and more computationally

---

<sup>1</sup>In this monograph, by *graph kernel* we refer to a kernel function between two *graphs*. Notice that the term *graph kernels* sometimes is also used to refer to the different subject of kernel functions between *nodes* of a single graph (e.g. Kondor and Lafferty (2002).)

efficient approaches to quantify the similarity of graphs, research on graph kernels has led to algorithms for supervised learning (Kriege *et al.*, 2020), dimensionality reduction (which can then be used to visualise graphs in a lower dimensional space) (Lee and Verleysen, 2012), and clustering (Aggarwal and Wang, 2010). Moreover, in doing so, the literature on graph kernels has produced a great amount of empirical results characterising the usefulness of different representations for graph-structured data in distinct application domains, which we exhaustively gather, reproduce and analyse. These experimental observations might not only pave the way to the development of novel graph kernels, but might also be of further use in the emerging field of graph neural networks, many of which can be understood as natural extensions of certain graph kernels in the context of representation learning (Xu *et al.*, 2019).

Before proceeding, we would like to mention two other recent graph kernel surveys and highlight how our review is different. Kriege *et al.* (2020) provide an excellent narrative overview of existing graph kernels; we additionally provide an in-depth description of the kernels. Their review is a good starting point for a researcher looking to understand the landscape at a high-level or looking for a reference on which graph kernel paper to read. Nikolentzos *et al.* (2019) provide more details about the kernels discussed; we additionally provide a conceptual categorisation of the kernels. Unlike these two reviews, our survey discusses trends and emerging topics in the field. Hence our review contributes to the literature in that it provides an in-depth description, categorisation and empirical comparison of graph kernels and gives a detailed outlook to the future of the field.

This review is divided into two parts: the first part focuses on the theoretical description of common graph kernels. After a short general introduction to graph theory and kernels in Chapter 2, we provide a detailed description, typology, and analysis of relevant graph kernels in Chapter 3. We take care to expose relations between different kernels and briefly comment on their applicability to certain types of data. The second part in Chapter 4 focuses on a large-scale empirical evaluation of graph kernels, as well as a description of desirable properties and requirements for benchmark data sets. We conclude our review with an outline of future trends and open challenges for graph kernels in Chapter 5.

## 2 Background on graph comparison and kernel methods

This chapter presents the required concepts and terminology from graph theory, while also providing a brief introduction into more classical approaches for graph comparison, such as graph isomorphism checking.

### 2.1 A primer in graph theory

This section presents all required concepts from graph theory. Care is taken to define everything unambiguously so that this review is self-contained, and we illustrate several of the following definitions in Figure 2.1.

**DEFINITION 2.1 (Graph).** A *graph*  $G$  is a tuple  $G = (V, E)$  of vertices  $V$  and edges  $E$ . For *undirected* graphs, edges are subsets of cardinality two of the vertices, so each edge is of the form  $(u, v)$  with  $u, v \in V$ . For *directed* graphs, the order of the edges in the tuple  $(u, v)$  is relevant to indicate the direction of the edge. If not mentioned otherwise, we will assume that a graph is undirected and has no self-loops, *i.e.* edges for which  $u = v$ .

The previous definition already gives rise to a basic graph invariant (a property that does not change under certain transformations such as node renumbering), namely the *degree* of a vertex.

**DEFINITION 2.2 (Degree).** The *degree* of a vertex  $v$  of an undirected graph  $G = (V, E)$  is the number of vertices that are connected to  $v$  by means of an edge, *i.e.*  $\deg(v) := |\{u \mid (u, v) \in E, u \neq v\}|$ . For directed graphs, a vertex has an *in-degree* and an *out-degree*, depending on the direction of the edges.

A graph  $G = (V, E)$  may also contain *labels* or *attributes*, for example in the form of node labels, edge labels, or edge weights. This is known as an *attributed graph*.

**DEFINITION 2.3 (Attributed graph).** An *attributed graph* is a graph that has either labels or attributes on the nodes and/or edges. When present, labels are each assumed to be defined over a common alphabet,  $\Sigma_V$  for nodes and  $\Sigma_E$  for edges, with a function,  $l_V$  for nodes and  $l_E$  for edges, to assign each entity its label. We thus have

$$\begin{aligned} l_V: V &\rightarrow \Sigma_V \\ l_E: E &\rightarrow \Sigma_E \end{aligned} \tag{2.1}$$

and both of these functions need to be *total*. A graph with additional attributes for vertices and or edges has attribute functions

$$\begin{aligned}\mathcal{A}_V: V &\rightarrow \mathbb{R}^d \\ \mathcal{A}_E: E &\rightarrow \mathbb{R}^d\end{aligned}\tag{2.2}$$

that are typically assumed to be real-valued, *i.e.*  $d = 1$ . Scalar-valued edge attributes are often also referred to as *weights*, with the tacit assumption that the values refer to the strength of a specific connection.

Generally speaking, most of the results in graph or kernel theory can be extended to other coefficients, such as the ring of integers, or the field of complex numbers, but in the interest of terseness, our definitions will stay in the field of real numbers. In order not to clutter up the notation, we will *not* mention additional attributes in the definition of the graph (for example by adding more values to its tuple), but rather mention whenever we assume or require their existence.

Since a graph defines a connectivity for each of its vertices, its edges induce sequences for visiting them. These sequences have specific names, depending on their properties.

**DEFINITION 2.4** (Walks, paths, and cycles). A sequence of  $k$  nodes  $v_1, \dots, v_k$  of the vertices of a graph  $G$  is called a *walk* of length  $k - 1$  if the edge between two consecutive vertices exists. More precisely, for an undirected graph,  $(v_{i-1}, v_i) \in E$  needs to be satisfied for  $1 < i \leq k$  (the case for a directed graph is analogous). Vertices of a walk are allowed to repeat. If, however, node repetition is not allowed, one typically refers to the node sequence as a *path*, the adjective *directed* often being added in the case of directed graphs. Special consideration is given to *cycles*, *i.e.* walks of length  $k - 1$  for which  $v_1 = v_k$ . If  $v_1$  and  $v_k$  are the only two nodes that are repeated in a cycle, the cycle is also called a *simple cycle*.

Cycles are considered to be relevant descriptors of the topology of a graph (Berger *et al.*, 2009). Their extraction has a high computational complexity, though, because even detecting the presence of a single Hamiltonian cycle—a cycle that visits all vertices exactly once, except for the start and end vertex, which is visited twice—is known to be an NP-complete problem (Karp, 1972).

The definition of walks can be extended to *edge walks* (as well as paths and cycles) by using the neighbour relationship (two vertices are said to be neighbours if they are connected by an edge; we shall return to this definition of neighbourhood shortly) between vertices: for example, an edge walk is a sequence of edges  $e_1, \dots, e_k$  such that exactly two vertices of each pair  $(e_{i-1}, e_i)$  coincide. The definitions for edge paths and edge cycles are completely analogous. In an edge path, a vertex may be visited multiple times, depending

on its degree. Certain walks are of special interest in graph theory because they involve an added element of stochasticity.

DEFINITION 2.5 (Random walks). A walk in a graph is referred to as a *random walk* if the next vertex (or edge) is picked in a probabilistic manner. Having picked a start node at random, a typical choice, for example, would be to pick any outgoing edge of the node with uniform probability (in case of unweighted graphs), or with a probability proportional to its weight.

The notion of walks (or, equivalently, paths and cycles), naturally leads to a definition of connectivity in graphs.

DEFINITION 2.6 (Connected graph). A graph is said to be *connected* if a walk between all pairs of nodes exists. Specifically, in a *fully connected* graph, each pair of nodes is connected by an edge. If a graph is not connected, the set of its nodes can be partitioned using an equivalence relation  $u \sim v$  if and only if a walk between  $u$  and  $v$  exists. The equivalence classes under this relation are called *connected components*.

Likewise, paths can also be used to assess distances in a graph. This viewpoint is often helpful when approximating high-dimensional manifolds through graphs, and it is possible to give bounds on the dissimilarity of graph-based distances and geodesic distances of the manifold (Bernstein *et al.*, 2000).

DEFINITION 2.7 (Shortest paths and distances). Given two vertices  $u$  and  $v$  of a graph that are in the same connected component, among all the paths connecting them, there is at least one *shortest path* that has the minimum number of vertices out of all other paths connecting the two vertices. The existence of such a path is a consequence of the fact that the number of all paths connecting the vertices is finite. The distance between  $u$  and  $v$  is thus the number of edges of the shortest path. In case the graph contains edge weights, the distance is typically set to be the *sum* of edge weights along the path. Although there can be multiple shortest paths between  $u$  and  $v$ , the length of these shortest paths is unique.

The shortest path between two vertices in a graph can be found in polynomial time using the seminal algorithm described by Dijkstra (1959). The notion of distance in graphs is only meaningful provided there are no negative weights along the path; in practice, this can always be achieved by a weight transformation.

The notion of distances as defined above gives rise to the useful concept of neighbourhoods in a graph, which extends the combinatorial perspective (graphs as sets and relationships) to that of a *metric space* (Ó Searcóid, 2007).

DEFINITION 2.8 ( $k$ -hop neighbourhood of a vertex). Given a vertex  $v$  of a graph  $G$  and  $k \in \mathbb{N}_{>0}$ , its  $k$ -hop neighbourhood  $N^{(k)}(v)$  is defined as all the vertices in  $G$  that are reachable



in at most  $k$  steps, which includes  $v$ , assuming uniform edge weights. For example,  $N^{(1)}(v)$  is just the set of vertices that are connected to  $v$  by an edge and  $v$ .

This definition can be connected to the idea of a “ball” in metric spaces by observing that each  $k$ -hop neighbourhood of a vertex  $v$  induces a subgraph of the original graph  $G$ . For increasing values of  $k$ , these induced subgraphs are nested—and for  $k$  sufficiently large, the original graph  $G$  is obtained. This concept will play an important role later on when we define graph kernels that operate at multiple scales, such as the Multiscale Laplacian graph kernel in Section 3.2.3.1 on p. 62.

We conclude this brief discussion of graph theory with a description of matrices assigned to graphs. For computational reasons, a graph is often represented through its *adjacency matrix*  $A$ . A graph with  $n$  vertices will thus be represented by an  $n \times n$  binary matrix whose entry  $A_{ij} = 1$  if the  $i$ th and  $j$ th vertex of the graph are connected by an edge. The adjacency matrix is symmetrical for undirected graphs, whereas for directed graphs  $A_{ij}$  and  $A_{ji}$  can be different depending on the edge structure. Furthermore, if edge weights are available, *i.e.*  $\mathcal{A}_E(\cdot)$  exists and  $d = 1$ , it is also possible to derive a *weighted* variant of the adjacency matrix by setting  $A_{ij}$  to the corresponding edge weight.

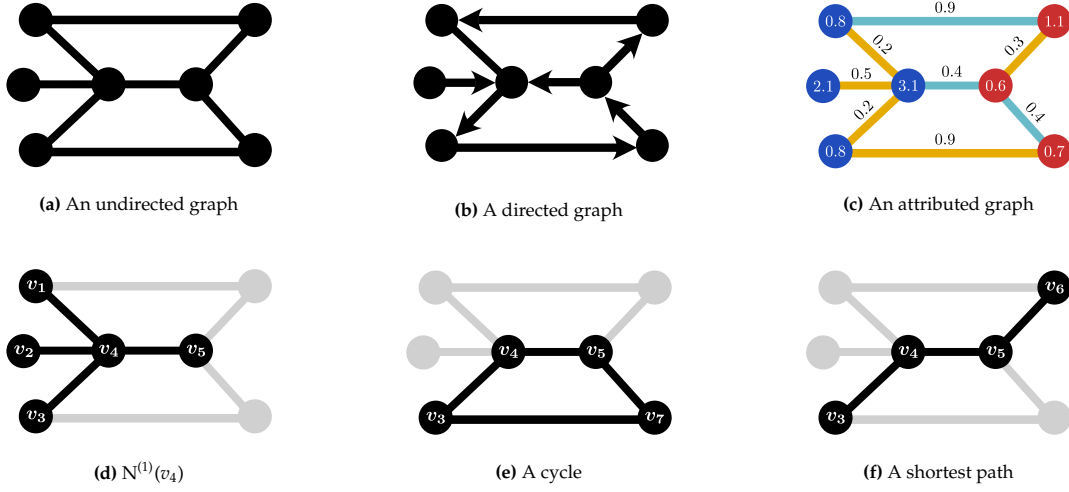
While the adjacency matrix  $A$  can already be used to perform random walks on graphs, another kind of matrix—the graph Laplacian—is often employed to measure topological properties. It is commonly defined using the adjacency matrix  $A$  and the degree matrix  $D$ ; other variants exist as well (Chung, 1997; Wilson and Zhu, 2008), but they mostly differ in terms of normalisation.

**DEFINITION 2.9 (Graph Laplacian).** Let  $A$  be the adjacency matrix of a graph  $G = (V, E)$ . If weights are available, each entry  $A_{ij}$  thus consists of the weight of the corresponding edge. Furthermore, let  $D$  be the degree matrix of  $G$ . This diagonal matrix contains the degree of each vertex  $v \in V$  in the unweighted case. For weighted graphs, each entry consists of the *sum* of all edge weights of all edges that are incident on the corresponding vertex. The *graph Laplacian* is then defined as

$$L := D - A \quad (2.3)$$

and will be a symmetric positive semi-definite matrix for undirected graphs. More precisely, each entry  $L_{ij}$  can be described as

$$L_{ij} = \begin{cases} -\mathcal{A}_E(e) & \text{if an edge } e \text{ between } v_i \text{ and } v_j \text{ exists} \\ \sum_{e \in N(v_i)} \mathcal{A}_E(e) & \text{if } i = j \\ 0 & \text{otherwise} \end{cases} \quad (2.4)$$



**Figure 2.1:** An example of an undirected graph (a) versus a directed graph (b), both of which are an example of a *fully connected* graph. (c) shows an example of an attributed graph, where the colour of the nodes and edges represent the node labels and edge labels respectively, and the nodes and edges also have 1-dimensional attributes. We show the 1-hop neighbourhood of vertex  $v_4$  in (d), and also mention its degree  $\deg(v_4) = 4$ . In (e) we show a simple cycle, and in (f) we see one of the several possible shortest paths between  $v_3$  and  $v_6$ . Cycles and paths are examples of the more general concept of a walk.

and in the undirected case, positive semi-definiteness is an immediate consequence of the (weak) diagonal dominance.

## 2.2 Classical approaches for graph comparison

Before diving into graph kernels, we first review earlier families of algorithms for graph comparison: methods based on graph isomorphism, edit distances and topological descriptors.

### 2.2.1 The graph isomorphism problem

A first family of approaches uses the most fundamental criterion for graph comparison, namely whether an isomorphism or subgraph isomorphism exists between the graphs. To formally define graph isomorphism, let  $G = (V, E)$  and  $G' = (V', E')$  be two graphs. A *graph isomorphism* between  $G$  and  $G'$  is a bijection between the vertex sets  $V$  and  $V'$  of  $G$  and  $G'$ , i.e.  $f: V \rightarrow V'$ , that preserves adjacency. Specifically,  $(v_i, v_j) \in E$  if and only if  $(f(v_i), f(v_j)) \in E'$  for all  $v_i, v_j \in V$ . Put differently, vertices  $v_i$  and  $v_j$  are adjacent in  $G$  if and only if  $f(v_i)$  and  $f(v_j)$  are adjacent in  $G'$ . If an isomorphism between  $G$  and  $G'$  exists, the

two graphs are referred to as being *isomorphic*. This gives rise to an equivalence relation that permits partitioning a set of graphs into different equivalence classes; graphs that belong to the same equivalence class are indistinguishable from each other. The notion of graph isomorphism thus gives rise to a simple similarity measure between graphs.

In terms of computational complexity, there are currently no known polynomial-time algorithms for solving this graph isomorphism problem, except for some specific classes of graphs such as trees. In fact, it is also not known to be NP-complete, making it an interesting problem to study (Read and Corneil, 1977). A rather recent publication (Babai, 2015) claims the existence of a quasi-polynomial algorithm.

In practical graph mining or graph classification, approaches based on graph isomorphism are too restrictive, in the sense that a single measurement error or noise in the observation of two graphs will render them non-isomorphic. The aforementioned computational complexity also directly results in poor scalability with the number of nodes of the graphs. For this reason, further families of graph comparison methods were developed and explored.

### 2.2.2 Graph edit distances

A second of these families are so-called graph edit distances. The concept of *edit distance* refers to a general concept of how to compare two structured objects, such as graphs. The main idea is to quantify how many transformations are necessary to turn the first graph into the second graph. Each transformation is measured in terms of a set of operations. For graphs, these *elementary graph operations* include (i) vertex/edge *insertions* (subject to the creation of a new label or new attributes if the input graph is equipped with those), (ii) vertex/edge *deletions*, and (iii) vertex/edge *substitutions*, *i.e.* the replacement of certain information, such as a label, of a given vertex/edge. Each of these operations is assigned a certain *cost*, and the graph edit distance between two graphs  $G$  and  $G'$  is defined as the *minimum cost sum* of all operations that are required to transform  $G$  and  $G'$  into each other.

The flexibility to define a cost function is both an advantage and disadvantage of edit distances; it allows for using application-specific or domain-specific costs, but at the same time poses the problem of careful parametrisation of the cost function. Once the cost function is fixed, numerous algorithms for computing these edit distance between graphs exist; for certain classes of graphs, such as trees, efficient polynomial-time algorithms are known, but in general, the problem is NP-complete, as it requires to determine the maximum common subgraph of the two given graphs (the interested reader is referred to Riesen (2015) for a more extensive introduction to graph edit distance, approximation algorithms, and applications). This rather high computational complexity and non-trivial

parametrisation of edit distances triggered interest in yet another approach to deal with graph data, namely to map them to a vectorial representation, as is described next.

In this manuscript, we will denote the graph edit distance between two graphs  $G$  and  $G'$  as  $\text{dist}_G(G, G')$ , with the tacit understanding that the edit distance is chosen appropriately depending on the type of the two graphs and on their attributes.

### 2.2.3 Invariants and topological descriptors

A third, computationally more feasible family of approaches for graph similarity assessment, involves computing *topological descriptors* and *graph invariants*. Common to both is the idea to map a graph to a vectorial representation: a topological descriptor is a vectorial representation of a topological property of a graph, and a graph invariant of a graph is a property that does not change under graph isomorphism, such as the *diameter*, *i.e.* the length of the longest shortest path, or the number of cycles. Representing a graph by topological descriptors or graph invariants opens the door to applying *any* of the numerous machine learning techniques for dealing with vectorial data.

A prominent example of this family is the *Wiener Index* (Wiener, 1947), which is defined as the average shortest length path in a graph.

**DEFINITION 2.10** (Wiener index). Let  $G = (V, E)$  be a graph and  $\mathcal{P}$  be the set of all shortest paths in a graph. Then the Wiener index  $W(G)$  of  $G$  is defined as

$$W(G) := \frac{1}{|\mathcal{P}|} \sum_{v_i \in V} \sum_{v_j \in V} \text{dist}(v_i, v_j), \quad (2.5)$$

where  $\text{dist}(v_i, v_j)$  is defined as the length of the shortest path between nodes  $v_i$  and  $v_j$  from  $G$ .

This index is identical for isomorphic graphs, making the Wiener index a (simple) graph invariant. The problem is that the converse does not hold in general—there are graphs with identical Wiener indices that are not isomorphic. A topological descriptor for which the converse direction holds is called a *complete graph invariant* (Köbler and Verbitsky, 2008). However, all known complete graph invariants require exponential runtime, as their computation is equivalent to solving the graph isomorphism problem.

Another one of the most commonly-used descriptors is the eigenspectrum of the graph Laplacian (see also Definition 2.9, p. 10): given the spectra of two graphs, potentially zero-padded to ensure that they are of the same size, their Euclidean distance can be used as a basic dissimilarity measure. Although it is known (Wilson and Zhu, 2008) that graphs that are *not* isomorphic might still have the *same* spectrum, the Laplacian is still

a useful tool in practice. Next to interesting theoretical properties, such as stability with respect to certain perturbations, the graph Laplacian can also be linked to diffusion-based measures via heat kernel signatures. The reader is referred to classical texts on spectral graph theory (Brouwer and Haemers, 2012; Chung, 1997) for more information.

The *circular fingerprints* framework (Glem *et al.*, 2006) constitutes a classical example of the use of topological information for specific graphs: given graphs of molecules, where each vertex represents an atom, it encodes information about the arrangement of other atoms (such as oxygen). This encoding takes into account the topological distance—the distance defined through graph edges—to generate descriptors at different length scales.

The central problem with topological descriptors is to find the right trade-off between efficiency and expressivity: As stated above, all known complete graph invariants require exponential runtime in the number of nodes of the graph, thereby lacking efficiency. Simple topological descriptors such as the Wiener index still lose a large amount of topological information represented by the graph, thereby lacking expressivity. Graph kernels, the focus of this survey, were proposed as a strategy to reach this middle ground that combines *efficiency* and *expressivity*.

## 2.3 A brief introduction to kernel methods

To understand the contributions of graph kernels to the field of graph comparison, we first have to familiarise ourselves with basic concepts from kernel-based machine learning.

Linear models operating on inputs belonging to some vector space have long been a staple of machine learning and statistics. Arguably some of the most famous algorithms for both unsupervised and supervised learning fall into this category. Examples include dimensionality reduction methods such as principal component analysis (Pearson, 1901; Hotelling, 1933), clustering approaches such as k-means (Lloyd, 1982), regression techniques such as ridge regression (Hoerl and Kennard, 1970) and classification algorithms such as support vector machines (Boser *et al.*, 1992). In a nutshell, kernel methods provide a rich mathematical formalism to adapt this large family of models to instead perform (possibly non-linear) modelling of inputs belonging to an arbitrary set  $\mathcal{X}$ . Intuitively, kernel-based approaches accomplish this by embedding inputs  $x \in \mathcal{X}$  as elements of a vector space  $\mathcal{H}$  (with special properties, which we will subsequently discuss) by means of a *feature map*  $\phi: \mathcal{X} \rightarrow \mathcal{H}$  and applying linear models on these transformed representations  $\phi(x) \in \mathcal{H}$ . Superficially, kernel methods might resemble topological descriptors, insofar as both of them rely on representing inputs as vectors by means of some transformation  $\phi$ . However, both differ crucially in aspects of great importance for machine learning applications.

Perhaps the most impactful distinction between both paradigms is that while topological descriptors require specifying the mapping  $\phi$  *explicitly*, kernel methods typically access the *feature space*  $\mathcal{H}$  only *implicitly*, namely in terms of the inner product  $\langle \phi(x), \phi(x') \rangle_{\mathcal{H}}$  for any pair of inputs  $x, x' \in \mathcal{X}$ . A key consequence of this is that, unlike topological descriptors, kernels can operate on a feature space  $\mathcal{H}$  of *arbitrary dimensionality* without major computational difficulties, as long as the algorithms implementing the linear model of choice are rewritten exclusively in terms of inner products. This observation is frequently referred to as the “kernel trick” by the machine learning community (Schölkopf and Smola, 2002; Hofmann *et al.*, 2008). Moreover, even though both designing an appropriate feature map  $\phi$  directly, as topological descriptors do, or indirectly, by means of a *kernel*  $k(x, x') := \langle \phi(x), \phi(x') \rangle_{\mathcal{H}}$ , can be seen as instances of feature engineering that require substantial domain knowledge, in many applications of interest it is arguably more natural to use this domain knowledge to define a notion of similarity between inputs—as captured by the kernel—than a (possibly high-dimensional) vectorial representation. Kernel methods also have strong ties with statistical learning theory, providing principled approaches to control the complexity of the function class being used by the model. In particular, this allows researchers to focus on designing a kernel function  $k(x, x')$  that captures a meaningful notion of similarity between objects for the task at hand, whereas other essential aspects of a learning algorithm, such as regularisation, follow naturally and generally from the theoretical foundations of kernel methods. These aspects make kernel methods a particularly appealing framework to deal with structured data types, such as graphs.

In the remainder of this chapter, we provide a brief background on kernel methods prior to diving into the specifics of kernel methods for graphs in Chapter 3. Interested readers can find additional, in-depth material on the theory of kernel methods and their applications in machine learning and statistics in Schölkopf and Smola (2002), Shawe-Taylor and Cristianini (2004), and Hofmann *et al.* (2008).

### 2.3.1 Fundamental concepts

As mentioned above, kernel methods define a feature map  $\phi: \mathcal{X} \rightarrow \mathcal{H}$  that represents inputs from a set  $\mathcal{X}$  as elements of a vector space  $\mathcal{H}$ . More precisely,  $\mathcal{H}$  will be a *Hilbert space* and, as such, will be endowed with an inner product.

**DEFINITION 2.11** (Real-valued Hilbert space). A real-valued Hilbert space  $\mathcal{H}$  is a vector space defined over  $\mathbb{R}$ , the field of real numbers, that has an *inner product*  $\langle \cdot, \cdot \rangle_{\mathcal{H}}$  and is *complete* (every Cauchy sequence in  $\mathcal{H}$  converges in to an element of  $\mathcal{H}$ ).

The existence of an inner product for  $\mathcal{H}$  is instrumental in the theory of kernel methods. In this way, the map  $\phi$ , as well as the Hilbert space  $\mathcal{H}$  in which inputs are represented, are

defined implicitly through a *kernel* function  $k(x, x')$  that corresponds to the inner product between the representations  $\phi(x), \phi(x')$  in  $\mathcal{H}$  of any pair of elements  $x, x'$  in  $\mathcal{X}$ .

**DEFINITION 2.12 (Kernel).** Given a non-empty set  $\mathcal{X}$ , we say that a function  $k: \mathcal{X} \times \mathcal{X} \rightarrow \mathbb{R}$  is a *kernel* if there exists a Hilbert space  $\mathcal{H}$  and some map  $\phi: \mathcal{X} \rightarrow \mathcal{H}$  that satisfies

$$k(x, x') = \langle \phi(x), \phi(x') \rangle_{\mathcal{H}} \quad (2.6)$$

for all  $x, x' \in \mathcal{X}$ .

Hence, the kernel function  $k(x, x')$  plays a central role in kernel methods, with the bulk of the research being devoted to proposing novel kernels with favourable properties (such as high expressivity with low computational costs) for specific tasks. In this regard, the field of graphs kernels is no exception. Consequently, characterising the properties that a function  $k: \mathcal{X} \times \mathcal{X} \rightarrow \mathbb{R}$  must satisfy to be a valid kernel is of utmost importance for theoretical and practical applications alike.

### 2.3.2 Characterisation of kernels

The Moore–Aronszajn theorem (Aronszajn, 1950), one of the seminal results in kernel theory, fully characterises the set of functions of the form  $k: \mathcal{X} \times \mathcal{X} \rightarrow \mathbb{R}$  that are kernels. Central to this result are the notions of *reproducing kernel Hilbert space* (RKHS) and *reproducing kernel*, which we enunciate next.

**DEFINITION 2.13 (Reproducing kernel Hilbert space and reproducing kernel).** A *reproducing kernel Hilbert space* on a non-empty set  $\mathcal{X}$  is a Hilbert space  $\mathcal{H}$  of functions  $f: \mathcal{X} \rightarrow \mathbb{R}$  with a *reproducing kernel*, that is, a function  $k: \mathcal{X} \times \mathcal{X} \rightarrow \mathbb{R}$  such that

- (i)  $k(\cdot, x) \in \mathcal{H}$  for all  $x \in \mathcal{X}$ ,
- (ii)  $f(x) = \langle f, k(\cdot, x) \rangle_{\mathcal{H}}$  for all  $f \in \mathcal{H}$  and  $x \in \mathcal{X}$ .

As a consequence of (ii), we note that the reproducing kernel  $k(x, x') = \langle k(\cdot, x), k(\cdot, x') \rangle_{\mathcal{H}}$  of a RKHS is itself *unique* and *symmetric*.

Another crucial concept towards the characterisation of kernels are *symmetric positive definite* functions.

**DEFINITION 2.14 (Symmetric positive definitive function).** Let  $\mathcal{X}$  be a set and  $g: \mathcal{X} \times \mathcal{X} \rightarrow \mathbb{R}$  be a bivariate real-valued function. We say that  $g$  is a symmetric positive definitive function if it satisfies the following two properties:

1. *Symmetry*: for  $x, x' \in \mathcal{X}$ , we have

$$g(x, x') = g(x', x). \quad (2.7)$$

2. *Positive definiteness*: for all  $\lambda_1, \dots, \lambda_k \in \mathbb{R}$  and all  $x_1, \dots, x_k \in \mathcal{X}$ , we have

$$\sum_{i=1}^k \sum_{j=1}^k \lambda_i \lambda_j g(x_i, x_j) \geq 0 \quad (2.8)$$

The second property is equivalent to saying that the matrix defined by the kernel function is *positive definite*, i.e. it only has non-negative eigenvalues.

If  $\mathcal{H}$  is a RKHS, its reproducing kernel  $k(x, x')$  is a kernel in the sense of Definition 2.12 under the map  $\phi: x \mapsto k(\cdot, x)$ . Likewise, any kernel in the sense of Definition 2.12 can be readily seen to be a symmetric, positive definite function. Crucially, the Moore–Aronszajn theorem completes the characterisation of kernels by proving that *any* symmetric positive definite function  $g(x, x')$  is the reproducing kernel  $k(x, x')$  of a *unique* RKHS  $\mathcal{H}$  and, thus, is also a kernel as in Definition 2.12. In other words, the concepts of (i) a kernel, (ii) a reproducing kernel and (iii) symmetric positive definite functions are equivalent. From a practical perspective, the take-away from this theoretical discussion is that a function  $k: \mathcal{X} \times \mathcal{X} \rightarrow \mathbb{R}$  will be a valid kernel if and only if it is symmetric and positive definite.

### 2.3.3 Examples of kernels

In this section, we will briefly mention some kernel functions defined for Euclidean space  $\mathcal{X} = \mathbb{R}^n$ . Despite the fact that  $\mathbb{R}^n$  is itself a Hilbert space and, thus, inputs are already elements of a vector space endowed with an inner product, kernel methods still provide great practical benefits. Indeed, in this case the purpose of the map  $\phi: \mathbb{R}^n \rightarrow \mathcal{H}$  implicitly defined by the kernel is not to embed the inputs into a vector space but rather to allow linear models to capture non-linear patterns.

We will begin by introducing what is perhaps one of the simplest kernel functions possible, the so-called *Dirac delta kernel*.

**DEFINITION 2.15** (Dirac delta kernel). The Dirac delta kernel takes two points  $x, x'$  from a set  $\mathcal{X}$  and compares their equality, i.e.

$$k_\delta(x, x') := \begin{cases} 1 & \text{if } x = x' \\ 0 & \text{otherwise.} \end{cases} \quad (2.9)$$



A key advantage of the Dirac delta kernel is that its simplicity makes it generally applicable. Not only it could be applied to Euclidean inputs, but also to categorical data, as well as structured objects such as strings or graphs. Most importantly, as we shall see in the next chapter, the practical importance of the Dirac delta kernel resides in its use as a building block for more sophisticated kernels.

Next, we describe two kernel functions that are ubiquitous in the literature, namely the *polynomial kernel* and the *radial basis function (RBF) kernel*.

**DEFINITION 2.16** (Polynomial kernel). Given two  $n$ -dimensional vectors  $x, x' \in \mathbb{R}^n$ , a non-negative scalar  $c$  and a *degree*  $d$ , the polynomial kernel is defined as

$$k_{\text{poly}}(x, x') = (\langle x, x' \rangle + c)^d, \quad (2.10)$$

where  $\langle \cdot, \cdot \rangle$  denotes the standard inner product in  $\mathbb{R}^n$ . The polynomial kernel can be generalised, being applicable to inputs belonging to other inner product spaces.

**DEFINITION 2.17** (Radial basis function (RBF) kernel). Given two  $n$ -dimensional vectors  $x, x' \in \mathbb{R}^n$  and a scale parameter  $\sigma \in \mathbb{R}$ , the RBF kernel is defined as

$$k_{\text{RBF}}(x, x') = \exp\left(-\frac{\|x - x'\|^2}{2\sigma^2}\right), \quad (2.11)$$

where  $\|\cdot\|$  refers to the standard Euclidean distance. The RBF kernel can also be defined for other inputs (in particular, the metric used for the calculation can be varied); the precise definition will become clear from the context.

It is also worth noting that kernels obey certain *closure properties*: for example, the sum of two kernels is another kernel, just as the product of a kernel with a positive scalar also remains a kernel (Vert *et al.*, 2004), thus forming a convex cone. These and related closure properties permit the construction of a plethora of novel kernels from existing ones. Finally, we conclude this chapter by discussing a general framework to define kernels on *structured* data sets such as graphs.

### 2.3.4 $\mathcal{R}$ -convolution kernels

The  $\mathcal{R}$ -convolution framework was developed by Haussler (1999). It provides an algorithmic way to obtain valid kernels for graphs based on substructure decomposition. The cornerstone of this method is the idea of describing *decompositions*.

DEFINITION 2.18 ( $\mathcal{R}$ -decomposition). Let  $\mathcal{G}$  denote a family of graphs. Given a graph  $G \in \mathcal{G}$ , an  $\mathcal{R}$ -decomposition is defined as a tuple

$$\mathcal{R}(g_1, \dots, g_d, G), \quad (2.12)$$

where  $g_i \in \mathcal{G}_i$  is a “part” of  $G$ , such as a *subgraph* or a subset of the vertices (the definition of a part is purposefully left open in order to be as generic as possible). The notation is supposed to describe a *relationship*, *i.e.* we can think of  $G$  as being composed of the  $g_i$ . Since such a decomposition is not unique, it is also important to define the *pre-image* or *fibre* of the relation as

$$\mathcal{R}^{-1}(G) := \{(g_1, \dots, g_d) \mid \mathcal{R}(g_1, \dots, g_d, G)\}. \quad (2.13)$$

We will use  $\vec{g} := (g_1, \dots, g_d)$  to denote the tuple.

If the fibre is finite, which is always the case for structural decompositions into paths or subgraphs, as long as the graph itself is finite, Haussler (1999) shows that the existence of kernels on individual substructures, *i.e.* for some  $g_i$ , guarantees the existence of a kernel on  $\mathcal{G}$ .

DEFINITION 2.19 ( $\mathcal{R}$ -convolution kernel). For  $i \in \{1, \dots, d\}$ , let  $\kappa_i$  be a base kernel on a subset of the parts  $\mathcal{G}_i$ . Then the  $\mathcal{R}$ -convolution kernel between two graphs  $G, G' \in \mathcal{G}$  is defined as

$$k_{\mathcal{R}}(G, G') := \sum_{\vec{g} \in \mathcal{R}^{-1}(G)} \sum_{\vec{g}' \in \mathcal{R}^{-1}(G')} \prod_{i=1}^d \kappa_i(g_i, g'_i), \quad (2.14)$$

and always constitutes a valid kernel on  $\mathcal{G}$  (Haussler, 1999).

In addition to the description of the kernel in terms of relations, the  $\mathcal{R}$ -convolution framework is also often expressed in terms of a decomposition of a graph into sets of substructures  $\mathcal{S}$ , such as (i) all nodes of a graph, (ii) all shortest paths of a graph. In this case, Eq. (2.14) can also be written as

$$k_{\mathcal{R}}(G, G') := \sum_{s \in \mathcal{S}} (G) \sum_{s' \in \mathcal{S}'} (G') \prod_{i=1}^d \kappa_i(s, s'), \quad (2.15)$$

with  $\mathcal{S}$  and  $\mathcal{S}'$  denoting the substructures of  $G$  and  $G'$ , respectively. This notation, being more accessible, will be used throughout the subsequent chapters.

### 3 Kernels for graph-structured data

The popularisation of kernel methods in machine learning during the early 2000s (Schölkopf and Smola, 2002), including successful applications to structured data types such as strings or trees, has led to almost two decades of research into designing kernels for graphs, spanning a wealth of approaches that greatly differ in the type of substructures they consider, their computational efficiency and the type of graphs they are applicable to. This chapter is devoted to describing how the field has evolved during this time, summarising the most relevant methods, discussing what motivated their development and ultimately presenting the state-of-the-art approaches in this domain.

Developing practically useful kernels for graph-structured data is particularly challenging due to the fundamental nature of graphs as discrete objects with a number of substructures that grows exponentially with the size of the graph. This creates an inherent trade-off between the goals of using as much of the information contained in the graphs as possible to define the kernel and of achieving computational tractability. In particular, it is known that computing *complete graph kernels*, that is, any kernel  $k(G, G') = \langle \phi(G), \phi(G') \rangle_{\mathcal{H}}$  such that the corresponding feature map  $\phi(G)$  is injective, is at least as hard as solving the graph isomorphism problem, for which no polynomial time algorithm is known (Gärtner *et al.*, 2003, Proposition 1). Crucially, this result suggests that, unless a breakthrough concerning the graph isomorphism problem occurs, graph kernels which can be computed in polynomial time must forego some information such that there will always exist at least one pair of graphs, not identical to each other, which nevertheless cannot be distinguished by the kernel. However, this seemingly negative theoretical result is not at odds with the excellent empirical performance of graph kernels in both unsupervised and supervised learning applications. Statistical learning algorithms typically operate under certain regularity assumptions, such as smoothness of the target function with respect to some appropriate metric or representation for the inputs. Therefore, the use of a function class of limited capacity might actually be instrumental in being able to generalise from finite data sets rather than being a practical liability.

Much of the existing research into graph kernels can hence be understood as instances of *feature engineering*, aiming to investigate which aspects of graphs are best suited to define a notion of graph similarity, quantified by the kernel function, that performs well in different statistical learning problems of interest. To this end, many graph kernels, including some of the state-of-the-art methods, have exploited the flexibility of the  $\mathcal{R}$ -convolution framework, exploring both the use of different types of substructures a graph can be decomposed into and of different base kernels to quantify the similarity of these substructures.

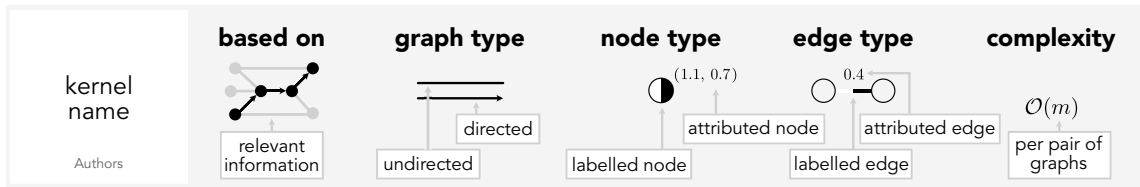
Another crucial driving force in the design of new graph kernels has been the quest for improved computational efficiency. This has motivated varied contributions ranging from the use of certain substructures that are more amenable to computation to the development of specialised algorithms to evaluate particular cases of formerly proposed graph kernels in a drastically more efficient manner. As a result of these efforts, the field has accomplished remarkable progress, with state-of-the-art approaches being orders of magnitude faster than the first ever proposed graph kernels while simultaneously performing better in many unsupervised and supervised learning tasks.

As a consequence of the emphasis on computational tractability, many existing graph kernels make assumptions that limit the type of graphs they can be applied to. Most often, these limitations concern the type of attributes or labels nodes and edges are allowed to have. For instance, some graph kernels are only applicable to graphs without attributes while many others can handle labels but not arbitrary continuous attributes. Overcoming these limitations by either proposing new graph kernels applicable to graphs with continuous attributes or providing ways to adapt previously existing graph kernels to this new setting has been another important motivation for contributions in this domain.

Finally, despite the great theoretical flexibility of the  $\mathcal{R}$ -convolution framework, most graph kernels based on this paradigm correspond to relatively simple particular cases. For example, a common simplification, once again motivated by computational considerations, is the use of Dirac kernels to compare the substructures of choice. However, despite being convenient from a computational viewpoint, exact matching of substructures has been known to cause difficulties such as diagonal dominance, which could impact the resulting generalisation performance (Greene and Cunningham, 2006). Motivated by this observation, some of the most recent developments in the field have aimed to extend the way in which the  $\mathcal{R}$ -convolution framework has been typically used to define graph kernels without compromising computational tractability.

We now seek to highlight a few important properties of the graph kernels we will subsequently describe. At a high level, we group the described graph kernels into three primary categories: (i) bag of structures, (ii) information propagation, and (iii) extensions of common frameworks. This hierarchy or categorisation can be seen in Figure 3.1. Each of these high-level categories can be further divided based on the type of approach within the category. We therefore organise our descriptions using both levels, in order to place these more granular categories into context, to understand the relationship with one another. Despite kernels within a given category sharing some higher-level principles, the specifics of what each kernel does can vary within a category, in particular in terms of what kind of information it can incorporate from a graph and in its computational complexity. We have therefore added a grey box after each kernel that we describe, summarising some of the key

information about the kernel. In the box, *based on* refers to the key aspect of the graph that the kernel uses. *Graph type* refers to the properties of the graph, namely whether the kernel can incorporate information from undirected graphs or directed graphs. *Node type* refers to whether the kernel can support node labels or node attributes, and *edge type* similarly details whether the kernel can incorporate edge labels or (continuous) edge attributes. Finally, *complexity* refers to the computational complexity of the kernel evaluation for a given pair of graphs. We provide a sample box here to indicate how this information will be represented in the boxes.



We leave a more detailed discussion on how to choose an appropriate kernel to Section 4.6, so as to incorporate also our findings from our experiments into such a recommendation. We note that it is also possible to choose a kernel a priori based on the various characteristics of a kernel, whether the graph kernel can incorporate the information in the data set, and using any relevant domain knowledge. More specifically, the factors guiding the choice of kernel could include:

- (i) Can the graph kernel handle graphs that are directed (or undirected)?
- (ii) Does it include whichever node or edge labels or attributes that are present in the graphs?
- (iii) Is the graph kernel (theoretically) efficient to compute for the given data set?
- (iv) Is there a particular substructure (e.g. tree patterns) that is relevant to the domain that would preclude the choice of a particular kernel?

We provide an initial reference in Figure 3.2 and in Table 3.1 to make such a decision. However, we would instead recommend choosing a kernel by not only considering what information it incorporates, but also based on its empirical performance on benchmark data sets. We provide a more detailed analysis of the performance of various kernels in Chapter 4, and provide the reader a more comprehensive guide on how to choose a kernel in Section 4.6.

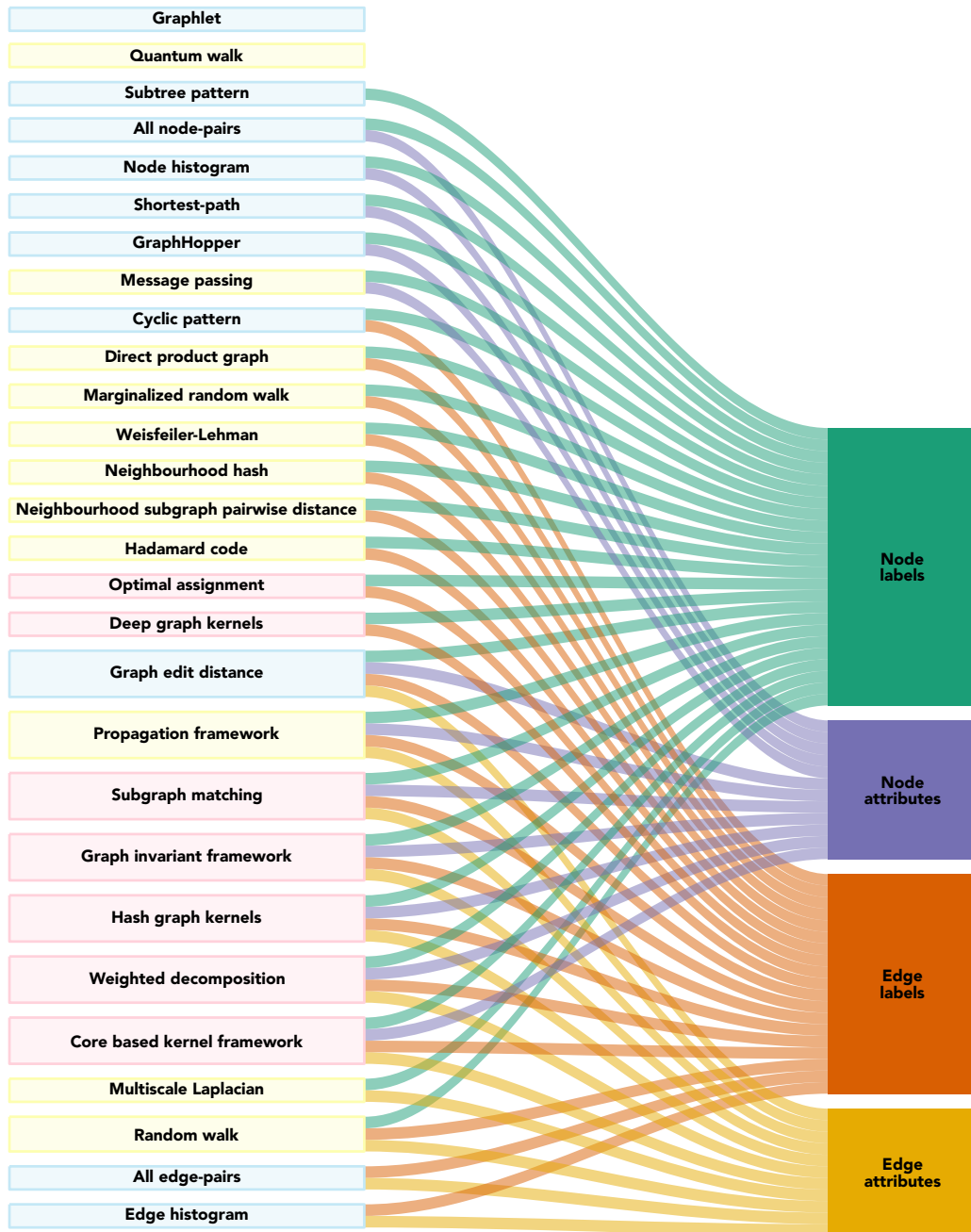
The remainder of this chapter aims to present the results of almost two decades of continued progress in graph kernel research in a concise, easy-to-follow manner. Sections have been structured to reflect an intuitive taxonomy of the different graph kernels covered in this review, depicted by the boxes in Figure 3.1. In this way, Sections 3.1.1-3.2.3 introduce



**Figure 3.1:** A taxonomy of the graph kernels presented in this survey. Despite the fact that each kernel was assigned a *single* category, following the structure of this chapter, some of the kernels (in particular the frameworks) are highly generic and could be seen as instances of multiple categories. The taxonomy is not to be understood as a “ranking” of kernels in terms of their expressivity or any other criteria.

**Table 3.1:** A brief summary of graph kernel properties.  $U$  and  $D$  stand for undirected and directed graphs, respectively, with the cell being blank if edge information is not taken into account by the kernel. Node and edge labels indicate (categorical) node and edge labels, whereas attributes refer to (continuous) node attributes and edge weights. A dagger (“†”) implies that continuous attributes can be handled if the underlying kernel has an explicit feature representation. Note that the multiscale Laplacian requires the edge attributes to be 1-dimensional. The complexity refers to the worst-case *theoretical* complexity for evaluating the kernel between two graphs. In practice, and for certain kinds of graphs, some graph kernels, such as the shortest-path and GraphHopper kernels, can be evaluated much more efficiently. Missing complexity entries correspond to frameworks whose complexity would depend on the underlying base kernel. The table uses notation that will be reintroduced in the respective graph kernel description:  $n$ : number of vertices,  $m$ : number of edges,  $d$ : maximum degree,  $d_v$ : dimension of the vertex labels/attributes,  $d_e$ : dimension of the edge labels/attributes,  $k$ : size of the subgraph,  $c$ : upper bound on the number of cycles in any graph,  $r$ : diameter,  $\tau$ : maximum number of matching substructures,  $l$ : maximum number of selector-context pairs.

Kernel	Graphs	N. labels	N. attr.	E. labels	E. attr.	Complexity
All node-pairs		✓	✓			$O(n^2 d_v)$
Node histogram		✓	✓ <sup>†</sup>			$O(nd_v)$
All edge-pairs	U, D			✓	✓	$O(m^2 d_e)$
Edge histogram	U, D			✓	✓ <sup>†</sup>	$O(md_e)$
Shortest-path	U, D	✓	✓			$O(n^4 d_v)$
GraphHopper	U, D	✓	✓			$O(n^4)$
Subtree pattern	U, D	✓				$O(n^2 h 4^d)$
Cyclic pattern	U, D	✓		✓		$O((c+2)n+2m)$
Graph edit distance	U, D	✓	✓	✓	✓	$O(n^3)$
Graphlet	U, D					$O(nd^{k-1})$
Direct product graph	U, D	✓		✓		$O(n^6)$
Marginalized random walk	U, D	✓		✓		$O(n^6)$
Random walk	U, D	✓		✓	✓ <sup>†</sup>	$O(n^3)$
Quantum walk	U					$O(n^3)$
Weisfeiler–Lehman	U, D	✓		✓		$O(hm)$
Neighbourhood hash	U, D	✓		✓		$O(hm)$
Neighbourhood subgraph pairwise distance	U	✓		✓		$O(mn_h m_h \log(m_h))$
Hadamard code	U, D	✓		✓		$O(hm)$
Propagation framework	U, D	✓	✓	✓	✓	$O(hm)$
Message passing	U, D	✓	✓			$O(n^2)$
Multiscale Laplacian	U	✓			✓	$O(n^2 h)$
Subgraph matching	U, D	✓	✓	✓	✓	$O(k(n^2)^{k+1})$
Graph invariant framework	U, D	✓	✓	✓	✓	$O(\tau n^2 d^{4r})$
Hash graph kernels	U, D	✓	✓	✓	✓	
Weighted decomposition	U, D	✓	✓	✓	✓	$O(l^2)$
Optimal assignment	U, D	✓		✓		$O(hm)$
Deep graph kernels	U, D	✓		✓		
Core based kernel framework	U	✓	✓	✓	✓	



**Figure 3.2:** An overview of the kernels and which node and edge information is used by the kernel. Labels refer to categorical features on the nodes or edges, whereas attributes refer to continuous features on the on nodes or edges. The kernels are coloured according to their higher level categorisation (blue: bag of structures, yellow: information propagation, pink: extensions), and are spaced according to the information that is included. The graphlet kernel and quantum walk kernel do not incorporate any node or edge labels or attributes.



some of the most prominent graph kernels, most of which fall under the  $\mathcal{R}$ -convolution framework, categorised according to the type of substructures they are based on. Next, Section 3.3.1 describes approaches to extend existing graph kernels that were designed for graphs with categorical attributes to the case where attributes might be continuous. Finally, Section 3.3.2 discusses methods to define graph kernels that seek to alleviate some of the limitations of simple instantiations of the  $\mathcal{R}$ -convolution framework. A high-level overview of computational complexity and supported labels and attributes for all graph kernels under consideration is provided in Table 3.1 on p. 23.

## 3.1 Bag of structures

Many graph kernels consider the enumeration and counting of given substructures in the graph. For example, one can consider using basic properties about the graph, such as the counts of node or edge labels, for use in a kernel. While these basic graph statistics are often efficient to compute, they lack the expressivity of more complex substructures. Another branch of this research accordingly considers more complex structures, such as patterns of special subgraphs or paths within a graph. The more expressive the feature, the more computationally intense the kernel evaluation typically is, resulting in a diverse range of time complexity within this category of kernels.

### 3.1.1 Graph kernels based only on nodes

Graphs jointly represent a collection of entities, referred to as *nodes*, as well as a set of relationships between those entities, referred to as *edges*. In particular, the relational information conveyed by a graph’s edges differentiates graphs from other data types, giving them great representational power, but also being responsible for most of the complexity in dealing with this type of data. As a consequence, one of the simplest ways to define a notion of graph similarity is to ignore the relational aspect of graphs altogether, effectively treating them as bags-of-nodes. Despite obvious limitations, graph kernels based exclusively on nodes are of great practical importance. Firstly, by ignoring edges, these methods provide a sensible baseline to ascertain the relative importance of graph topology for each specific task. Moreover, as we will see in Chapter 4, node-only graph kernels can exhibit competitive performance in certain data sets, suggesting that modelling inputs as “fully-fledged” graphs might be unnecessary in some particular cases. Instead, a bag-of-nodes representation might lead to a more parsimonious and computationally efficient model for such data sets. Finally, and perhaps most importantly, graph kernels defined on nodes are used as building blocks for some of the most successful graph kernels

to-date, which apply a node-only kernel to graphs that have been modified so that the attributes of each node encode information about the topology of the original graph.

### 3.1.1.1 All node-pairs kernel

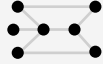
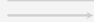
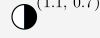
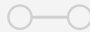
A fully general, node-only graph kernel can be instantiated using the  $\mathcal{R}$ -convolution framework by defining the  $\mathcal{R}$ -decomposition so that its pre-image  $\mathcal{R}^{-1}(G)$  corresponds to the set of nodes of the graph  $G$ . This leads to the *all node-pairs kernel*.

**DEFINITION 3.1** (All node-pairs kernel). Let  $G = (V, E)$  and  $G' = (V', E')$  be two graphs with node attributes. The *all node-pairs kernel* is defined as

$$k_N(G, G') := \sum_{v \in V} \sum_{v' \in V'} k_{\text{node}}(v, v') \quad (3.1)$$

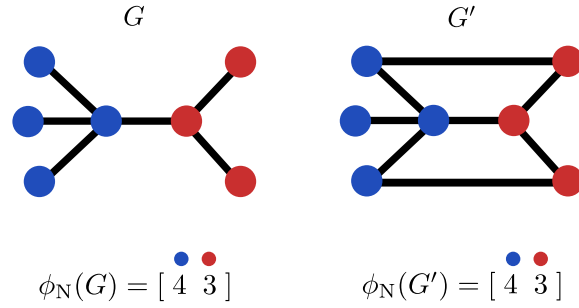
where  $k_{\text{node}}$  stands for any p.d. (*positive definite*) kernel defined on the node attributes.

The all node-pairs kernel can trivially handle both categorical and continuous node attributes by using an appropriate p.d. kernel  $k_{\text{node}}$  between node attributes. Under the assumption that evaluating  $k_{\text{node}}$  has complexity  $\mathcal{O}(d_v)$ , the resulting graph kernel can be computed with complexity  $\mathcal{O}(n^2 d_v)$  for graphs having  $n$  nodes each.

	based on	graph type	node type	edge type	complexity
all node-pairs kernel	 nodes	 none	 labelled attributed	 none	$\mathcal{O}(n^2 d_v)$

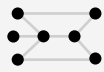

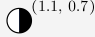
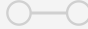
### 3.1.1.2 Node histogram kernel

Denoting the feature map corresponding to the kernel on node attributes  $k_{\text{node}}$  as  $\phi_{\text{node}}(\cdot)$ , the all node-pairs kernel can be expressed as  $k_N(G, G') = \langle \phi_N(G), \phi_N(G') \rangle_{\mathcal{H}}$ , where  $\phi_N(G) := \sum_{v \in V} \phi_{\text{node}}(v)$  can be interpreted as the RKHS embedding of a graph  $G = (V, E)$ . An important particular case arises whenever  $\phi_{\text{node}}(\cdot)$  can be computed explicitly. This occurs, for instance, when node attributes are categorical labels over a finite alphabet  $\Sigma_V$  and  $k_{\text{node}}$  is a Dirac kernel. Then, denoting the  $i$ th canonical basis vector of  $\mathbb{R}^{|\Sigma_V|}$  as  $\mathbf{e}_i$ , one can define  $\phi_{\text{node}}(v) := \mathbf{e}_{l_V(v)}$ , where  $l_V(v)$  stands for the label of node  $v$ . The graph embedding  $\phi_N(G)$  induced by this kernel simply corresponds to an unnormalised histogram that counts the occurrence of each node label in the graph. More formally, this kernel should be referred to as a node-based kernel with an explicit feature map, whose features are defined by label



**Figure 3.3:** Given a graph  $G$  and  $G'$  with node labels, the node histogram kernel can be efficiently computed using the unnormalised histogram of node labels:  $k_N(G, G') = \langle \phi_N(G), \phi_N(G') \rangle_{\mathcal{H}} = 25$ .

counts. With a slight abuse of terminology, we will refer to this implementation of the all node-pairs kernel as the *node histogram kernel*, which is visualised in Figure 3.3, even in cases where  $\phi_N(G)$  cannot be interpreted as a histogram. Under the assumption that  $\phi_{\text{node}}(\cdot)$  can be explicitly represented as a  $d_v$ -dimensional vector, the computational complexity of the node histogram kernel is simply  $O(nd_v)$ , making it one of the most computationally efficient graph kernels for sufficiently small values of  $d_v$ .

	based on	graph type	node type	edge type	complexity
node histogram kernel	 nodes	 none	 labelled attributed	 none	$\mathcal{O}(nd_v)$

### 3.1.2 Graph kernels based only on edges

A straightforward alternative to treating graphs as a bag-of-nodes is to model them instead as a bag-of-edges. This allows accounting for some of the relational information contained in the graph, though only in terms of direct relationships between entities (nodes). Any higher-order relations defined implicitly by paths between non-adjacent nodes are effectively ignored by this approach. Nevertheless, much like graph kernels based only on nodes, these methods are useful in the sense that they can serve as a basis to construct more sophisticated graph kernels as well as provide a baseline to characterize the relative importance of indirect relationships between nodes for any task of interest. More generally, node-only and edge-only graph kernels can be combined to construct a strong baseline restricted to use only node and/or edge attributes while ignoring other aspects of the topology of the graphs.

### 3.1.2.1 All edge-pairs kernel

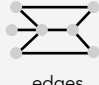
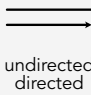


Similarly to the all node-pairs kernel, defining an  $\mathcal{R}$ -decomposition so that its pre-image  $\mathcal{R}^{-1}(G)$  corresponds to the set of edges of the graph  $G$  leads to the *all edge-pairs kernel*.

DEFINITION 3.2 (All edge-pairs kernel). Let  $G = (V, E)$  and  $G' = (V', E')$  be two graphs with node and/or edge attributes. The *all edge-pairs kernel* is defined as

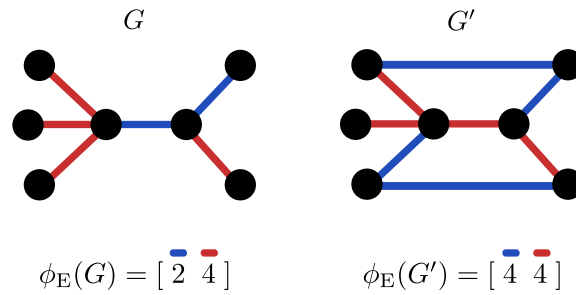
$$k_E(G, G') := \sum_{e \in E} \sum_{e' \in E'} k_{\text{edge}}(e, e') \quad (3.2)$$

where  $k_{\text{edge}}$  stands for any p.d. kernel defined on the edge attributes and/or the node attributes of the edge's endpoints.

The all edge-pairs kernel can also handle both categorical and continuous attributes depending on the choice for the edge kernel  $k_{\text{edge}}$ . If evaluating this function takes time  $O(d_e)$ , the resulting graph kernel would have complexity  $O(m^2 d_e)$  for graphs having  $m$  edges.

	based on	graph type	node type	edge type	complexity
all edge-pairs kernel	 edges	 undirected directed	 none	 0.4 labelled attributed	$O(m^2 d_e)$

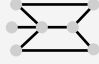
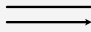

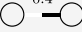
### 3.1.2.2 Edge histogram kernel



**Figure 3.4:** Given a graph  $G$  and  $G'$  with edge labels, the edge histogram kernel can be efficiently computed using the unnormalised histogram of edge labels:  $k_E(G, G') = \langle \phi_E(G), \phi_E(G') \rangle_{\mathcal{H}} = 24$ .

Analogously to the node histogram kernel, whenever the feature map  $\phi_{\text{edge}}(\cdot)$  corresponding to the edge kernel  $k_{\text{edge}}$  can be computed explicitly, the all edge-pairs kernel can

be efficiently calculated in terms of the induced graph embeddings  $\phi_E(G) := \sum_{e \in E} \phi_{\text{edge}}(e)$ , which can be interpreted as an unnormalised histogram of edge label counts. Assuming  $\phi_{\text{edge}}(\cdot)$  admits an explicit  $d_e$ -dimensional representation, the computational complexity of the *edge histogram kernel* is reduced to  $\mathcal{O}(md_e)$ . We present an illustration of the edge histogram kernel in Figure 3.4.

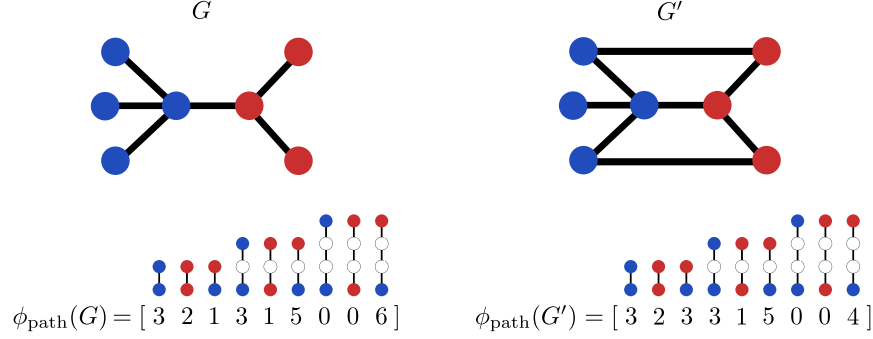
	based on	graph type	node type	edge type	complexity
edge histogram kernel	 edges	 undirected directed	 none	 labelled attributed	$\mathcal{O}(md_e)$

### 3.1.3 Graph kernels based on paths

Graph kernels built around pairwise comparisons of the node and edge sets make limited use of the topology of graphs, failing to capture any indirect relationships between non-adjacent nodes. Instead, representing a graph by the *paths* that are present provides a way to account for such relations. This is the idea we will study in this subsection. A major disadvantage, however, is that paths are less amenable to efficient computation than comparing edges or nodes. For example, one could propose a kernel based on comparing each path of graph  $G$  to each path of graph  $G'$ . However, computing this *all path-pairs kernel* has been proven to be NP-hard (Borgwardt and Kriegel, 2005, Lemma 2). To circumvent this limitation, popular graph kernels based on paths focus instead on shortest paths since, like walks, these can be obtained in polynomial time.

#### 3.1.3.1 Shortest-path kernel

As its name suggests, the idea behind the *shortest-path kernel* (shown in Figure 3.5) is to define the similarity between two graphs in terms of the similarities of their shortest-paths. Borgwardt and Kriegel (2005) accomplish this by transforming a given graph  $G = (V, E)$  into its *shortest-paths graph*  $S = (V, E_S)$ , which is a weighted graph. As indicated,  $S$  shares the vertices with the original graph, but its edges  $E_S$  are defined by the constraint that  $(v_i, v_j) \in E_S$  if and only if nodes  $v_i$  and  $v_j$  are connected by a walk. Furthermore, the weight  $w_{ij}$  of this edge will be set to the shortest path distance of  $v_i$  and  $v_j$ . The transformed graph  $S$  is also referred to as the *Floyd-transformation* (Borgwardt and Kriegel, 2005) of  $G$  because the original publication uses Floyd’s algorithm (Floyd, 1962; Warshall, 1962) to calculate shortest paths between all pairs of nodes at the same time. This permits us to define the shortest-path kernel.



**Figure 3.5:** A possible implementation of the shortest-path kernel which counts the number of matching shortest paths with the same node labels at the end points. Here, white nodes indicate that the node can have any label. This instance of the shortest-path kernel is the multiplication of three Dirac delta kernels: two node kernels comparing the labels of the source nodes and target nodes respectively, and one edge kernel comparing the length of the shortest path. Such an instance gives rise to an explicit feature representation (this is not always the case), and the resulting kernel computation is  $k_{\text{SP}}(G, G') = \langle \phi_{\text{path}}(G), \phi_{\text{path}}(G') \rangle_{\mathcal{H}} = 75$ . While there may exist several shortest paths between two nodes, the length of the shortest path is unique.

**DEFINITION 3.3 (Shortest-path graph kernel).** Given graphs  $G$  and  $G'$  and their shortest-paths graphs  $S = (V, E_S)$  and  $S' = (V', E'_S)$ , the *shortest-path graph kernel* is defined as

$$k_{\text{SP}}(G, G') := \sum_{e \in E_S} \sum_{e' \in E'_S} k_{\text{path}}^{(1)}(e, e'), \quad (3.3)$$

where  $k_{\text{path}}^{(1)}$  is a kernel on edge paths of length one in the shortest-paths graphs. Given two edges  $e := (u, v)$  and  $e' := (u', v')$ , Borgwardt and Kriegel (2005) suggest such an edge path kernel to take the form of




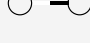
$$k_{\text{path}}(e, e') := k_{\text{node}}(u, u') \cdot k_{\text{edge}}(e, e') \cdot k_{\text{node}}(v, v'), \quad (3.4)$$

*i.e.* a product of node kernels with an edge kernel.

The definition of  $k_{\text{path}}$  allows for some flexibility in assessing the similarity of paths. The node kernel, for example, can be a Dirac delta kernel that compares the labels of nodes at the beginning and end of the path (purposefully ignoring all other labels along the path), while the edge kernel  $k_{\text{edge}}$  can be a Dirac kernel on the length of the shortest path, and can also be easily extended to incorporate edge features by using a measure of the difference in edge lengths of weighted graphs (Borgwardt and Kriegel, 2005).

The computational complexity of this kernel depends on the number of edges that have to be considered in the Floyd-transformed graphs, leading to a worst-case runtime of  $\mathcal{O}(n^4)$  for  $n$  vertices. Even though this might seem prohibitive for some applications, one of the advantages of this kernel is its great flexibility with respect to the node and edge kernels

that can easily be adapted to make use of arbitrary attributes. Alternatively, if the feature map  $\phi_{\text{path}}(\cdot)$  corresponding to the edge path kernel  $k_{\text{path}}$  admits a  $d$ -dimensional explicit representation, the computational complexity can be sharply reduced to  $\mathcal{O}(n^2d)$ .

	based on	graph type	node type	edge type	complexity
shortest path kernel <small>Borgwardt and Kriegel, 2005</small>	 paths	 undirected directed	 labelled	 labelled	$\mathcal{O}(n^4d_v)$

### 3.1.3.2 GraphHopper kernel

A drawback of the shortest-path kernel is its  $\mathcal{O}(n^4)$  asymptotic runtime for a graph with  $n$  nodes, which can quickly become prohibitive as graphs grow in size. This motivated Feragen *et al.* (2013) to develop the GraphHopper kernel. Just like the shortest-path kernel, it is applicable for undirected graphs with edge weights and optional node attributes—provided a kernel function for comparing them is available; this is the case for real-valued (“continuous”) attributes, whose dissimilarity can be assessed, for example, by means of an RBF kernel (see Definition 2.17 on p. 17).

The central idea of the GraphHopper kernel is to compare graphs by nodes that are encountered while the eponymous “hopping” along shortest paths happens. This leads to the following general form of the kernel.

**DEFINITION 3.4** (GraphHopper kernel). Given graphs  $G$  and  $G'$  and node kernel  $k_{\text{node}}$ , the GraphHopper kernel is a sum of node kernels over shortest paths, *i.e.*

$$k_{\text{GH}}(G, G') := \sum_{p \in \mathcal{P}, p' \in \mathcal{P}'} k_p(p, p'), \quad (3.5)$$





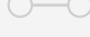
where  $k_p$  is a special path kernel that evaluates the node kernel  $k_{\text{node}}$  along paths of *equal* length  $|p| = |p'|$ , *i.e.*

$$k_p(p, p') := \begin{cases} \sum_{j=1}^m k_{\text{node}}(p^{(j)}, p'^{(j)}) & \text{if } |p| = |p'| \\ 0 & \text{otherwise} \end{cases}, \quad (3.6)$$

where  $p^{(j)}$  refers to the  $j$ th vertex of a shortest path  $p$ .

While there is a worst-case complexity of  $\mathcal{O}(n^4)$ , it was shown (Feragen *et al.*, 2013) that the previous equation decomposes into a weighted sum of node kernels. These weights can

be calculated efficiently, leading to an average overall worst-case complexity of  $O(n^2d)$  per kernel evaluation, where  $n$  denotes the number of vertices and  $d$  denotes the dimension of the node attributes. This estimate assumes that the node kernel  $k_{\text{node}}$  can be calculated in time  $O(d)$ , which is the case for most common kernels, such as the linear kernel.

	based on	graph type	node type	edge type	complexity
 GraphHopper kernel <small>Feragen et al., 2013</small>	 paths	 undirected directed	 labelled attributed	 none	$O(n^4)$

### 3.1.4 Graph kernels based on special subgraphs

Arguably, the most powerful representation of graphs one could obtain would count the number of occurrences in a graph of each subgraph occurring at least once in a given graph data set. From the perspective of the  $\mathcal{R}$ -convolution framework, this corresponds to decomposing each graph into the set of all its subgraphs and using a Dirac kernel to quantify the similarity between these substructures. However, it is also known that computing this kernel is an NP-hard problem (Gärtner *et al.*, 2003, Proposition 2). As a consequence, existing graph kernels based on subgraph enumeration focus instead on counting the occurrence of special subtypes of subgraphs, as we will discuss next.

#### 3.1.4.1 Subtree pattern kernel

Due to the limitations mentioned above, Ramon and Gärtner (2003) proposed to limit the subgraphs considered to subtree patterns from a root node up to a specified height  $h$ . For  $h = 1$ , this amounts to a Dirac delta kernel on the node labels, *i.e.* for two vertices  $v$  and  $v'$ ,

$$k_{\text{st}}^{(1)}(v, v') = \begin{cases} 1 & \text{if } l_V(v) = l_V(v') \\ 0 & \text{otherwise.} \end{cases} \quad (3.7)$$

For  $h > 1$ , this considers all possible matchings  $M_{v,v'}$  between the nodes in the neighbourhood of the root nodes,  $N(v)$  and  $N(v')$ , and checks whether the size of the neighbourhood is equivalent, and whether there is a suitable match of node labels, while finally counting how many such matchings there are. We note that this kernel uses *subtree patterns*, as opposed to *subtrees*, to allow for the repetition of nodes and edges. While Ramon and Gärtner defined the neighbourhood to be specifically the out-degree neighbourhood, we will use our normal neighbourhood notation since this is equivalent to



the out-degree neighbourhood in unlabelled graphs. More formally, this is to say that  $M_{v,v'} = \{R \subseteq N(v) \times N(v') \mid (\forall (a, a'), (b, b') \in R: a = a' \Leftrightarrow b = b' \wedge (\forall (a, a') \in R: l_V(a) = l_V(a'))\}$ . This leads to the following definition.

**DEFINITION 3.5.** Given graphs  $G = (V, E)$  and  $G' = (V', E')$  with node labels defined on the common alphabet  $\Sigma_V$ , labelling function  $l_V$ , and vertices  $v \in V, v' \in V'$ , the *subtree pattern kernel* is defined as


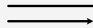

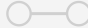
$$k_{\text{ST}}^{(h)}(G, G') = \sum_{v \in V} \sum_{v' \in V'} k_{\text{st}}^{(h)}(v, v'), \quad (3.8)$$

where  $k_{\text{st}}^{(h)}$  is defined as

$$k_{\text{st}}^{(h)} = \lambda_v \lambda_{v'} \sum_{R \in M_{v,v'}} \prod_{a, a' \in R} k_{\text{st}}^{(h-1)}(v, v'), \quad (3.9)$$

and  $\lambda_v, \lambda_{v'}$  are used as a way to give smaller weights to higher-order subtree patterns on the nodes  $v$  and  $v'$ .

Due to the matching step, the subtree pattern kernel is not trivial to compute, having a complexity of  $O(n^2 h 4^d)$ , where  $n^2$  represents the pairwise comparison of nodes in the two graphs, where  $h$  represents the number of iterations, and  $4^d$  represents the calculation of all matchings, where  $d$  is the maximum degree in the graph for a pair of two graphs. Nevertheless, the kernel provided the foundation for many future kernels. For instance, Mahé and Vert (2009) extend the idea by adding a more general parameter based on the tree patterns considered (versus at the node level here), in order to control the effect of more complex subtree patterns.

	based on	graph type	node type	edge type	complexity
subtree pattern kernel <small>Ramon and Gärtner, 2003</small>	 subgraphs	 undirected directed	 labelled	 none	$O(n^2 h 4^d)$

### 3.1.4.2 Cyclic pattern kernel

Horváth *et al.* (2004) proposed a kernel based on the patterns of cycles and trees observed in a graph. As opposed to other kernels that compare the frequency of given patterns, which typically places larger importance on the patterns which are frequent, Horváth *et al.* (2004) instead developed a kernel to capture the diversity of different patterns present in a given graph.

The principal idea is to represent a graph by its set of simple cycles  $C(G)$  and the set of trees  $\mathcal{T}(G)$  present in a graph  $G$ . A graph  $G$  can be decomposed into cycles and trees by removing any *cut vertices*, *i.e.* vertices that will disconnect the graph when both the vertex and its incident edges are removed. What remains are *maximal biconnected components* of  $G$  and trees formed by the cut vertices. These components form the sets  $C(G)$  and  $\mathcal{T}(G)$ , which are ordered using a canonical representation that is obtained by using a function  $\pi(\cdot)$ , which finds the smallest lexicographic ordering of the sequences of nodes and edges in each cycle and tree by using the labels assigned to the nodes and edges. For the ordering of cycles, this function is defined as

$$\pi(C) := \min\{\sigma(w) \mid w \in \rho(s)\}, \quad (3.10)$$

where  $\rho(s)$  is the set of all possible orderings of a cycle  $s$ , and  $\sigma(w)$  assigns a value to the particular ordering  $w$  using the labels of the nodes  $l_V$  and edges  $l_E$  in the sequence, *i.e.*

$$\sigma(w) = l_V(v_0) l_E((v_0, v_1)) l_V(v_1) \cdot \dots \cdot l_V(v_{k-1}) l_E((v_{k-1}, v_0)) \quad (3.11)$$

for vertices  $v_i$  and edges  $(v_i, v_{i+1})$  in the cycle (considering both possible directions of the sequence in a cycle). A similar process is carried out to provide an ordering for the trees present in the graph, and therefore ensures that identical cycles and trees will be comparable in different graphs. The sets of cycles and trees of a graph  $G$  are therefore


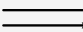

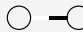
$$\begin{aligned} C(G) &:= \{\pi(C) \mid C \in \mathcal{S}(G)\} \\ \mathcal{T}(G) &:= \{\pi(T) \mid T \in \mathcal{T}(G)\}. \end{aligned}$$

**DEFINITION 3.6** (Cyclic pattern kernel). Given two graphs  $G$  and  $G'$  with node and edge labels from their respective alphabets  $\Sigma_V$  and  $\Sigma_E$ , the *cyclic pattern kernel* kernel is defined the cardinality of the intersection between these two sets, *i.e.*

$$k_{CP}(G, G') := |C(G) \cap C(G')| + |\mathcal{T}(G) \cap \mathcal{T}(G')|. \quad (3.12)$$

The computation of this kernel is, as acknowledged by the authors (Horváth *et al.*, 2004, Proposition 1), NP-hard, since a graph with  $n$  nodes can have more than  $2^n$  cycles or tree patterns. However, the authors propose a variation of their kernel that works when all the graphs in a data set (or a high proportion thereof) have a bounded number of simple cycles (graphs with more than such a bound can be disregarded). Such a modification results in an upper bound on the runtime of  $O((c+2)n+2m)$  for a given pair of graphs, where  $c$  is the bound on the number of simple cycles in any graph,  $n$  is the maximum number of

nodes in any graph in the data set, and  $m$  is the maximum number of edges in any graph in the data set.

<p>cyclic pattern kernel</p> <p>Horváth et al., 2004</p>	<p><b>based on</b></p>  <p>subgraphs</p>	<p><b>graph type</b></p>  <p>undirected directed</p>	<p><b>node type</b></p>  <p>labelled</p>	<p><b>edge type</b></p>  <p>labelled</p>	<p><b>complexity</b></p> <p><math>\mathcal{O}((c+2)n + 2m)</math></p>
--	---	---	---	---	---

### 3.1.4.3 Graph edit distance kernels

Another approach to counteract the computational bottleneck of enumerating and counting all possible subgraphs is to select a subset of important subgraphs, *i.e.* *prototypes*, a concept equivalently known as *landmarks* (Hsieh et al., 2014), and then assess how many graph edits are necessary for a given graph to include such prototypes. Specifically, the key ideas behind this approach are to instead (i) select the subgraphs on which the feature map will be based directly from the data set of graphs we wish to represent, *i.e.* data-driven *prototypes*, and (ii) define the feature map in terms of the graph edit distances to each of these prototypes, which can be computed for any type of attributed graphs, rather than counting exact matches.

This makes it possible to obtain a kernel from a metric defined on graphs (which is normally fraught with difficulties, such as having to prove that the resulting kernel is p.d.; however, since this formulation directly defines a feature map, *any* p.d. kernel can be used to compare the resulting feature vectors). For example, the *graph edit distance*, as briefly described in Section 2.2.2, has the advantage of being applicable to different types of graphs: by modifying the cost functions in the appropriate fashion, it is possible to handle directed graphs, graphs with continuous attributes, and so on. Bunke and Riesen (2007) thus proposed using graph edit distances to *embed* graphs into a feature space. This permits using either feature-based classification algorithms, *i.e.* algorithms that work directly on the vector representation, or kernel-based methods. In the following, let  $\mathcal{G} := \{G, \dots, G_n\}$  be a set of  $n$  input graphs and  $\text{dist}_{\mathcal{G}}(\cdot, \cdot)$  their corresponding graph edit distance calculation function. With a suitably-selected subset of graphs, this gives rise to an embedding.

**DEFINITION 3.7** (Graph edit distance embedding). Given  $\mathcal{G}$  as defined above, let  $\mathcal{P} := \{P_1, \dots, P_m\} \subseteq \mathcal{G}$  be a subset of *prototype* graphs (we will subsequently discuss several

strategies for choosing them), where  $m \leq n$  by definition. The *graph edit distance embedding* of a graph  $G \in \mathcal{G}$  is then defined as

$$\phi_{\mathcal{G}}(G) := (\text{dist}_{\mathcal{G}}(G, P_1), \text{dist}_{\mathcal{G}}(G, P_2), \dots, \text{dist}_{\mathcal{G}}(G, P_m)), \quad (3.13)$$

which creates a mapping  $\phi_{\mathcal{G}}: \mathcal{G} \rightarrow \mathbb{R}^m$ .

The graph edit distance mapping can now be used either directly as the feature vector for feature-based algorithms, or provided with an appropriate kernel on a feature vector space.

**DEFINITION 3.8** (Graph edit distance kernel). Let  $\kappa$  be a well-defined kernel defined for real-valued vector spaces of dimension  $m$ . Then the *graph edit distance kernel* between two graphs  $G$  and  $G'$  is defined as

$$k_{\text{edit}}(G, G') := \kappa(\phi_{\mathcal{G}}(G), \phi_{\mathcal{G}}(G')), \quad (3.14)$$


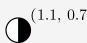
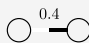
which is a valid kernel between graphs by definition.

Bunke and Riesen (2007) use a variant of an RBF kernel for their experiments, *i.e.*  $\kappa(\phi_{\mathcal{G}}(G), \phi_{\mathcal{G}}(G')) := \exp(-\gamma \|\phi_{\mathcal{G}}(G) - \phi_{\mathcal{G}}(G')\|)$ , where  $\|\cdot\|$  denotes the usual Euclidean norm, and  $\gamma \in \mathbb{R}$  is a scaling parameter. However, other choices of  $\kappa$  are possible, such as linear kernels. The choice of the *prototype set*  $\mathcal{P}$  is crucial for the suitability of the embedding. Bunke and Riesen (2007) discuss the properties of various selection schemes, such as a *spanning* selection, which starts from randomly-selected graph and iteratively extends the selection by taking the graph that has the maximum graph edit distance from all selected graphs. Specifically, given a set of graphs  $\mathcal{G}$ , suppose that a subset of graphs  $\tilde{\mathcal{G}} = \{G, G', \dots\} \subseteq \mathcal{G}$  has already been selected by the prototype selection algorithm (the base case for  $\tilde{\mathcal{G}} = \emptyset$  is typically solved by selecting a graph from  $\mathcal{G}$  at random). The next graph to include in  $\tilde{\mathcal{G}}$  is the graph  $G^* \in \mathcal{G} \setminus \tilde{\mathcal{G}}$  that *maximises* the function

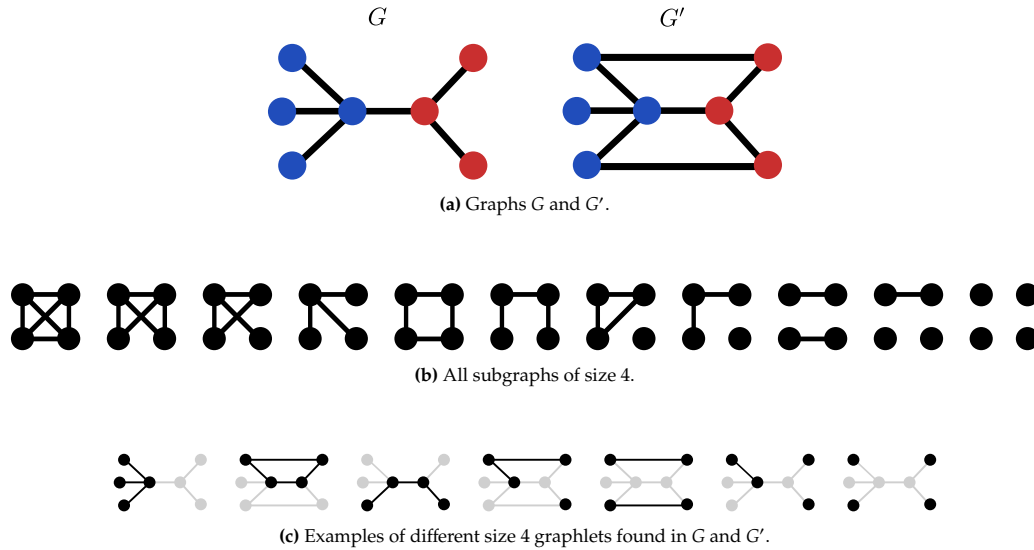
$$G \mapsto \min\{\text{dist}_{\mathcal{G}}(G, G), \text{dist}_{\mathcal{G}}(G, G'), \dots\}, \quad (3.15)$$

*i.e.* the  $G^*$  whose minimum distance to the set of selected prototype graphs  $\tilde{\mathcal{G}}$  is as *large* as possible—this ensures that the most “diverse” set of graphs is selected; similar strategies are very common for landmark selection algorithms in computational geometry, for example (Silva and Carlsson, 2004). Without loss of generality, we may assume that the graph maximising Eq. 3.15 is *unique*. If this is not the case,  $G^*$  can be selected at random from the set of candidates. For real-world applications, prototype selection can also be treated as a hyperparameter of the algorithm, which is thus subject to cross-validation.

In terms of complexity, the feature vector creation hinges on fast algorithms for the graph edit distance. These algorithms depend on the graph structure; we refer to Riesen (2015) for a detailed introduction to state-of-the-art algorithms. A recent preprint (Bai *et al.*, 2018) also deals with graph edit distance computation through the lens of graph neural networks, the key idea being that the network *learns* how to calculate the graph edit distance. Preliminary results indicate that the quality of the approximation is highly dependent on the data set. Hence, there is still a need for other algorithmic approximations.

	based on	graph type	node type	edge type	complexity
graph edit distance kernel Bunke and Riesen, 2007	 subgraphs	$\rightleftarrows$ undirected directed	 <sup>(1.1, 0.7)</sup> labelled attributed	 <sup>0.4</sup> labelled attributed	$\mathcal{O}(n^3)$

#### 3.1.4.4 Graphlet kernel



**Figure 3.6:** The graphlet kernel counts the number of matching subgraphs of size  $k$  in a given graph, resulting in an explicit feature representation for each graph. This representation, called the  $k$ -spectrum, can be done using either all possible graphlets of size  $k$ , as visualised in (b), or using only the connected graphlets of size  $k$ . The  $k$ -spectra are then typically normalised, and the resulting kernel is the linear kernel between the two spectra:  $k_{GL}(G, G') := \phi_{gd}(G)^\top \phi_{gd}(G')$ .

The *graphlet kernel* bypasses the difficulties arising from the need to enumerate a potentially enormous number of subgraphs by restricting its feature space to counts of subgraphs of a fixed size. Specifically, we will use subgraphs with a small number of nodes, often referred to as *graphlets*. This term was introduced by Pržulj *et al.* (2004) in the context of describing protein–protein interaction networks and subsequently extended with a more efficient estimation procedure (Pržulj *et al.*, 2006). Shervashidze *et al.* (2009) then developed a kernel, based on the notion that two graphs should be considered to be similar if their graphlet distributions are similar.


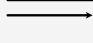

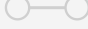
This results in a simple algorithm, which we will subsequently describe. Given  $k$ , let  $\mathcal{G} := \{g_1, \dots, g_{N_k}\}$  refer to the set of graphlets of size  $k$ . This method ignores all labels and attributes for this enumeration and merely focuses on connectivity. Generating different graphlets is a combinatorial problem and the set of  $k$ -graphlets, even though exponential in  $k$ , is fully enumerable. We show an example of enumerating graphlets and matching their occurrences in a given graph in Figure 3.6. Having enumerated all graphlets, we count their occurrence in a graph  $G$ , which yields an  $N_k$ -dimensional vector  $\phi_{gd}(G)$  whose  $i$ th entry contains the frequency of occurrence of  $g_i$  in  $G$ . We will refer to this vector as the *k-spectrum* of a graph; it leads to a graphlet comparison kernel.

DEFINITION 3.9 (Graphlet kernel). Given graphs  $G$  and  $G'$  and their corresponding  $k$ -spectrum vectors for a fixed  $k$ ,  $\phi_{gd}(G)$  and  $\phi_{gd}(G')$ , the graphlet kernel is defined as

$$k_{GL}(G, G') := \phi_{gd}(G)^\top \phi_{gd}(G') = \phi_{gd}(G')^\top \phi_{gd}(G), \quad (3.16)$$

*i.e.* a linear kernel between the two spectra. The  $k$ -spectra are typically normalised by dividing them by the total number of graphlets that occur in the graph.

The computational bottleneck of the graphlet kernel is the enumeration of all graphlets. Since the number of arbitrary graphlets is exponential in the number of vertices in the graphlet, Shervashidze *et al.* (2009) suggest that only graphlets for  $k \in \{3, 4, 5\}$  be computed; the closure properties of graph kernels make it possible to evaluate Eq. 3.16 for different values of  $k$  and combine the results. Moreover, Shervashidze *et al.* (2009) show that their computation has a complexity of  $O(nd^4)$ , where  $d$  refers to the maximum degree in a graph. Notably, Kondor *et al.* (2009) proposed a follow-up approach that uses notions from group representation theory to extend the graphlet kernel in order to account for the relative position of different graphlets in a graph, as well as to incorporate node and edge attributes.

	based on	graph type	node type	edge type	complexity
graphlet kernel <small>Shervashidze et al., 2009</small>	 subgraphs	 undirected directed	 none	 none	$\mathcal{O}(nd^{k-1})$

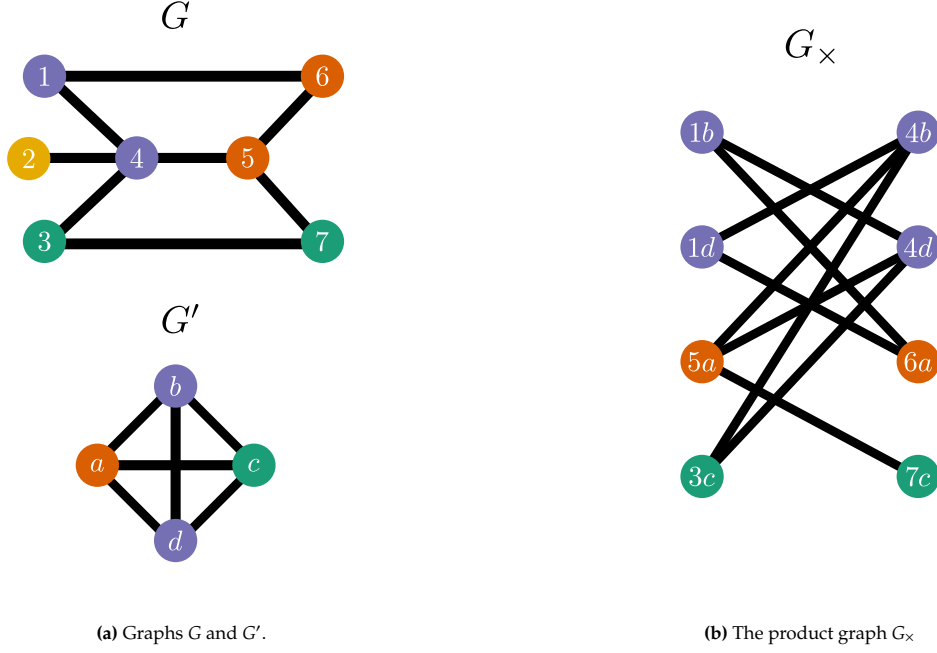
## 3.2 Information propagation

Our second high-level category, information propagation, includes methods that observe how information can be diffused throughout the graph. Walks and spectral methods can be seen as special instances of graph-based information diffusion processes. Similarly, iterative label refinement methods may also be considered as iteratively propagating information between neighbouring nodes. We now consider each of these in turn.

### 3.2.1 Graph kernels based on walks

A crucial property of walks is that they are amenable to efficient computation, unlike many other substructures. In particular, letting  $A$  denote the adjacency matrix of a graph  $G = (V, E)$  and using the definition of matrix multiplication, one can show by induction that  $A_{i,j}^k$  equals the number of walks of length  $k$  from node  $v_i$  to node  $v_j$  in  $G$ . As a consequence, the number of walks of a certain length between any pair of nodes in a graph can be computed in polynomial time. This observation motivated the use of walks as the substructure of choice for the first graph kernels proposed in the literature (Kashima *et al.*, 2003; Gärtner *et al.*, 2003).

However, they are not without important limitations. A well-known problem of graph kernels based on walks is the phenomenon often referred to as *tottering* (Mahé *et al.*, 2004). In brief, tottering occurs as a consequence of walks allowing vertices to be visited multiple times, potentially inflating the similarity of graphs that have matching edges as these could be visited infinitely many times. Another disadvantage of walks, investigated in-depth more recently, is the phenomenon of *halting* (Sugiyama and Borgwardt, 2015). Halting occurs because, for sufficiently small values of the hyperparameter  $\lambda$ , the random walk kernel is dominated by the constant and first-order terms of the infinite series, corresponding to walks of length 0 and 1, respectively. In these cases, the random walk kernel effectively degenerates to treating the graphs as bags-of-nodes-and-vertices, much like the baselines introduced in Sections 3.1.1 and 3.1.2. However, in real-world applications, small values of  $\lambda$  might be required to guarantee convergence of the series. One possibility to ameliorate these issues is to truncate the series defining the random walk kernel, as discussed in (Sugiyama and Borgwardt, 2015, Section 4). Despite these limitations, their



**Figure 3.7:** The direct product graph  $G_{\times}$  of graphs  $G$  and  $G'$ . In  $G_{\times}$ , the node uses the number of  $G$  and the letter from  $G'$  as the index. The node in  $G_{\times}$  exists if the labels of the nodes are the same in the two graphs, and an edge exists between two nodes in  $G_{\times}$  if there are edges between the corresponding nodes in  $G$  and  $G'$ .

ability to capture higher-order relationships between nodes while having computationally favourable properties has made walks a critical pillar of graph kernel methods. In this subsection, we will describe those approaches, as well as follow-up work that improved the computational efficiency of walk-based graph kernels and methods that aimed to investigate alternative types of walks.

### 3.2.1.1 Direct product graph kernel

Given a graph  $G = (V, E)$  with categorical node and edge attributes, any walk  $\omega = (v_1, v_2, \dots, v_{k+1})$  of length  $k$  in  $G$  can be represented as the sequence of node and edge labels encountered along the walk, that is,  $s(\omega) = (l_V(v_1), l_E((v_1, v_2)), l_V(v_2), \dots, l_E((v_k, v_{k+1})), l_V(v_{k+1}))$ . If node and edge attributes take values in finite alphabets  $\Sigma_V$  and  $\Sigma_E$ , then the collection of all sequences that can be obtained this way forms a countable set. Conceptually, a graph could then be represented by a feature map that counts the number of occurrences of each possible label sequence in the graph. This is precisely the idea behind the *direct product graph kernel* introduced by Gärtner *et al.* (2003).



An indispensable tool to tractably compute a kernel based on this feature map is the *direct product graph*, from which the kernel derives its name. We provide an example of a direct product graph in Figure 3.7.

**DEFINITION 3.10** (Direct product graph). Given two graphs  $G = (V, E)$  and  $G' = (V', E')$ , the *direct product graph*  $G_{\times} := (V_{\times}, E_{\times})$  is a graph that captures walks that induce identical label sequences in  $G$  and  $G'$ . More precisely, we have  $V_{\times} := \{(v, v') \in V \times V' \mid l_V(v) = l_V(v')\}$  and  $E_{\times} := \{((u, v), (u', v')) \in E \times E' \mid l_E((u, v)) = l_E((u', v'))\}$ . Thus,  $V_{\times}$  and  $E_{\times}$  correspond to matching pairs of nodes and edges in  $G$  and  $G'$ .

As shown in Gärtner *et al.* (2003, Proposition 3), the key property of the product graph is that any walk in  $G_{\times}$  is in one-to-one correspondence to a pair of walks in  $G$  and  $G'$  that have the same sequence of node and edge labels. Thus, the problem of counting matching walks between  $G$  and  $G'$  can be reduced to the problem of counting walks in  $G_{\times}$  which, as described above, can be solved in polynomial time via matrix multiplication. Using this property, the direct product graph kernel can then be defined as follows.


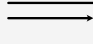

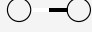
**DEFINITION 3.11** (Direct product graph kernel). Given two graphs  $G$  and  $G'$  the direct product graph kernel is calculated as

$$k_{\text{CP}}(G, G') := \sum_{i=1}^{|V_{\times}|} \sum_{j=1}^{|V_{\times}|} \left[ \sum_{k=0}^{\infty} \lambda_k A_{\times}^k \right]_{ij}, \quad (3.17)$$

where  $A_{\times}^k$  denotes the  $k$ -th power of the adjacency matrix of the direct product graph and  $(\lambda_k)_{k=0}^{\infty}$  is a sequence of non-negative scalars such that  $\lambda_k$  weights the contribution of  $k$ -length walks to the resulting kernel.

The direct product graph kernel can also be applied to graphs without node and/or edge labels by considering all missing attributes to be identical, in which case the conditions  $l_V(v) = l_V(v')$  and/or  $l_E((u, v)) = l_E((u', v'))$  in the definition of the direct product graph would become trivially true. Early attempts to define the sequence of weights  $(\lambda_k)_{k=0}^{\infty}$  focused on computational considerations. One of the most common choices, originally proposed in Gärtner *et al.* (2003), is to set  $\lambda_k := \lambda^k$ . This reduces the number of kernel hyperparameters to just one and guarantees convergence of the infinite series defining the kernel provided that  $|\lambda| < 1/\rho(A_{\times})$ , where  $\rho(A_{\times})$  stands for the spectral norm of the adjacency matrix of the direct product graph. Moreover, in this case, it can be shown that  $\sum_{k=0}^{\infty} \lambda^k A_{\times}^k = (\mathbf{I} - \lambda A_{\times})^{-1}$  and, thus, the kernel can be expressed in closed-form using matrix inversion. Since matrix inversion has complexity  $\mathcal{O}(p^3)$  for a  $p \times p$  matrix and, given graphs  $G, G'$  with  $n$  nodes each, the dimension of  $A_{\times}$  can be  $n^2 \times n^2$  in the worst case, evaluating

$k_{CP}(G, G')$  with  $\lambda_k = \lambda^k$  in this manner results in worst-case computational complexity of the order  $\mathcal{O}(n^6)$ .

	based on	graph type	node type	edge type	complexity
<div>direct product graph kernel</div> <div>Gärtner et al., 2003</div>	 walks	 undirected directed	 labelled	 labelled	$\mathcal{O}(n^6)$

### 3.2.1.2 Marginalized random walk kernel




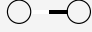
The direct product graph kernel represents a simple instantiation of the  $\mathcal{R}$ -convolution framework, decomposing a graph  $G$  into the set of all its walks  $\mathcal{W}$  and defining the base kernel between walks to be a Dirac kernel on the induced node and edge label sequences. By considering a more general base kernel  $k_{\text{walk}}$ , the direct product graph kernel can be extended to handle continuous node and edge attributes. The *marginalized random walk kernel*, introduced by Kashima *et al.* (2003), can be understood as such a generalization.

DEFINITION 3.12 (Marginalized random walk kernel). Given two graphs  $G$  and  $G'$  the marginalized random walk kernel is obtained as

$$k_{\text{MRW}}(G, G') := \sum_{\omega_1 \in \mathcal{W}_1} \sum_{\omega_2 \in \mathcal{W}_2} k_{\text{walk}}(s(\omega_1), s(\omega_2)) p(\omega_1 | G) p(\omega_2 | G'), \quad (3.18)$$

where  $k_{\text{walk}}$  is a non-negative p.d. kernel between node and edge attribute sequences and  $p(\omega | G)$  is the probability of  $\omega$  being the outcome of a random walk in  $G$ .

Importantly, Kashima *et al.* (2003) shows that, given some restrictions on  $k_{\text{walk}}$ , the marginalized random walk kernel can also be computed by inverting a  $n^2 \times n^2$  matrix for graphs  $G, G'$  with  $n$  nodes each, resulting in the same worst-case computational complexity as the direct product graph kernel, that is,  $\mathcal{O}(n^6)$ .

	based on	graph type	node type	edge type	complexity
<div>marginalized random walk kernel</div> <div>Kashima et al., 2003</div>	 walks	 undirected directed	 labelled	 labelled	$\mathcal{O}(n^6)$

### 3.2.1.3 Fast computation of walk-based kernels

Both the direct product graph kernel and the marginalized random walk kernel can be computed in polynomial time. However, their asymptotic complexity, in the order of  $O(n^6)$  for graphs having  $n$  nodes, severely limits their practical applicability. Vishwanathan *et al.* (2006) introduced an advance in the way graph kernels based on walks are computed, drastically reducing the computational complexity with respect to the size of the graphs to  $O(n^3)$ . Their method applies to a broad family of walk-based kernels, which include the direct product graph kernel as well as the marginalized random walk kernel whenever continuous node and edge attributes are compared using kernels whose feature maps can be computed explicitly. We will refer to the graph kernels that can be derived from this framework simply as *random walk kernels*.

**DEFINITION 3.13** (Random walk kernel). Given two graphs  $G$  and  $G'$ , the random walk kernel is calculated as

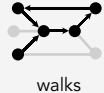
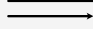

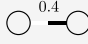
$$k_{RW}(G, G') := q_x^\top \left[ \sum_{k=0}^{\infty} \lambda_k W_x^k \right] p_x, \quad (3.19)$$

where (i)  $W_x := W_1 \otimes W_2$ , with  $W_1$  and  $W_2$  being matrices whose entries are elements of a RKHS and have the same sparsity pattern as the adjacency matrices of  $G$  and  $G'$ , respectively; (ii)  $p_x$  and  $q_x$  represent the initial and stopping probability distributions of the random walk and (iii)  $(\lambda_k)_{k=0}^{\infty}$  is a sequence of non-negative scalars such that  $\lambda_k$  weights the contribution of  $k$ -length walks to the resulting kernel.

As previously discussed in Section 3.2.1.1, choosing exponentially-decaying weights  $\lambda_k = \lambda^k$  leads to  $k_{RW}(G, G') = q_x^\top (\mathbf{I} - \lambda W_x)^{-1} p_x$ . Efficiently evaluating the random walk kernel therefore hinges on exploiting the Kronecker structure of  $W_x$  to obtain  $(\mathbf{I} - \lambda W_x)^{-1} p_x$  with a series of matrix-vector products of the form  $W_x r$  using techniques such as fixed-point iterations or conjugate gradient methods (Vishwanathan *et al.*, 2006). As a result, if the entries in  $W_1$  and  $W_2$  are elements of a RKHS whose feature map can be represented by a  $d$ -dimensional vector, the computational complexity of the random walk kernel is  $O(n^3 d)$  as opposed to  $O(n^6)$  for a naive implementation.

Recent extensions of random walk kernels include RetGK, a kernel based on the return probabilities of random walks (Zhang *et al.*, 2018). This kernel is based on a new descriptor of random walks that incorporates their return probabilities. Next to being invariant under graph isomorphism, this descriptor also permits treating attributed and non-attributed graphs within the same framework. This is achieved by *enriching* the obtained walk representations, which do not require attribute information to be available, with additional information about node attributes, for instance. While RetGK exhibits

improved expressivity and thus improved predictive performance, its computation has a marginally higher computational complexity of  $O(n^3 + (k+1)n^2) = O(n^3 + kn^2)$  for random walks of at most  $k$  steps.

	based on	graph type	node type	edge type	complexity
random walk kernel <small>Vishwanathan et al., 2006</small>	 walks	 undirected directed	 labelled	 labelled attributed	$O(n^3)$

### 3.2.1.4 Continuous-time quantum walk kernel

Recent work has sought inspiration in the formalisms of quantum mechanics to make use of an alternative type of random walk in a graph such that, at any given time, the state of the walk does not correspond to a single vertex but rather to an arbitrary superposition of basis states. Quantum walks have several properties that are not present in “classical” random walks, such as reversibility and non-ergodicity (Bai *et al.*, 2013). For this subsection, we assume that we are dealing with unlabelled, undirected graphs. Given such a graph  $G = (V, E)$ , we first define the evolution of a general quantum walk in close analogy to random walks.

**DEFINITION 3.14** (Continuous-time quantum walk). Let  $n := |V|$  be the number of vertices in the graph and  $U := \{u_1, \dots, u_n\}$  be an orthonormal basis of a complex Hilbert space  $\mathcal{H}$ . Given a set of time-varying amplitude vectors  $\alpha(u_j, t) \in \mathbb{C}$ , the state of a *continuous-time quantum walk* is defined as

$$\psi(t) = \sum_{j=1}^n \alpha(u_j, t) u_j. \quad (3.20)$$

The amplitude vectors can be defined using the Laplacian matrix  $L$  of  $G$ , leading to

$$\psi(t) = \exp(-iLt)\psi(0), \quad (3.21)$$

which can be seen as a solution of the Schrödinger equation for this graph (Bai *et al.*, 2013). The initial state  $\psi(0)$  in the previous equation is defined using the *degree* of a given vertex, *i.e.*

$$\psi(0) := \sum_{j=1}^n \frac{d_{u_j}}{\sqrt{\sum_{k=1}^n d_{u_k}^2}} u_j, \quad (3.22)$$

which is equal to the steady state of a classical random walk on the graph.

To obtain a kernel for comparing different quantum walks, a notion of *entropy* is introduced (Bai *et al.*, 2013). The underlying idea is to define a density matrix over the individual states of the graph. This is achieved by rephrasing the continuous formulation from above into a discrete form (as proposed by Bai *et al.* (2013), we use the same terminology as before to make the link clearer). Specifically, we define a maximum number of time steps  $s \in \mathbb{N}$  and using a uniform probability  $p := 1/s$  for assuming each of the states  $\psi(1), \dots, \psi(s)$ . This leads to a *density operator*  $\rho_G$  of the graph  $G$  as

$$\rho_G = \sum_{t=1}^s p \cdot \psi(t)\psi(t)^\top, \quad (3.23)$$

*i.e.* the weighted sum of an *outer product* of two state vectors. Finally, the *von Neumann entropy* of this density operator is defined as

$$H_N(\rho_G) := -\text{tr}(\rho_G \log \rho_G), \quad (3.24)$$

where  $\text{tr}$  refers to the trace of the resulting matrix. In practice, Bai *et al.* (2013) note that the von Neumann entropy is calculated from a spectral decomposition of the density matrix, but for notational simplicity, we refrain from doing so. This leads to the definition of the quantum Jensen–Shannon kernel for graphs.

**DEFINITION 3.15 (Quantum Jensen–Shannon kernel).** Let  $G$  and  $G'$  be two undirected graphs, and  $s \in \mathbb{N}$  be the maximum number of time steps. With the respective density operators  $\rho_G$  and  $\rho_{G'}$ , the *Jensen–Shannon divergence* between  $G$  and  $G'$  is defined as

$$\text{JSD}(G, G') := H_N\left(\frac{\rho_G + \rho_{G'}}{2}\right) - \frac{1}{2}H_N(\rho_G) - \frac{1}{2}H_N(\rho_{G'}), \quad (3.25)$$

where  $H_N(\cdot)$  refers to the von Neumann entropy as defined in Equation 3.24. From this, the *quantum Jensen–Shannon kernel* is defined by an appropriately-scaled exponential expression, *i.e.*

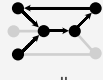


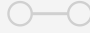
$$\text{k}_{\text{QS}}(G, G') := \exp(-\lambda \text{JSD}(G, G')), \quad (3.26)$$

where  $0 < \lambda < 1$  is a decay factor that ensures that large values do not tend to dominate the kernel value.

The computational complexity of the kernel is dominated by the calculation of the eigendecomposition of the Laplacian, which has a complexity of the order  $\mathcal{O}(n^3)$ , where  $n$  is the maximum number of vertices in the two graphs for which the kernel is calculated.

Several types or variants of this kernel exist (Bai *et al.*, 2014; Bai *et al.*, 2015). For example, an extension (Bai *et al.*, 2015) employs an additional matching or assignment procedure (see

also Section 3.3.2.2 for more details). In a more general setting, quantum walks based on graphs have also demonstrated favourable performance in other application domains, such as edge detection in images (Curado *et al.*, 2015).

	based on	graph type	node type	edge type	complexity
quantum walk kernel <small>Bai et al., 2013</small>	 walks	 undirected	 none	 none	$O(n^3)$

### 3.2.2 Graph kernels based on iterative label refinement

An important advance in the field of graph kernels occurred in 2009, when (Shervashidze and Borgwardt, 2009; Hido and Kashima, 2009) concurrently introduced two graph kernels based on the same underlying idea. Most previously existing approaches defined graph similarity directly in terms of pairwise comparisons between a large number of graph substructures. Instead, these methods proposed to first substitute the original node attributes in each graph by a new set of node attributes that also incorporate topological information about the  $k$ -hop neighbourhood of each node. Then, one can subsequently apply a simple graph kernel based only on nodes to the modified graphs to obtain a computationally efficient graph kernel that nonetheless can make use of fine-grained information about graph topology.

More precisely, these approaches recursively *refine the node labels* by applying local transformations of the form

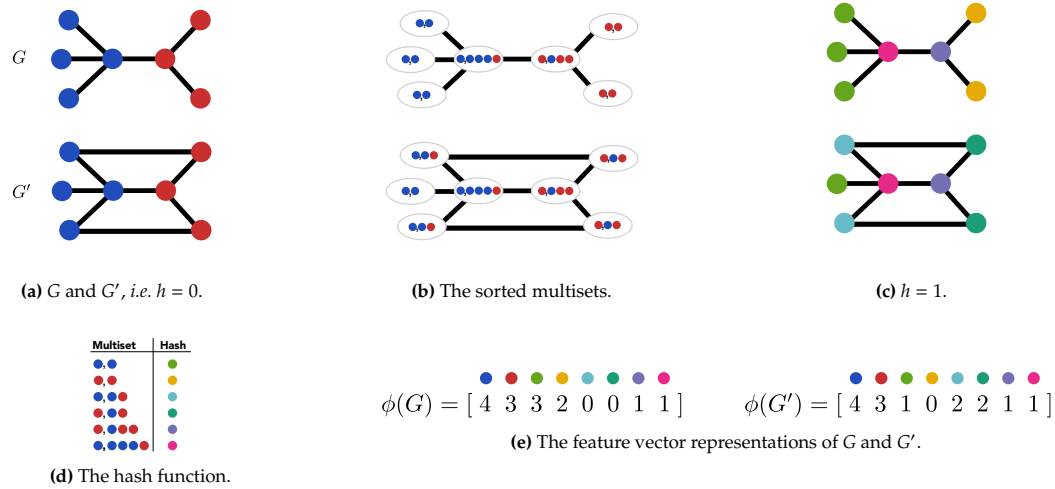
$$l_v^{(\text{new})}(v) = f\left(l_v^{(\text{old})}(v), g\left(\{l_{v'}^{(\text{old})}(v') \mid v' \in \mathcal{N}(v)\}\right)\right),$$

where  $\mathcal{N}(v)$  denotes the set of nodes adjacent to  $v$ ,  $g$  a permutation-invariant function and  $f$  an arbitrary function. As we shall see, these operations can be defined to be very efficient, such that computing  $l_v^{(\text{new})}(v)$  for all nodes in a graph can be done in only  $O(m)$  time for a graph with  $m$  edges. Applying these transformations in succession results in a sequence of modified graphs, each of which has node attributes that aggregate information about increasingly large  $k$ -hop neighbourhoods. This general idea can give rise to a multitude of distinct graph kernels, depending on (i) the specific form of the functions  $f$  and  $g$ ; (ii) which kernels are used to compare the resulting modified graphs and (iii) how the graph similarities at multiple scales ( $k$ -hop neighbourhoods), captured by the different modified graphs obtained during the sequence of label refinement operations, are aggregated into a single similarity value.

The success of this family of methods has been three-fold. Firstly, they lead to extremely efficient graph kernels, often orders of magnitude faster than previously existing methods for sufficiently large graphs. Secondly, as will be seen in Chapter 4, approaches based on such iterative label refinement schemes achieve state-of-the-art performance in many different supervised learning tasks, often outperforming kernels based on other substructures by a significant margin. Finally, as will be discussed in Chapter 5, these graph kernels have strong ties to more recent approaches, being *de facto* the precursors of most modern *graph neural networks*.

In this section, we will study this family of graph kernels by first introducing the two original methods, as proposed by Shervashidze and Borgwardt (2009) and Hido and Kashima (2009). Next, we will describe follow-up approaches that aim to further speed-up these kernels as well as to extend them to handle continuous node and edge attributes.

### 3.2.2.1 The Weisfeiler–Lehman kernel framework



**Figure 3.8:** An example of the Weisfeiler–Lehman kernel where  $h = 1$ . The nodes in graphs  $G$  and  $G'$  are relabeled using a hash function of the multiset of the given node’s label and the sorted labels of its neighbours. The expanded alphabet from this hashing procedure  $\Sigma_{WL}^{(1)}$  gives rise to a feature vector representation of the graphs which counts the instances of each label. We obtain our kernel value as  $k_{WL}^{(1)}(G, G') = \langle \phi(G), \phi(G') \rangle_{\mathcal{H}} = 30$ .

The first of the two original approaches that pioneered the use of iterative label refinement operations to derive graph kernels (Shervashidze and Borgwardt, 2009; Shervashidze *et al.*, 2011) was inspired by the Weisfeiler–Lehman test for isomorphism (Weisfeiler and Lehman, 1968), which gave it its name. A central component of this test is the concept

of a *multiset*. Informally put, a multiset is a generalization of a set that permits the same element to be added multiple times. By this definition, a set can be considered as a multiset, in which all elements have a count of 1. For a formal definition, please see Blizard (1988). Briefly put, the Weisfeiler–Lehman test now uses two undirected graphs  $G = (V, E)$  and  $G' = (V', E')$  with a set of node labels from the same alphabet and repeatedly augments node labels by the sorted multiset of labels of the neighbours of a vertex. The augmented label is subsequently compressed, and the process is repeated until the label multisets of the two graphs are different (indicating that the graphs cannot be isomorphic), or until the maximum number of iterations  $h_{\max} := \max(|V|, |V'|)$  has been reached. This procedure is guaranteed to produce identical sequences for isomorphic graphs. While it remains possible for two non-isomorphic graphs to also have identical sequences, if the generated label sequences are equal, the two graphs are isomorphic with high probability (Babai and Kucera, 1979).

It was observed by Shervashidze and Borgwardt (2009) that the Weisfeiler–Lehman test can be seen to give rise to an iteration that creates subsequent refinements of vertex labels  $l_V(v)_{\text{WL}}^{(h)}$  for a vertex  $v$  and  $h \in \mathbb{N}$ . The base case for  $h = 0$  of this iteration uses the original labels of the graph, so that  $l_V(v)_{\text{WL}}^{(0)} := l_V(v)$ . For  $h > 0$ , each vertex is assigned a new label that uniquely identifies the tuple formed by the current Weisfeiler–Lehman label of the vertex,  $l_V(v)_{\text{WL}}^{(h)}$ , and the multiset of the current Weisfeiler–Lehman labels of its neighbours,  $\{l_V(v')_{\text{WL}}^{(h)} \mid v' \in N(v)\}$ , i.e. the updates take the form

$$l_V(v)_{\text{WL}}^{(h+1)} := f\left(\left(l_V(v)_{\text{WL}}^{(h)}, \{l_V(v')_{\text{WL}}^{(h)} \mid v' \in N(v)\}\right)\right), \quad (3.27)$$

where  $f(\cdot)$  is a hashing function that compresses the tuple into a *single* integer-valued label. Crucially, as we shall see, what sets this method apart from the approach concurrently proposed by Hido and Kashima (2009) is the use of *perfect hashing* for  $f(\cdot)$ , following the Weisfeiler–Lehman test for graph isomorphism. This leads to a highly expressive representation of topological information, able to differentiate neighbourhoods differing by a single node. To accomplish this, Shervashidze *et al.* (2011) proposed an approach based on Counting Sort and Radix Sort, that manages to keep the time complexity linear with respect to the number of edges in the graph. Applying this relabelling scheme recursively gives rise to a sequence of *Weisfeiler–Lehman graphs*.

**DEFINITION 3.16** (Weisfeiler–Lehman sequence). Given an undirected graph  $G = (V, E)$  with a label function  $l_V(\cdot)$  and  $h \in \mathbb{N}$ , the Weisfeiler–Lehman relabelling operation as described in Eq. 3.27 results in a sequence of graphs  $(G_0, G_1, \dots, G_h)$ , where

$$G_h := \left(V, E, l_V(\cdot)_{\text{WL}}^{(h)}\right) \quad (3.28)$$



and each graph only differs in terms of its labels. This sequence is referred to as the *Weisfeiler–Lehman sequence*.

The sequence of graphs can be seen as a multiscale description of its neighbourhoods. By comparing them with a suitable kernel function, it is possible to obtain a kernel for the graph itself (Shervashidze *et al.*, 2011).

**DEFINITION 3.17** (Weisfeiler–Lehman kernel). Let  $G$  and  $G'$  be two undirected graphs with node labels defined over the same alphabet. Given a well-defined base kernel  $\kappa$  for graphs and  $h \in \mathbb{N}$ , the *Weisfeiler–Lehman kernel* is defined as

$$k_{\text{WL}}^{(h)}(G, G') := \sum_{i=0}^h \kappa(G_i, G'_i), \quad (3.29)$$

where  $G_i$  and  $G'_i$  refer to the  $i$ th graph of the Weisfeiler–Lehman sequences of  $G$  and  $G'$ , respectively.

This framework gives rise to a multitude of kernels (Shervashidze *et al.*, 2011); we only discuss the *subtree kernel* here, which makes direct use of the label sequence. Letting  $\Sigma_{\text{WL}}^{(h)} := \{\sigma_1^{(h)}, \sigma_2^{(h)}, \dots\}$  refer to the alphabet of *all* compressed labels in step  $h$  of the Weisfeiler–Lehman relabelling operation, the subtree kernel uses a *count* function  $c(\cdot)$  such that  $c(G, \sigma_i^{(h)})$  is the number of occurrences of the label  $\sigma_i^{(h)}$  in  $G$ . Thus, a graph  $G$  is assigned a feature vector

$$\phi(G) = \left( c(G, \sigma_1^{(0)}), \dots, c(G, \sigma_i^{(1)}), \dots, c(G, \sigma_j^{(h)}), \dots \right) \quad (3.30)$$


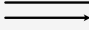

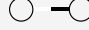
for a total of  $h$  steps of the Weisfeiler–Lehman iteration, and the *Weisfeiler–Lehman subtree kernel* is defined as the *inner product* of these features vectors, *i.e.*

$$\kappa_{\text{subtree}}(G, G') := \langle \phi(G), \phi(G') \rangle, \quad (3.31)$$

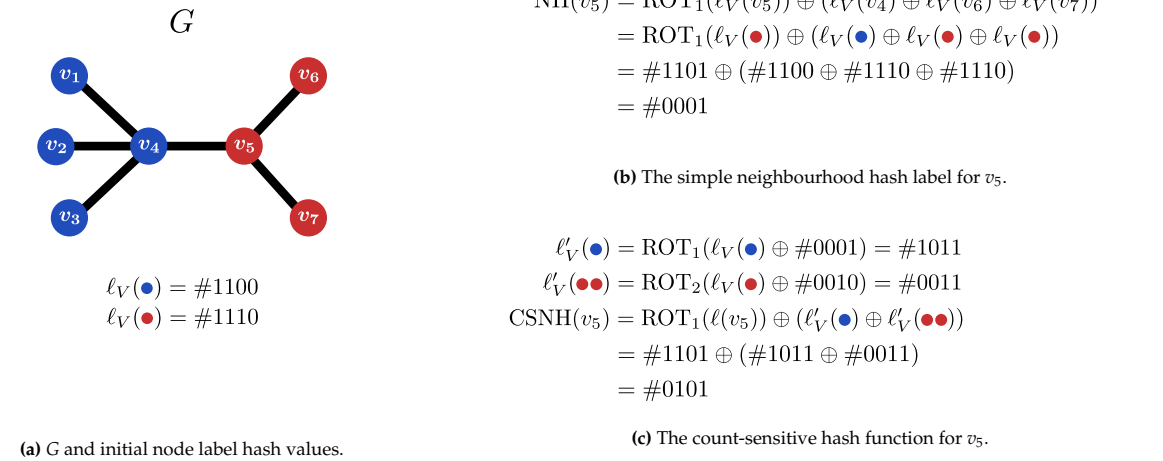
where  $G$  and  $G'$  are undirected labelled graphs as described above. This sort of propagation scheme is simple but extremely powerful, as it automatically makes it possible to represent the graph at coarse scales (small values of  $h$ ) or fine scales (large values of  $h$ ). Multiple variants of this kernel exist. For instance, it is simple to extend this to incorporate edge labels as well as node labels by using the triple of  $(l_V(v), l_V(v_i), l_E((v, v_i)))$  to represent a given neighbour  $v_i$  of node  $v$ , rather than using only  $l_V(v_i)$ , as is done in the base case implementation of the kernel. Nevertheless, the aforementioned subtree kernel is the most common one, and is depicted in Figure 3.8.

The complexity of the Weisfeiler–Lehman kernel computation depends on the selected base kernel. For the subtree kernel, Shervashidze *et al.* (2011) show that, given a perfect

hashing function, the computation of a full kernel matrix for  $N$  graphs and  $h$  steps of the Weisfeiler–Lehman iteration has a complexity of  $O(Nhm + N^2hn)$ , where  $n$  is the maximum number of vertices of a graph and  $m$  is the maximum number of edges. More generally, the complexity of  $h$  Weisfeiler–Lehman relabelling iterations (not accounting for any kernel calculations) is  $O(hm)$ . Compared to previously existing, popular graph kernels, such as the random walk kernel, the shortest-paths kernel or the graphlet kernel, the availability of an approach whose runtime scales only linearly with the number of nodes and edges while simultaneously achieving state-of-the-art performance in a variety of statistical learning tasks constituted an important step forward in the field.

	based on	graph type	node type	edge type	complexity
Weisfeiler-Lehman kernel <small>Shervashidze and Borgwardt, 2009</small>	 label refinement	 undirected directed	 labelled	 labelled	$O(hm)$

### 3.2.2.2 Neighbourhood hash kernel



**Figure 3.9:** An example relabeling of the node  $v_5$  in a graph  $G$  with initial node label function (a), with nodes indexed as  $v_1, \dots, v_7$ , using the simple neighbourhood hash function (b) and the count-sensitive hash function (c). After each node has been hashed, the vector representation is a count vector of each unique hash label. The neighbourhood hash kernel is then calculated according to Eq. 3.36.

In parallel, Hido and Kashima (2009) developed the *neighbourhood hash kernel* with the same goal: to obtain a highly computationally efficient graph kernel that accounts

for information about the graph topology and achieves good predictive performance in real-world problems.

Conceptually, the neighbourhood hash kernel, shown in Figure 3.9, and the Weisfeiler–Lehman framework converged to similar ideas. Both are based on iteratively refining node labels, combining information about the current node label of a vertex and those of its neighbours, to create a sequence of graphs which can then be compared by means of simple criteria. Moreover, both approaches use hashing-based schemes to implement this refinement step. However, while the Weisfeiler–Lehman framework relies on perfect hashing, Hido and Kashima (2009) instead use simpler hashing techniques based on binary arithmetic. While both approaches have the same asymptotic scaling with respect to the size of the graphs, the neighbourhood hash kernel has better constant factors thanks to its simpler hashing function, being slightly faster in practice, and is also more memory-efficient. However, this comes at the cost of the possibility of having accidental hashing *collisions*, which can limit the expressivity of the resulting feature map if nodes that are rather different get hashed to the same value. Notice that collisions are not problematic per se. In fact, the primary lesson of the Weisfeiler–Lehman iteration is that graph isomorphism is a perspective that is too restrictive—for most applications, graph *similarity* is much more relevant. Collisions that result in similar graphs being hashed together are therefore less problematic than collisions that result in highly dissimilar graphs being assigned the same hash.

The neighbourhood hash kernel assumes that node labels can be embedded into binary strings (“bit arrays”) of a pre-determined length  $s$ . Thus, for the remainder of this section, we assume that each node label  $l$  is represented by a sequence of bits  $l = \{b_1, b_2, \dots, b_s\}$ , where  $b_i \in \{0, 1\}$ . Shorter strings (small values for  $s$ ) will lead to faster hashing but increase the probability of accidental collisions occurring. The hashing schemes in Hido and Kashima (2009) are based on this binary representation of node labels, making use of XOR operations and bit rotations (also known as *shifts*).

The XOR operation between two bits  $b_i, b_j$  is defined as

$$b_i \oplus b_j = \begin{cases} 1 & \text{if } b_i \neq b_j \\ 0 & \text{otherwise} \end{cases} \quad (3.32)$$

and can be extended to bit strings of the same lengths. A key aspect of the XOR operation is that it is associative and commutative, making the output permutation invariant. Consequently, it is a suitable function to hash multisets of labels of neighbouring nodes.

The bit rotation function circularly shifts all bits by a pre-defined amount, *i.e.*

$$\text{ROT}_k(b_1, \dots, b_l) := \{b_{k+1}, b_{k+2}, \dots, b_l, b_1, \dots, b_k\}, \quad (3.33)$$

which does not change the size of the bit string. In this context, bit-rotations are useful to treat certain elements *asymmetrically* during the hashing process. This allows, for example, hashing the tuple formed by the current node label of a vertex and the multiset of labels of neighbouring nodes.

Building on these ideas, the first of the hashing schemes in Hido and Kashima (2009) is defined as follows.

**DEFINITION 3.18** (Simple neighbourhood hash function). Given a vertex  $v \in V$  and its neighbours  $v_1, \dots, v_k$ , the *simple neighbourhood* hash is calculated as

$$\text{NH}(v) := \text{ROT}_1(l_V(v)) \oplus (l_V(v_1) \oplus \dots \oplus l_V(v_k)). \quad (3.34)$$

The label of the initial vertex is shifted by one bit in order to make it distinct from the other vertices. This hash function can now be applied multiple times, and each iteration will thus use information from higher-order neighbourhoods, since every vertex receives propagated information from its direct neighbours.

Hido and Kashima (2009) note that this hashing scheme is severely limited in its ability to handle repeated occurrences of the same node label in the multisets. Indeed, the XOR operation can be seen to compute the bitwise *parity* of the bit strings being hashed. Thus, the only information retained about the number of occurrences of each node label in the multisets is whether the count is even or odd. To alleviate this limitation, Hido and Kashima (2009) proposed a second hashing scheme that makes explicit use of the label counts using bit rotations.

**DEFINITION 3.19** (Count-sensitive neighbourhood hash function). If a specific label  $l_V(v_j)$  occurs  $l$  times in the neighbourhood, let  $l_V'(v_j) := \text{ROT}_l(l_V(v_j) \oplus l)$  denote its transformed version: by shifting a label by  $l$  bits after calculating its XOR, hash values are unique and only depend on the number of occurrences of a label. This leads to the *count-sensitive neighbourhood hash function*

$$\text{CSNH}(v) := \text{ROT}_1(l_V(v)) \oplus (l_V'(v_1) \oplus \dots \oplus l_V'(v_k)). \quad (3.35)$$

The *count-sensitive neighbourhood hash function*, while still prone to collisions, manages to avoid some of the main pitfalls of the previous hashing scheme. However, to obtain the label counts in each multiset, a sorting operation must be applied, which reduces the computational advantage with respect to the Weisfeiler–Lehman framework.

Based on either of the two hash functions, the neighbourhood hash kernel can now be defined as the overlap between the label sets of two graphs.

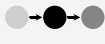
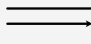

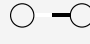
**DEFINITION 3.20** (Neighbourhood hash kernel). Given two labelled graphs  $G$  and  $G'$ , select a hash function as described above and calculate its hashed labels according to Eq. 3.34 or Eq. 3.35 above. This results in two sets of labels  $\mathcal{L}$  and  $\mathcal{L}'$ . The *neighbourhood hash kernel* is the *Tanimoto coefficient* (Tan et al., 2019, Chapter 2) of  $\mathcal{L}$  and  $\mathcal{L}'$ , i.e.

$$k_{\text{NH}}(G, G') := \frac{c}{n + n' - c}, \quad (3.36)$$

where  $c$  is the number of matching labels between  $\mathcal{L}$  and  $\mathcal{L}'$ , and  $n, n'$  denotes the number of vertices in  $G$  and  $G'$ , respectively.

Ignoring the fact that the quantities involved are bit strings, the previous equation can also be seen as an instance of the Weisfeiler–Lehman framework, which takes the linear kernel between two count vectors instead of an overlap measure.

The asymptotic complexity of the neighbourhood hash kernel with respect to the size of the graphs is comparable to that of the Weisfeiler–Lehman framework. However, as discussed above, it offers certain advantages in terms of runtime; in the best case, hash function calculations and comparisons can be performed in a single CPU instruction, respectively.

	based on	graph type	node type	edge type	complexity
neighbourhood hash kernel <small>Hido and Kashima, 2009</small>	 label refinement	 undirected directed	 labelled	 labelled	$\mathcal{O}(hm)$

### 3.2.2.3 Fast Neighbourhood Subgraph Pairwise Distance Kernel

Costa and De Grave (2010) present another method that also uses a node's neighbourhood as a mechanism to propagate information to a node. In graphs without edge weights, this neighbourhood corresponds to the  $k$ -hop neighbourhood of a node  $v$  defined in Chapter 2, where  $k$  is now referred to as the radius  $r$ , i.e.  $N^{(r)}(v)$ , and accordingly includes any node  $u$  that is reachable from  $v$  in at most  $r$  hops. In weighted graphs, we can extend this definition using the sum of edge weights to define the shortest distance to  $v$ , and in both cases, require that the distance  $d$  between the two nodes is less than or equal to the radius  $r$ . For a root node  $v$  in a graph  $G = (V, E)$ , with a given radius  $r$ , we can therefore generalise the definition of its radius  $r$  neighbourhood  $N^{(r)}(v)$  as  $\{u \in V \mid d(u, v) \leq r\}$ . The subgraph we will use is the corresponding induced subgraph of  $G$ , denoted by  $G_v^{(r)}$ .

The neighbourhood subgraph pairwise distance kernel does a pairwise comparison using pairs of subgraphs in each graph, where the two root nodes  $v_1$  and  $v_2$  have a

shortest path distance to one another less than or equal to  $d$ . It then evaluates this for increasing values of  $r$  and  $d$ . While the original formulation wants to test the subgraphs for isomorphism, we have mentioned this is not yet computationally tractable, and so the authors instead settle for a proxy test.

**DEFINITION 3.21** (Neighbourhood subgraph pairwise distance kernels). Let  $G = (V, E)$  and  $G' = (V', E')$  be two graphs with node and edge labels defined on alphabets  $\Sigma_V$  and  $\Sigma_E$  and labelling functions  $l_V$  and  $l_E$  respectively. A subgraph of root node  $v$  of radius  $r$ ,  $G_v^{(r)}$  is represented as the lexicographically sorted list of updated edge labels in the subgraph,  $l_E^{(r)}(e_{ij})$ , which contains the updated node labels incident to the edge, as well as its original edge label. That is,

$$l_E^{(r)}(e_{ij}) = (l_V^{(r)}(i), l_V^{(r)}(j), l_E(e_{ij})), \quad (3.37)$$

and where the updated node labels are again a sorted representation of

$$l_V^{(r)}(i) = ((d(i, u), l_V(u)) \forall u \in V(G_v^{(r)}), d(i, v)) \quad (3.38)$$

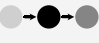
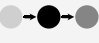


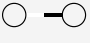
*i.e.* the distance of node  $i$  to all other nodes in the subgraph combined with the label of the other node, and the distance of  $i$  to the root node  $v$ . This representation is then hashed to an integer to be used in the Dirac delta kernel. For a given radius  $r$ , the neighbourhood subgraph pairwise distance kernel is calculated as

$$k_{\text{NSPD}}(G, G') = \sum_r \sum_d \kappa_{r,d}(G, G'), \quad (3.39)$$

where  $\kappa_{r,d}(G, G')$  assesses the similarity of the pairs of subgraphs induced by pairs of root nodes whose distance is less than or equal to  $d$ . If we call  $\mathfrak{R}$  the set of tuples of root nodes  $(v_1, v_2) \in V$  where  $d(v_1, v_2) \leq d$ , and  $\mathfrak{R}'$  is the set of tuples  $(v'_1, v'_2) \in V'$  where  $d(v'_1, v'_2) \leq d$ , and  $k_\delta$  is the Dirac delta kernel, this leads to the final formulation of

$$\kappa_{r,d}(G, G') = \sum_{(v_1, v_2) \in \mathfrak{R}} \sum_{(v'_1, v'_2) \in \mathfrak{R}'} k_\delta(G_{v_1}^{(r)}, G_{v'_1}^{(r)}) k_\delta(G_{v_2}^{(r)}, G_{v'_2}^{(r)}). \quad (3.40)$$

The complexity of the neighbourhood subgraph pairwise distance kernel is determined primarily from the repeated process of relabelling the nodes and edges in the induced subgraphs, resulting in an overall complexity of  $O(nm_h m_h \log(m_h))$ , where  $n$  is the maximum number of nodes in a graph,  $n_h$  and  $m_h$  are the maximum number of nodes and edges respectively in the induced subgraphs from the root nodes. Since  $d$  and  $r$  are typically small, this reduces to being linear in the number of nodes in a graph.

neighbourhood subgraph pairwise distance kernel	based on	graph type	node type	edge type	complexity
 Costa and De Grave, 2010	 label refinement	 undirected	 labelled	 labelled	$\mathcal{O}(nm_h m_h \log(m_h))$

### 3.2.2.4 Hadamard code kernel

The two hashing schemes proposed by Hido and Kashima (2009) incur a trade-off between computational efficiency and expressivity. The simple neighbourhood hash function is highly efficient, but can also result in accidental collisions. In contrast, the count-sensitive neighbourhood hash function circumvents some of the most obvious cases of collisions in the previous scheme, such as those due to node label duplications, but at the price of requiring a sorting step that might slow down the resulting algorithm.

Motivated by this observation, Kataoka and Inokuchi (2016) proposed a different hashing scheme, aiming to keep the computational efficiency of the simple neighbourhood hash function while being more robust to collisions. The key element of their construct are Hadamard matrices, which we introduce next.

**DEFINITION 3.22** (Hadamard matrix and Hadamard code). A square matrix  $H$  of dimension  $n$  whose entries are from  $\{-1, 1\}$  is called a *Hadamard matrix* if its rows are mutually orthogonal. Hence, given  $i \neq j$ , for rows  $h_i$  and  $h_j$  we have  $\langle h_i, h_j \rangle = 0$ , where  $\langle \cdot, \cdot \rangle$  denotes the usual real-valued dot product. Any row  $h_i$  of  $H$  is called a *Hadamard codeword* (there is also the notion of *Hadamard codebook*, which refers to the union of rows of  $H$  and  $-H$ , but we do not require it here).

Hadamard codes can be shown to have interesting mathematical properties, such as the ability to self-correct; we refer the reader to Arora and Barak (2009, Chapter 17.5) for more details.

The key idea behind the Hadamard code kernel is to represent each categorical node label in a finite alphabet  $\Sigma_V$  by a different Hadamard codeword rather than a bit string. Since distinct codewords are mutually orthogonal, this can be understood as an alternative feature map for a Dirac kernel defined on the set of node labels. However, compared to the more commonly used embeddings given by the canonical basis vectors of  $\mathbb{R}^{|\Sigma_V|}$ , Hadamard codewords have favourable computational properties when many such embeddings are to be summed together. In particular, since entries of Hadamard codewords take values  $-1$  or  $+1$  with equal probability, the expected value of most entries of a sum of Hadamard codewords is 0. Kataoka and Inokuchi (2016) argue that, due to this property, a small number of bits should suffice to represent them faithfully. In contrast, if one were to use

the canonical basis instead, entries would explode as the number of embeddings being summed grows, requiring many bits to be represented accurately. Building on this idea, the relabelling step of the Hadamard code kernel is defined as a simple aggregation of individual Hadamard codewords.

**DEFINITION 3.23** (Hadamard code relabelling). Let  $G = (V, E)$  be an undirected graph with a set of vertex labels from a common label alphabet  $\Sigma_V$ . Let  $s := 2^{\lceil \log_2 |\Sigma_V| \rceil}$  and  $H$  be a Hadamard matrix of dimension  $s$ , such that there is at least one different codeword in  $H$  per label in  $\Sigma_V$ . For a vertex  $v$  with original label  $l_V(v) = \sigma_i$ , set its initial Hadamard label  $l_V(v)_H^{(0)}$  to be  $h_i$ , the  $i$ th row of  $H$ . Given  $h \in \mathbb{N}$ , the Hadamard code label of  $v$  at stage  $h + 1$  is calculated recursively as

$$l_V(v)_H^{(h+1)} = l_V(v)_H^{(h)} + \sum_{v' \in N(v)} l_V(v')_H^{(h)}, \quad (3.41)$$

where  $N(v)$  are the vertices adjacent to  $v$ .

Due to Hadamard codewords being mutually orthogonal,  $l_V(v)_H^{(h)}$  can be understood as an unnormalised, rotated histogram of node label counts. Indeed, the dot product of  $l_V(v)_H^{(h)}$  with  $h_i$  yields a scaled count of occurrences of node label  $\sigma_i$  in a  $k$ -hop neighbourhood around  $v$ , whose size depends on  $h$ . However, as previously mentioned, the entries of these rotated histograms fluctuate symmetrically around zero, rather than growing monotonically as  $h$  increases, hence requiring fewer bits to store. In this way, as noted by Kataoka and Inokuchi (2016), the Hadamard relabelling step bears some resemblance to the Weisfeiler–Lehman relabelling step, but has some key differences, such as not treating the central vertex of each  $k$ -hop neighbourhood asymmetrically when computing the new node labels. The Hadamard code kernel is finally defined as an iterative summation of Dirac delta kernels on the sequence of relabelled graphs.

**DEFINITION 3.24** (Hadamard code kernel). Given two graphs  $G = (V, E)$  and  $G' = (V', E')$  with node labels that are defined over the same node label alphabet  $\Sigma_V$  and  $h \in \mathbb{N}$ , the Hadamard code base kernel at step  $h$  is defined as

$$k_H^{(h)}(G, G') := \sum_{v \in V} \sum_{v' \in V'} \delta(l_V(v)_H^{(h)}, l_{V'}(v')_H^{(h)}), \quad (3.42)$$

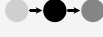
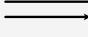

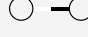
where  $l_V(v)_H^{(h)}$  refers to Hadamard code label of  $v$  at stage  $h$  according to Definition 3.23, and  $\delta$  denotes a Dirac delta kernel. Building on this, the *Hadamard code kernel* is defined as

$$k_H(G, G') := \sum_h^{h_{\max}} k_H^{(h)}(G, G'), \quad (3.43)$$



where  $h_{\max}$  denotes the maximum number of iterations of the relabelling step.

In terms of computational efficiency, Kataoka and Inokuchi (2016) exploit that the Hadamard codewords can be stored as bit strings of a fixed length. While collisions, as for the neighbourhood hash kernel, still occur with a non-zero probability, the kernel is able to perform well in practice without requiring any sorting operations. Hence, even though its asymptotic computational complexity is the same as that of the neighbourhood hash kernel and the Weisfeiler-Lehman framework, it is faster than the version of the neighbourhood hash kernel based on the count-sensitive neighbourhood hash function while matching its predictive performance.

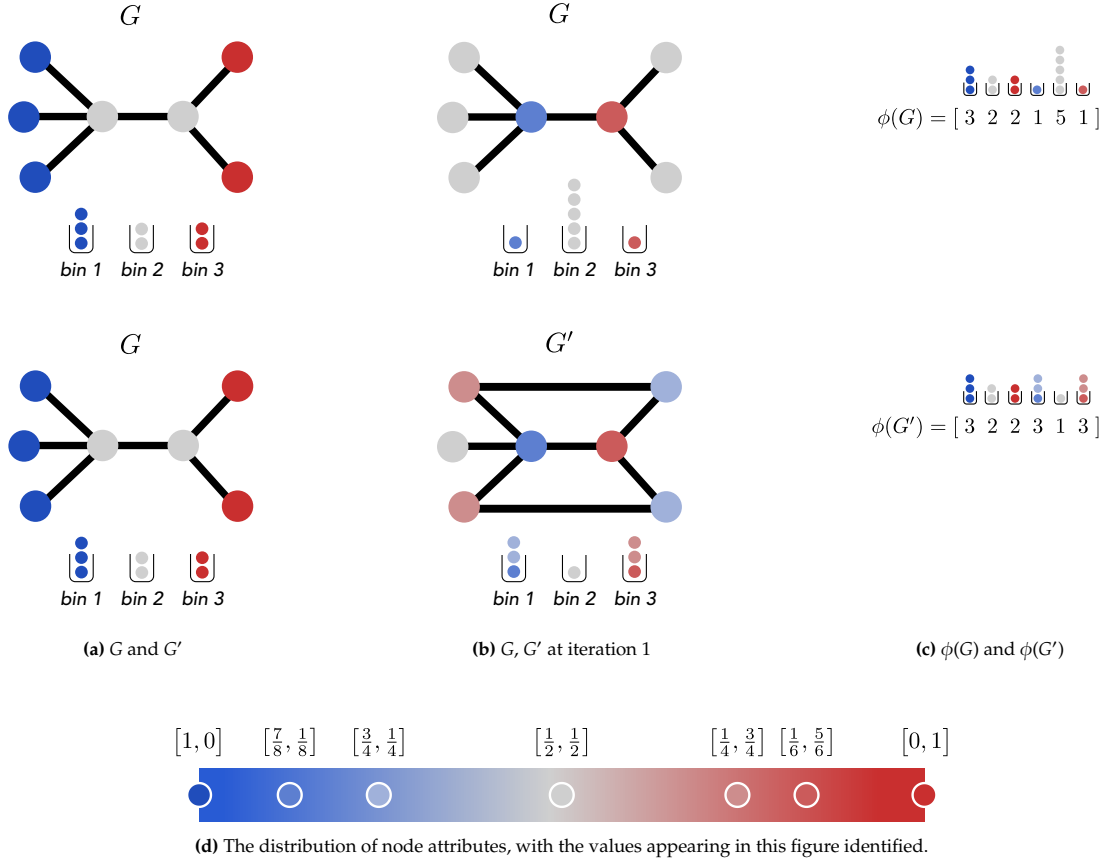
	based on	graph type	node type	edge type	complexity
Hadamard code kernel <small>Kataoka and Inokuchi, 2016</small>	 label refinement	 undirected directed	 labelled	 labelled	$\mathcal{O}(hm)$

### 3.2.2.5 Propagation kernels

An important limitation of many of the first graph kernels based on iterative label refinement is their reliance on categorical node and/or edge labels. Indeed, all approaches described so far exploit the fact that node labels are discrete to construct efficient hashing schemes that lie at the core of their respective relabelling steps. Motivated by this, Neumann *et al.* (2016) introduced the propagation kernels, a *family* of graph kernels that, much like the Weisfeiler-Lehman framework, are flexible with respect to the choice of base kernel, but can be applied to a more general class of graphs, including those having continuous node and/or edge attributes or even graphs with partially-missing attributes.

Their central idea is similar to other approaches already introduced in this section. Information, such as label sequences, is *propagated* through a series of local transformations to assign a sequence of relabelled graphs to each graph of the input data set. The similarity of two graphs may then be assessed by using any valid kernel that compares their individual sequences.

**DEFINITION 3.25** (Propagation kernels). Let  $G$  and  $G'$  be two graphs (with or without attributes). We assume that there is a *propagation scheme*, which we will discuss later, that assigns a *sequence* (of equal length  $t$ ) of graphs to each graph. We thus have a sequence  $G_0, G_1, \dots, G_{t-1}$  for  $G$  and a sequence  $G'_0, G'_1, \dots, G'_{t-1}$  for  $G'$ . Letting  $V_i$  and  $V'_i$  refer to the vertex sets



**Figure 3.10:** A visualisation of a one iteration propagation kernel. The node attribute distributions at iteration  $t$  is  $P_t \in \mathbb{R}^{n \times k}$ , where  $k$  is the dimension of the node attributes. Node attributes are denoted by colour, and their corresponding values in (d).  $P_0$  thus contains  $[1, 0]$  in the indices corresponding to blue nodes in the original graphs,  $[\frac{1}{2}, \frac{1}{2}]$  for the gray nodes corresponding to gray nodes, and  $[0, 1]$  to the red nodes. The node attribute distributions are updated via the following:  $P_{t+1} = TP_t$ , where  $T = D^{-1}A$ , i.e. the row-normalised adjacency matrix. In each propagation, the node label distributions are binned, the feature vector of a graph is the count of nodes in each bin throughout all propagation steps.

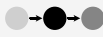
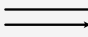

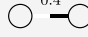
of the  $i$ th graph in the propagation scheme of  $G$  and  $G'$ , respectively, we can use any node kernel  $k_{\text{node}}(\cdot)$  to define a propagation kernel as

$$k_{\text{Prop}}(G, G') := \sum_{i=0}^{t-1} \sum_{v \in G_i} \sum_{v' \in G'_i} k_{\text{node}}(v, v'), \quad (3.44)$$

which amounts to the sum of individual node kernels over the propagation process.

The node kernel in the previous equation should be chosen according to the problem domain. Typical examples include the linear kernel (for real-valued attributes) or a Dirac kernel (for labels). The most important property of this kernel is that the propagation scheme can be adapted easily to deal with missing information in the graph. Neumann *et al.* (2016) present multiple suitable schemes for this purpose: for labelled and unlabelled graphs, there is a simple *diffusion scheme* based on iterative updates of the labels (or degrees, for unlabelled graphs) of the vertices in a one-hop neighbourhood around each vertex. For partially labelled graphs, this scheme can be slightly adapted (Neumann *et al.*, 2016), whereas for graphs with continuous attributes, the simplest propagation scheme assumes that attributes can be modelled according to a mixture of Gaussian distributions, whose parameters are then adjusted in every step. We provide an example of a propagation kernel in Figure 3.10.

The computational complexity of this kernel clearly depends on the calculation of the kernel for each propagation scheme. Neumann *et al.* (2016) note that in many cases, it is possible to use a *hashing* function (or, similarly, *binning* of node features) to perform the evaluation of the kernel on two graphs  $G_i$  and  $G'_i$  in *linear* (linear in the number of bins) time. Such a binning process is straightforward in the case of discrete attributes; see the discussion of hashing functions in Section 3.2.2.1 for more details. In the case of continuous node attributes, Neumann *et al.* (2016) propose using *locality-sensitive hashing* (Datar *et al.*, 2004), *i.e.* a family of hashing functions, for this purpose. Using these speed-up techniques, propagation kernels have a computational complexity of order  $\mathcal{O}(tNm + tN^2n)$  for computing features based on counts, where  $t$  is the number of iterations of the kernel,  $N$  is the number of graphs, and  $n$  and  $m$  are the maximum number of vertices and edges, respectively. Thus, its asymptotic complexity is comparable to the Weisfeiler–Lehman framework or the neighbourhood hash kernel.

	based on	graph type	node type	edge type	complexity
propagation kernels Neumann <i>et al.</i> , 2016	 label refinement	 undirected directed	 <sup>(1.1, 0.7)</sup> labelled attributed	 <sup>0.4</sup> labelled attributed	$\mathcal{O}(hm)$

### 3.2.2.6 Message passing graph kernels

We conclude the section of graph kernels based on iterative label refinement with an approach by (Nikolentzos and Vazirgiannis, 2018) that introduces the *message passing* framework. Like propagation kernels, the message passing framework aims to extend

existing approaches in order to handle graphs with continuous attributes. Nevertheless, this framework accomplishes this by means of a message passing step inspired by graph neural networks (see Zhou *et al.* (2018) for an in-depth review of these techniques). This step, however, is defined in terms of auxiliary kernel functions, rather than parametric transformations instantiated as neural networks.

DEFINITION 3.26 (Vertex-based message passing graph kernel). Given a vertex-based kernel function  $k_v$  and a neighbourhood-based kernel  $k_N$ , the message passing graph kernel is an iterative scheme satisfying the recurrence formula

$$k_v^{t+1}(v_1, v_2) := \alpha k_v^t(v_1, v_2) + \beta k_N(N(v_1), N(v_2)), \quad (3.45)$$

where  $t$  denotes the iteration step,  $\alpha, \beta \in \mathbb{R}_{>0}$  are non-negative scale factors, and  $N(\cdot)$  refers to the neighbourhood of a vertex.

This is a valid vertex kernel because of the closure properties of kernel functions (see Section 2.3 on p. 13 for more details). The vertex-based kernel can be trivially extended to handle two graphs  $G, G'$  by setting

$$k_{MP}(G, G') := k_V(V, V'), \quad (3.46)$$

where  $k_V$  denotes a kernel between the vertex sets  $V$  and  $V'$  of  $G$  and  $G'$ , respectively. Nikolentzos and Vazirgiannis (2018) suggest two different families of vertex set kernels, which make up their proposed message passing graph kernel.

DEFINITION 3.27 (Graph-based message passing kernel). Given two sets of vertices  $V$  and  $V'$  of two graphs  $G$  and  $G'$ , the graph-based message passing kernel is defined by replacing  $k_V$  in Eq. 3.46 with either

$$k_V(V, V') := \sum_{v \in V} \sum_{v' \in V'} k_v(v, v'), \quad (3.47)$$

leading to a standard graph kernel formulation which is based on the  $\mathcal{R}$ -convolution framework (see Section 2.3.4 on p. 17 for more details), or, alternatively,

$$k_V(V, V') := \max_{B \in \mathcal{B}(V, V')} \sum_{v, v' \in B} k_v(v, v'), \quad (3.48)$$

where  $\mathcal{B}(V, V')$  denotes the set of all bijections between  $V$  and  $V'$ , leading to a kernel formulation based on *optimal assignment*. Nikolentzos and Vazirgiannis (2018) use a Dirac delta kernel for  $k_v$  in the case of graphs with discrete node labels, or a linear kernel for graphs with attributes.

Given a kernel function for vertex sets as shown in Definition 3.27, Eq. 3.46 can be easily adjusted to integrate the recurrence formula from Definition 3.26. Using a maximum of  $t$  iterations, this leads to

$$k_{\text{MP}}(G, G') := \sum_{v \in V} \sum_{v' \in V'} k_v^t(v, v'), \quad (3.49)$$

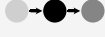
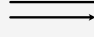

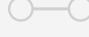
or

$$k_{\text{MP}}(G, G') := \max_{B \in \mathcal{B}(V, V')} \sum_{v, v' \in B} k_v^t(v, v'), \quad (3.50)$$

respectively. As the subsequent discussion of optimal assignment kernels in Section 3.3.2.2 on p. 74 will show, the kernel function  $k_v$  in Eq. 3.48 has to satisfy certain properties—in the terminology of Kriege *et al.* (2016), it has to be a *strong* kernel, *i.e.* one induced by a hierarchy. To satisfy this, Nikolentzos and Vazirgiannis (2018) suggest using a clustering scheme, such as  $k$ -means clustering (Kanungo *et al.*, 2002).

In terms of computational complexity, evaluating the message passing kernel based on  $\mathcal{R}$ -convolution (Eq. 3.47) has a complexity of  $\mathcal{O}(|V|^2)$ , where  $|V|$  denotes the maximum cardinality of a vertex set. By contrast, an evaluation of the optimal assignment message passing kernel (Eq. 3.48) has a complexity of  $\mathcal{O}(\bar{d}^2)$ , where  $\bar{d}$  refers to the average degree of a graph. Asymptotically, the two kernels behave the same in the case of complete graphs; in practice, however, graph data tend to contain sparse graphs, implying  $\bar{d} \ll |V| - 1$ . Nikolentzos and Vazirgiannis (2018) showed that, with a pre-calculated hierarchy, it is possible to employ a Nyström method (Williams and Seeger, 2001) to compute Eq. 3.48 with *linear* time complexity in the cardinality of the vertex set, *i.e.* in  $\mathcal{O}(|V|)$  time, giving the message passing kernel desirable scaling properties.

The message passing kernel is linked to the Weisfeiler–Lehman subtree kernel (see Section 3.2.2.1 on p. 3.2.2.1 for more details). In fact, as the authors note, the message passing kernel framework *includes* the Weisfeiler–Lehman subtree kernel (Nikolentzos and Vazirgiannis, 2018): following the terminology of this section, the subtree kernel satisfies the  $\mathcal{R}$ -convolution formulation from Eq. 3.47, where the kernel between two vertices at every step  $t$  of the iteration is equal to the kernel of the previous time step followed by a Dirac delta kernel between their new labels. However, the formulation of the Weisfeiler–Lehman subtree kernel that we give in this survey is computationally more efficient and to be preferred for real-world applications.

message passing kernels	based on	graph type	node type	edge type	complexity
Nikolentzos and Vazirgiannis, 2018	 label refinement	 undirected directed	 <sup>(1.1, 0.7)</sup> labelled attributed	 none	$\mathcal{O}(n^2)$

### 3.2.3 Graph kernels based on spectral theory

Graph spectral theory provides a wealth of well-known results that allow the characterisation of a graph in terms of the eigenvalues and eigenvectors of its corresponding graph Laplacian matrix (see Definition 2.9). The graph Laplacian can be intuitively understood as a discretised differential operator. Given any function  $f: V \rightarrow \mathbb{R}$ , one can show that  $L := D - A$  satisfies  $(Lf)(v) = \sum_{v' \in \mathcal{N}(v)} w(v, v')(f(v) - f(v'))$ , where  $w(v, v')$  is the weight of the edge between the vertices  $v$  and  $v'$ . Moreover, one can also show that

$$\langle f, Lf \rangle = \sum_{(v, v') \in E} w(v, v')(f(v) - f(v'))^2 \quad (3.51)$$

holds in general. Thus, eigenvectors of  $L$  corresponding to small eigenvalues can be seen as smoothly-varying functions defined on the nodes of the graph, capturing a notion of “shape” of the graph. These and other properties of the graph Laplacian matrix have been exploited, for example, to design kernels to quantify the similarity being nodes of a single graph (Kondor and Lafferty, 2002). The resulting kernels admit multiple theoretical interpretations, including close connections to random walks and stochastic diffusion processes (Kondor and Lafferty, 2002, Section 3).

Extending these approaches to instead compare graphs presents multiple challenges. Firstly, it is not immediate how to ensure that the resulting kernel will be invariant with respect to graph isomorphism. Secondly, a direct implementation would not make use of node attributes, when available. Finally, and perhaps most importantly, the graph Laplacian mostly captures “global” properties of the graph yet localized information about graph topology is likely to be essential for many practical applications. In the remainder of this section, we will introduce a recent graph kernel based on spectral theory that overcomes all of these drawbacks.

#### 3.2.3.1 Multiscale Laplacian graph kernel

The *multiscale Laplacian graph kernel* of Kondor and Pan (2016) solves the aforementioned limitations by combining two different contributions. Firstly, they propose the *feature space Laplacian graph kernel* (FLG kernel), a novel graph kernel based on spectral theory that is able

to take node attributes into account while introducing invariance to vertex permutations. However, the FLG kernel only models global aspects of the graphs being compared. In order to capture structural information of graphs at multiple scales, Kondor and Pan (2016) introduce a graph kernel defined recursively in terms of a suitably-defined *hierarchy* of subgraphs “centered” around each vertex. Typically, these subgraph hierarchies will correspond to  $k$ -hop neighbourhoods for increasing values of  $k$ . In a nutshell, the recursive construction of graph kernels in this framework builds on the FLG kernel, exploiting the fact that it admits any p.d. kernel to compare pairs of nodes. Thus, to obtain a graph kernel at scale  $k + 1$ , their method uses the previous graph kernel at scale  $k$  to define a p.d. kernel between *nodes*, which compares their respective  $k$ -hop neighbourhoods.

We will begin by introducing the FLG kernel. The core idea behind this approach is to define a random variable for each graph that combines spectral information with its node attributes. Then, the problem of comparing two graphs can be reduced to the problem of comparing the probability densities of these random variables, for which Kondor and Pan (2016) use the Bhattacharyya kernel (Jebara and Kondor, 2003). The FLG kernel assumes the existence of a suitable p.d. kernel to compare pairs of vertices,  $k_{\text{node}}$ . Suppose that  $\phi_{\text{node}}(\cdot)$  is the feature map corresponding to this kernel. By definition, the linear combination

$$\phi(G) := \sum_{v \in V} \alpha(v) \phi_{\text{node}}(v) = \Phi_V \alpha_V, \quad (3.52)$$

where  $\Phi_V$  contains the feature map representations of all nodes and  $\alpha$  is a vector of the vertex weights  $\alpha(v)$ , is invariant to vertex permutations. Kondor and Pan (2016) define the set  $\{\alpha(v) \mid v \in V\}$  to be random variables distributed according to a Gaussian Markov Random Field (Koller and Friedman, 2009) sharing structure with the graph. This accomplishes three objectives: (1) the probability density of  $\{\alpha(v) \mid v \in V\}$ , which is a Normal distribution  $\mathcal{N}(0, L^{-1})$ , is endowed with information about the (global) structure of the graph; (2) this density transforms in the same way as  $\{\phi_{\text{node}}(v) \mid v \in V\}$  under vertex reorderings, achieving the desired invariance and (3) the Bhattacharyya kernel between the densities of  $\phi(G_1) \sim \mathcal{N}(0, \Phi_{V_1} L_1^{-1} \Phi_{V_1}^T)$  and  $\phi(G_2) \sim \mathcal{N}(0, \Phi_{V_2} L_2^{-1} \Phi_{V_2}^T)$ , can be computed in closed form. This leads to the following definition of the *generalized feature space Laplacian graph kernel*.

**DEFINITION 3.28** (Generalized feature space Laplacian graph kernel). Let  $G = (V, E)$  and  $G' = (V', E')$  be two undirected graphs whose vertex sets are subsets of the same vertex space  $\mathfrak{V}$ , i.e.  $V \subseteq \mathfrak{V}$  and  $V' \subseteq \mathfrak{V}$ . Furthermore, let  $\kappa: \mathfrak{V} \times \mathfrak{V} \rightarrow \mathbb{R}$  be a base kernel on said vertex space. In the case that each vertex can be assigned a one-hot encoded feature vector,

$\kappa$  might be chosen as a linear kernel on these vectors, for example. The *generalized feature space Laplacian graph kernel* induced by  $\kappa$  is then defined as

$$k_{\text{FSL}}^\kappa(G, G') := \frac{\left| \left( \frac{1}{2}S_1^{-1} + \frac{1}{2}S_2^{-1} \right)^{-1} \right|^{\frac{1}{2}}}{|S_1|^{\frac{1}{4}}|S_2|^{\frac{1}{4}}}, \quad (3.53)$$

where  $|\cdot|$  denotes the determinant of the given matrix. In the preceding equation,  $S_1$  and  $S_2$  are transformed variants of the graph Laplacian matrices that take the base kernel into account. More precisely, for  $i \in \{1, 2\}$ , we have

$$S_i := Q_i^\top L_i^{-1} Q_i + \eta \mathbb{1}, \quad (3.54)$$

where  $Q_i$  contains those eigenvectors of the joint Gram matrix of the base kernel  $\kappa$  that correspond to the vertices of  $G_i$ , while  $\eta$  denotes a small regularization factor, and  $\mathbb{1}$  is the identity matrix of appropriate size.

The generalized feature space Laplacian kernel may now be extended and applied recursively to capture the similarity between subgraphs. We first give the definition in terms of *one* graph but will subsequently extend it.

**DEFINITION 3.29** (Multiscale Laplacian subgraph kernel). Let  $G = (V, E)$  be an undirected graph and  $\kappa: \mathfrak{B} \times \mathfrak{B} \rightarrow \mathbb{R}$  a base kernel on its nodes, with  $V \subseteq \mathfrak{B}$  as defined above. Furthermore, suppose that there is a sequence of nested neighbourhoods such that for each vertex  $v \in V$ , we have

$$v \in N_1(v) \subseteq N_2(v) \subseteq \cdots \subseteq N_h(v) \quad (3.55)$$

where  $N_j(v) \subseteq V$ . Kondor and Pan (2016) propose that such a *filtration* of neighbourhoods be obtained by extending the usual “hop” neighbourhoods (see Definition 2.8, p. 9) around a vertex, for example. Letting  $G_i(v)$  denote the graph that is induced by  $v$  and a certain neighbourhood, the hierarchy of *multiscale Laplacian subgraph kernels*  $k_{\text{MLS}_1}, \dots, k_{\text{MLS}_h}$  is defined recursively:

1. The first multiscale Laplacian subgraph kernel is the *generalized feature space Laplacian graph kernel* induced by the base kernel  $\kappa$ , i.e.

$$k_{\text{MLS}_1}(v_1, v_2) := k_{\text{FSL}}^\kappa(G(v_1), G(v_2)), \quad (3.56)$$

which is evaluated on the induced subgraphs of the first stage of the neighbourhood filtration.



2. The higher stages of the neighbourhood filtration, by contrast, use the generalized feature space Laplacian kernel induced by lower stages, *i.e.*

$$k_{\text{MLS}}^{(j)}(v_1, v_2) := k_{\text{FSL}}^{k_{\text{MLS}}^{(j-1)}}(G_j(v_1), G_j(v_2)), \quad (3.57)$$

where  $j \in \{1, \dots, h\}$ .



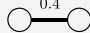
Finally, to extend this definition to the comparison of two graphs  $G$  and  $G'$ , Kondor and Pan (2016) note that the kernel can be extended under the assumption that the *same* base kernel is used. This leads to the *multiscale Laplacian graph kernel*.

DEFINITION 3.30 (Multiscale Laplacian graph kernel). Given two graphs  $G$  and  $G'$  with the same vertex space as in Definition 3.28, the *multiscale Laplacian graph kernel* is defined as

$$k_{\text{ML}}(G, G') := k_{\text{FSL}}^{k_{\text{MLS}}^{(h)}}(G, G'), \quad (3.58)$$

where  $k_{\text{MLS}}^{(h)}$  denotes the multiscale Laplacian subgraph kernel at the highest level, following Definition 3.29.

In terms of computational complexity, it is possible to evaluate the kernel between two graphs in time proportional to  $\mathcal{O}(hn^2)$ , where  $h$  denotes the number of scales (recursion steps) and  $n$  denotes the number of vertices.

	based on	graph type	node type	edge type	complexity
multiscale Laplacian kernel  Kondor and Pan, 2016	$\left[ \lambda \right]$ graph Laplacian	 undirected	 labelled	 attributed	$\mathcal{O}(n^2h)$

### 3.3 Extensions of common graph kernels

Finally, some methods can be considered an extension of the previously defined categories. We now describe two important categories of such methods, namely approaches that extend existing methods to continuous attributes, and methods that define graph kernels outside the popular  $\mathcal{R}$ -convolution framework.

#### 3.3.1 Extending graph kernels to handle continuous attributes

Many of the graph kernels introduced so far, including some of the most commonly used such as the Weisfeiler-Lehman framework (Section 3.2.2.1), forego the possibility to

use continuous node and/or edge attributes, often due to computational considerations. Some approaches have been motivated precisely by the goal to overcome this limitation, such as the family of propagation kernels (Section 3.2.2.5) or the message passing kernels (Section 3.2.2.6). These new methods, however, focus on one particular type of substructure. In this section, we will instead describe three different generic approaches that allow using most graph kernels, including those limited to categorical attributes, to compare graphs that might nonetheless have continuous node and/or edge attributes.

The first method, subgraph matching kernels (Section 3.3.1.1) counts the number of common subgraph isomorphisms between two graphs. This kernel relies on using the direct product graph, introduced in Section 3.2.1.1, to identify the maximum common subgraphs, and then weights these findings using the node and edge labels or attributes.

The idea behind the second of these approaches, the graph invariant kernel framework (Section 3.3.1.2), is to augment a simple node-only graph kernel, which can easily accommodate continuous node attributes by defining a suitable p.d. kernel  $k_{\text{node}}$  but misses topological information, with a *weight function*, which is computed using previously existing graph kernels to capture higher-order graph substructures.

The third method, hash graph kernels (Section 3.3.1.3), instead propose to transform each input graph into an ensemble of “discretised” graphs, each of them obtained by applying a randomly sampled hash function that maps each real-valued attribute to an integer-valued “bin”. These graph ensembles can then be compared to each other using existing graph kernels, and the final similarity between any two input graphs is obtained as the average similarity between elements of their respective ensembles.

### 3.3.1.1 Subgraph matching kernels

Kriege and Mutzel (2012) provided an early approach to extend graph kernels to graphs with continuous attributes. The foundation of the method hinges upon counting the number of common subgraph isomorphisms using the direct product graph. Whereas the graphlet kernel described in Section 3.1.4.4 counts the number of matching common subgraphs of two graphs  $G$  and  $G'$ , Kriege and Mutzel (2012) propose counting the number of matching subgraph isomorphisms, since there can be multiple isomorphisms for a given common subgraph. After providing a framework on how to do this for a simple graph with node and edge labels, they provide extensions to incorporate continuous node and label attributes.

**DEFINITION 3.31** (Common subgraph isomorphism kernel). Let  $G = (V, E)$  and  $G' = (V', E')$  be two undirected graphs, with node and edge labels from the alphabets  $\Sigma_V$  and  $\Sigma_E$  respectively. For a subset of vertices  $V_i \in V$  and  $V'_i \in V'$ , and their corresponding induced subgraphs  $G[V_i]$  and  $G'[V'_i]$ , a common subgraph isomorphism (CSI) is the mapping

$\varphi: V_i \rightarrow V'_i$ . The *common subgraph isomorphism kernel* can thus be defined as the sum over all common subgraph isomorphisms  $\mathcal{I}$  in  $G$  and  $G'$ , weighted by some weight function  $\lambda$ , i.e.

$$k_{\text{CSI}}(G, G') := \sum_{\varphi \in \mathcal{I}(G, G')} \lambda(\varphi). \quad (3.59)$$

$k_{\text{CSI}}$  is used to then compute the subgraph matching kernel.

**DEFINITION 3.32** (Subgraph matching kernel). Again let  $G = (V, E)$  and  $G' = (V', E')$  be two undirected graphs, with node and edge labels from the alphabets  $\Sigma_V$  and  $\Sigma_E$  respectively, and  $\lambda$  representing all bijections from  $V_i$  to  $V'_i$ . The subgraph matching kernel is thus defined as


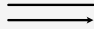
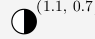
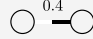
$$k_{\text{SM}}(G, G') := \sum_{\varphi \in \mathcal{B}(G, G')} \lambda(\varphi) \prod_{v \in V_i} k_{\text{node}}(v, \varphi(v)) \prod_{e \in V_i \times V_i} k_{\text{edge}}(e, \psi_\varphi(e))$$

where  $V_i = \text{dom}(\varphi)$ , and  $k_{\text{node}}$  and  $k_{\text{edge}}$  are predefined kernels on the nodes and edges.

The authors recommended a simple Dirac kernel on the node and edge labels for  $k_{\text{node}}$  and  $k_{\text{edge}}$  when the graphs have categorical labels, and offered an extension to node/edge attributed graphs by multiplying these Dirac kernel by an additional kernel evaluated on the continuous attributes, such as the Brownian bridge kernel for node attributes or the triangular kernel for edge attributes. Moreover, the authors used a uniform value of  $\lambda$  in their experiments.

The key step in this process is to use the result of Levi (1973), who found that each maximum clique in the product graph  $G_{\times}$  from graphs  $G$  and  $G'$  corresponds to a maximal common subgraph of  $G$  and  $G'$ . Indeed, determining all such cliques equates to finding all common subgraph isomorphisms, and thus reduces the problem to finding all maximal cliques in the product graph. The product graph is further extended by creating a weighted product graph, which has the effect of assigning a weight to the maximal cliques.

The complexity of the subgraph matching kernel depends on the number of nodes in the two graphs and the upper bound on the size of subgraphs considered,  $k$ . This leads to a complexity of  $\mathcal{O}(k(n^2)^{k+1})$ .

subgraph matching kernel <small>Kriege and Mutzel, 2012</small>	<b>based on</b>  continuous attributes	<b>graph type</b>  undirected directed	<b>node type</b>  labelled attributed	<b>edge type</b>  labelled attributed	<b>complexity</b> $\mathcal{O}(k(n^2)^{k+1})$
--	---	--	---	---	--

### 3.3.1.2 Graph invariant kernel framework

The framework of graph invariant kernels was developed by Orsini *et al.* (2015) to extend existing graph kernels to graphs with continuous attributes, based on the calculation of certain *vertex invariants*. This makes it possible to quickly adapt certain graph kernels—most prominently the Weisfeiler–Lehman graph kernel framework—to graphs with continuous attributes.

The central concept of the framework by Orsini *et al.* (2015) is the vertex invariant. A vertex invariant is a function

$$\mathcal{I}: V \rightarrow C \quad (3.60)$$

that assigns each vertex  $v \in V$  a “colour”  $c \in C$ , also known as *colour refinement*. The assigned colour  $c = \mathcal{I}(v)$  needs to be *invariant* under graph isomorphism, *i.e.*  $\mathcal{I}(v) = \mathcal{I}(f(v))$  for any isomorphism  $f$ . This leads to the generic formulation of the graph invariant kernels framework.

**DEFINITION 3.33** (Graph invariant kernels). Let  $G = (V, E)$  and  $G' = (V', E')$  be two undirected graphs, potentially with additional node attributes. The general *graph invariant kernel* is defined as

$$k_{\text{GI}}(G, G') := \sum_{v \in V} \sum_{v' \in V'} \mathcal{A}(v, v') k_{\text{node}}(v, v'), \quad (3.61)$$

where  $k_{\text{node}}(\cdot)$  represents a suitable kernel defined on the nodes—and their attributes—and  $\mathcal{A}(\cdot)$  is a *weight function* that counts the number of invariants that  $G$  and  $G'$  have in common. Following the  $\mathcal{R}$ -convolution framework (see also Section 2.3.4), it is calculated over all substructures  $g \in \mathcal{R}^{-1}(G)$  and  $g' \in \mathcal{R}^{-1}(G')$

$$\mathcal{A}(v, v') := \begin{cases} \sum_{(g, g')} \kappa(v, v') \frac{\delta_{\text{m}}(g, g')}{|g||g'|} & \text{if } v \in g \text{ and } v' \in g' \\ 0 & \text{otherwise.} \end{cases} \quad (3.62)$$

In the previous equation,  $\kappa(\cdot)$  refers to a kernel that measures the similarity of the vertex colours under a selected vertex invariant  $\mathcal{I}$ , while  $\delta_{\text{m}}(\cdot)$  is a function that determines if two substructures *match*. Subsequently, we will describe some example choices of these two functions.

We first describe suitable choices for the match function  $\delta_{\text{m}}(\cdot)$  because this function admits a more intuitive explanation. In general,  $\delta_{\text{m}}(\cdot)$  can be expressed as an equivalence check, *i.e.*

$$\delta_{\text{m}}(g, g') := \begin{cases} 1 & \text{if } g \sim g' \\ 0 & \text{otherwise.} \end{cases} \quad (3.63)$$

Thus,  $\delta_m(g, g')$  checks whether the two substructures are *equivalent*. For example, if  $\mathcal{R}(G)$  decomposes a graph with node labels into its shortest paths,  $\delta_m(g, g')$  could be defined to check whether two shortest path have the same length *and* the same sequence of labels when following the path. The kernel  $\kappa(\cdot)$ , by contrast, can be defined by reusing other graph kernels that are defined on substructures. For example, suppose we are given a graph with node labels. We may then use the Weisfeiler–Lehman framework (see also Section 3.2.2.1) to obtain a sequence of neighbourhood-based labels per vertex. Letting  $\mathcal{L}(v)$  and  $\mathcal{L}(v')$  refer to the Weisfeiler–Lehman node label sequences of two vertices  $v \in G$  and  $v' \in G'$ , respectively, we can define


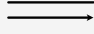

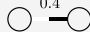
$$\kappa(v, v') := \left| \left\{ \mathcal{L}^{(i)}(v), \mathcal{L}^{(i)}(v') \mid \mathcal{L}^{(i)}(v) = \mathcal{L}^{(i)}(v') \right\} \right|, \quad (3.64)$$

which counts the number of equal labels for the two vertices. Other kernel choices are possible as well; please refer to Orsini *et al.* (2015) for more information.

In terms of complexity, the graph invariant kernels framework depends on the complexity of the node label kernel and the complexity of the match function. In general, for an undirected graph  $G = (V, E)$  with a diameter bounded by  $r$  and maximum vertex degree  $d$ , the complexity is of order  $\mathcal{O}\left(n^2(C_1 + C_2\tau d^{4r})\right)$ , where  $n$  is the number of vertices,  $C_1$  and  $C_2$  are costs that depend on  $k_{\text{node}}(\cdot)$  and  $\kappa(\cdot)$ , and  $\tau$  is the maximum number of matching substructures, *i.e.*

$$\tau := \sum_{(g, g')} \delta_m(g, g') \quad (3.65)$$

for substructures  $g \in \mathcal{R}^{-1}(G)$  and  $g' \in \mathcal{R}^{-1}(G')$ . Typically,  $C_1 = n_1$  for a node label kernel with  $n_1$  features, and  $C_2 = n_2$  for an invariant kernel with  $n_2$  features. If *global* invariants, such as the degree, are used, it is possible to simplify the equation such that  $C_2 = 1$  (Orsini *et al.*, 2015).

	based on	graph type	node type	edge type	complexity
graph invariant framework Orsini <i>et al.</i> , 2015	 continuous attributes	 undirected directed	 <sup>(1.1, 0.7)</sup> labelled attributed	 <sup>0.4</sup> labelled attributed	$\mathcal{O}(\tau n^2 d^{4r})$

### 3.3.1.3 Hash graph kernels

Hash functions are prevalent in several kernel frameworks—see Section 3.2.2.1 or Section 3.2.2.2, for example—but their utility was mostly restricted to graphs with discrete labels. Morris *et al.* (2016) thus developed a framework that makes it possible to “convert”

any graph kernel that supports discrete attributes to a graph kernel that supports continuous attributes. The key concept of this framework is the use of multiple hash functions that map continuous attributes to discrete labels, which in turn permits the use of a discrete graph kernel.



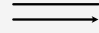

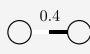
**DEFINITION 3.34** (Hash graph kernel). Let  $\kappa$  be a base graph kernel, such as a Weisfeiler–Lehman kernel (Definition 3.17 on p. 49). Moreover, let  $\mathfrak{H} = \{h_1, h_2, \dots\}$  be a finite family of hash functions. Each element  $h_i \in \mathfrak{H}$  should be a function  $h_i: \mathbb{R}^d \rightarrow \mathbb{N}$ , where  $d$  denotes the dimensionality of the graph attributes. While the function  $h_i$  is applied to individual components of  $G$ , such as the nodes, we will use  $h_i(G)$  to refer to the discretised graph resulting from applying  $h_i$  to continuous attributes of the graph. Given two graphs  $G$  and  $G'$ , the *hash graph kernel* is defined as

$$k_{\text{HGK}}(G, G') := \frac{1}{|\mathfrak{H}|} \sum_{i=1}^{|\mathfrak{H}|} \kappa(h_i(G), h_i(G')), \quad (3.66)$$

i.e. the *average* of kernel values under multiple hash functions, which are drawn randomly from  $\mathfrak{H}$ .

This formulation is advantageous because it is highly generic and supports arbitrary kernels—moreover, explicit feature map representations are available in case the base kernel  $\kappa$  supports them. The run time can easily be shown to only depend on the employed base kernel, the cardinality of  $\mathfrak{H}$ , and the complexity of evaluating a single hash function (Morris *et al.*, 2016).

Typical choices for  $\mathfrak{H}$  include, but are not limited to, locality-sensitive hashing schemes (Datar *et al.*, 2004; Paulevé *et al.*, 2010). As for the base kernel function, typical choices discussed by Morris *et al.* (2016) include the *shortest-path kernel* (Section 3.1.3.1) and the *Weisfeiler–Lehman subtree kernel* (Section 3.2.2.1). We will abbreviate them with HGK-SP and HGK-WL, respectively.

	based on	graph type	node type	edge type	complexity
 hash graph kernels <small>Morris et al., 2016</small>	 continuous attributes	 undirected directed	 labelled attributed	 labelled attributed	---

### 3.3.2 Beyond simple instances of the $\mathcal{R}$ -convolution framework

As has been argued throughout this chapter, a large number of graph kernels, including some of the most successful ones, belong to the  $\mathcal{R}$ -convolution framework, introduced in Section 2.3.4. The  $\mathcal{R}$ convolution framework is extremely general. However, most  $\mathcal{R}$ -convolution-based graph kernels can be seen as simple instances of this framework that implement an “all substructure-pairs” kernel for a certain substructure of choice, such as walks, shortest-paths, graphlets or  $k$ -hop neighbourhoods. If  $\mathcal{R}^{-1}(G)$  denotes the set of all such substructures in a graph  $G$ , these kernels could be generically expressed as

$$k(G, G') = \sum_{g \in \mathcal{R}^{-1}(G)} \sum_{g' \in \mathcal{R}^{-1}(G')} k_{\text{base}}(g, g'),$$

where  $k_{\text{base}}$  is a p.d. kernel that quantifies the similarity between any two instances of the specific type of substructures under consideration. Moreover, for many of the graph kernels that can be expressed this way, the base kernel is defined to be a Dirac kernel, in which case the feature map of  $k$  can be interpreted as an unnormalised histogram that counts the number of occurrences of each possible variation of the substructure of choice. To obtain a representation of graphs that is highly expressive, often complex substructures that can present many variations, such as long walks or  $k$ -hop neighbourhoods, are preferred over simpler ones, such as vertices, edges or short walks. However, there is an implicit statistical trade-off incurred when making such a choice; the feature map of the kernel could be extremely high-dimensional and, most importantly, could contain a very large number of features mostly irrelevant for the task at hand. This phenomenon often manifests itself as *diagonal dominance* in the resulting kernel matrix, indicating that graphs are mostly deemed similar only to themselves, leading to models prone to overfitting.

Ultimately, this limitation arises due to the underlying lack of adaptivity in the way feature maps are defined by these approaches. When large collections of annotated graph data sets are available, graph neural networks (Zhou *et al.*, 2018) are emerging as a powerful generalization of graph kernels that, borrowing many of their implicit biases, attempt to directly learn a feature map optimised end-to-end for the task of interest. Nevertheless, the graph kernels community has also explored alternative methods to alleviate these limitations by different means. In the final section of this chapter, we will describe three such approaches.

Weighted decomposition kernels (Section 3.3.2.1) are, in a nutshell, based on the idea of decomposing graphs into two different types of substructures simultaneously, referred to as *selectors* and *contexts* in their terminology. These two types serve complementary roles.

Selectors are simple substructures, often chosen to be single vertices, and are compared using a Dirac kernel. In contrast, the contexts are typically chosen to be more complex substructures, such as the  $k$ -hop neighbourhoods surrounding the selectors, and are compared with a base kernel that accounts for partial similarities. The (partial) similarity between these contexts provides an adaptive *weight* for the contribution to the kernel of the exact matching performed on their corresponding selectors, from which the method derives its name. In this way, the authors aim to define a more parsimonious feature map that retains sufficient expressivity to capture higher-order information about the graph topology.

Unlike the previous approach, the family of optimal assignment kernels (Section 3.3.2.2) represent a departure from the  $\mathcal{R}$ -convolution framework. Much like the “all substructure-pairs” kernel, they consider a decomposition of graphs into a set of substructures. However, rather than computing  $k(G, G')$  by comparing every substructure in graph  $G$  to every substructure in graph  $G'$ , they compare each substructure in  $G$  only to one substructure in  $G'$ . This requires learning an *optimal assignment* between substructures of  $G$  and  $G'$  so as to maximise the resulting value of  $k(G, G')$ . By construction, this approach alleviates the diagonal dominance problem. However, as we shall see, there are important restrictions in the type of base kernels that can be used in this scheme to guarantee that the resulting kernel is positive definite.

Deep graph kernels (Section 3.3.2.3), the last approach we will discuss, take the idea behind weighted decomposition kernels one step further. The contribution of each individual dimension in the feature maps of highly expressive graphs kernels, such as those arising from the Weisfeiler-Lehman framework, could be weighted by a free parameter learnt from the data. If suitable weights are found, this would allow prioritizing the most predictive features while down-weighting those which are irrelevant for a specific task. As will be described later, the authors propose to accomplish this with a method inspired by recent advances in natural language processing.

### 3.3.2.1 Weighted decomposition kernels

In some applications, for example molecular classification, it makes sense to assign different weights to a specific  $\mathcal{R}$ -decomposition in order to accentuate a given property of a molecule, for example. Menchetti *et al.* (2005) thus developed a *weighted* variant of the  $\mathcal{R}$ -convolution framework to handle molecular classification better (Ceroni *et al.*, 2007). The central idea is to decompose a graph  $G$  into a certain *subgraph*  $s_G \subseteq G$  and a *context*  $c_G \subseteq G$ . The subgraph is also referred to as a *selector*, while the context subgraph typically contains  $s_G$ ; we will also use  $s$  and  $c$  to denote these variables when the corresponding graph  $G$  is clear. Following



the notation of  $\mathcal{R}$ -convolution, we will denote this by  $\mathcal{R}(s_G, c_G, G)$ . While the subgraphs are typically only compared using a Dirac delta kernel, the contexts are supposed to be compared in terms of their attributes (in the original application of Ceroni *et al.* (2007), edges are assigned attributes that refer to the chemical properties of the corresponding bonds in a molecule, for example). To this end, Ceroni *et al.* (2007) introduce a novel set of kernels based on probability distributions over attributes. In the following, we assume that we are given two graphs  $G$  and  $G'$  with a set of  $m$  attributes  $\mathcal{A} := \{A_1, \dots, A_m\}$ . This notation can be seen as a generalization of the notation presented in Definition 2.3 on p. 7, which discusses a single attribute function. Here, we assume that more than one attribute is present, but we leave the definition of each attribute purposefully open.

DEFINITION 3.35 (Graph probability distribution kernel). Let  $\rho \in \mathbb{R}$  be a scaling parameter and  $p_i(\cdot), p'_i(\cdot)$  be probability distributions over the individual attributes in  $\mathcal{A}$  for  $G$  and  $G'$  respectively. Assuming that the  $i$ th attribute only has  $n_i$  distinct values, a family of *graph probability kernels* is obtained as

$$\kappa_i(G, G') := \sum_{j=1}^{n_i} p_i(j)^\rho p'_i(j)^\rho. \quad (3.67)$$

For *continuous* attributes, Menchetti *et al.* (2005) note that previous work (Jebara *et al.*, 2004) provides a theoretical framework.

In the previous definition, the topology of the graph is not used—making it possible to perform a “soft matching” of smaller substructures in kernels. This results in the following generic framework.

DEFINITION 3.36 (Weighted decomposition kernel). Given a decomposition of  $G$  and  $G'$  into subgraphs  $s_G$  and  $s_{G'}$  with corresponding contexts  $c_G$  and  $c_{G'}$ , the *weighted decomposition kernel* is defined as


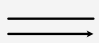

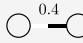
$$k_{\text{WD}}(G, G') = \sum_{(s, c) \in \mathcal{R}^{-1}(G)} \sum_{(s', c') \in \mathcal{R}^{-1}(G')} \delta(s, s') \sum_{i=1}^m \kappa_i(c, c'), \quad (3.68)$$

where  $\kappa_i(c, c')$  refers to a kernel according to Definition 3.35.

The choice of  $s$  and  $c$  depends on the application. Ceroni *et al.* (2007), for example, propose setting  $c$  to a neighbourhood of fixed radius  $k$ , comprising all vertices that are *reachable* with paths of length at most  $k$ , while  $s$  is just the source vertex (meaning that the Dirac delta boils down to comparing vertex labels).

The computational efficiency of this kernel depends to a large extent on the choice of subgraph and context. Given  $l$  substructures in the pre-image of the  $\mathcal{R}$ -convolution

relationship, the kernel between two graphs can be computed in  $\mathcal{O}(l^2)$  time, which can be reduced to linear time for sparser indices (Menchetti *et al.*, 2005).

	based on	graph type	node type	edge type	complexity
weighted decomposition kernels <small>Ceroni <i>et al.</i>, 2007</small>	$\mathcal{R}$  beyond $\mathcal{R}$ -convolutions	 undirected directed	 <sup>(1.1, 0.7)</sup> labelled attributed	 <sup>0.4</sup> labelled attributed	$\mathcal{O}(l^2)$

### 3.3.2.2 Optimal assignment kernels

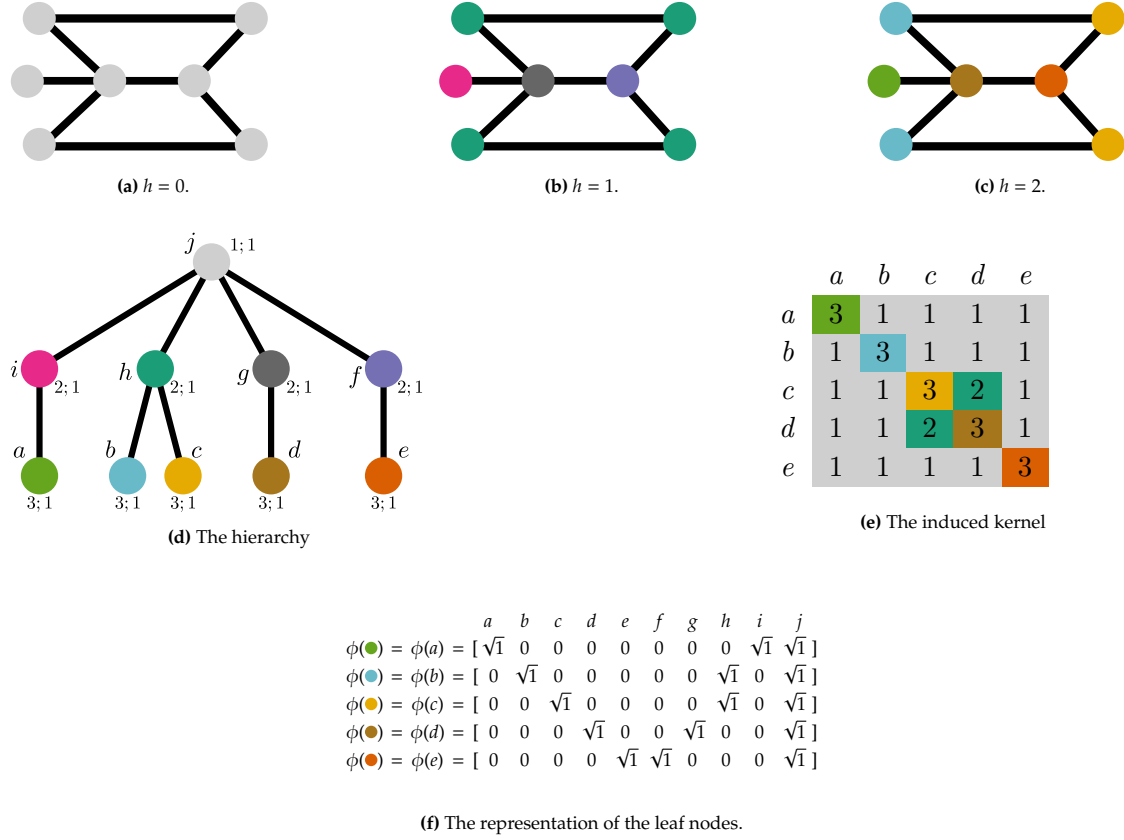
In some application domains, such as chemoinformatics, additional information for graph nodes, is available. Molecules, for examples, might have additional information about their structure attached. These structural information cannot always be easily expressed in terms of continuous attributes. Fröhlich *et al.* (2005) thus developed a kernel based on finding an optimal assignment between substructures of these graphs. The underlying idea is reminiscent of  $\mathcal{R}$ -convolution kernels (see Section 2.3.4 for more information) and requires a graph to be decomposable into a set of parts. However, the original optimal assignment kernel is not guaranteed to be positive semi-definite for all choices of substructure kernels (Vert, 2008). Kriege *et al.* (2016) showed that certain base kernels lead to positive semi-definite kernels. Following their terminology, let  $\mathcal{X}$  be a set (such as all potential vertex labels),  $X, Y \subseteq \mathcal{X}$  subsets of the same cardinality, and  $\mathfrak{B}(X, Y)$  the set of all bijections between  $X$  and  $Y$ . This leads to the optimal assignment kernel.

**DEFINITION 3.37** (Optimal assignment kernel). Given a base kernel  $\kappa$  between individual elements of  $\mathcal{X}$ , such as a vertex kernel, the *optimal assignment kernel* is defined as

$$k_{\text{OA}}(X, Y) := \max_{B \in \mathfrak{B}(X, Y)} \sum_{x \in X} \kappa(x, B(y)), \quad (3.69)$$

where  $\kappa(x, y) = 0$  is used to account for subsets of different cardinalities.

Kriege *et al.* (2016) show (by virtue of defining strong kernels, *i.e.* a function  $\kappa: \mathcal{X} \times \mathcal{X} \rightarrow \mathbb{R}_{\geq 0}$  such that  $\kappa(x, y) \geq \min\{\kappa(x, z), \kappa(y, z)\}$  for all  $x, y, z \in \mathcal{X}$ ; notice that in a strong kernel, an object is most similar to itself, such that  $\kappa(x, x) \geq \kappa(x, y)$  for objects  $x, y$ ) that certain base kernels, namely the ones arising from hierarchical partitions of the kernel domain, lead to positive semi-definite optimal assignment kernels. This gives rise to a general framework for kernel construction, leading to a *vertex optimal assignment kernel*, for example, which employs a Dirac delta kernel on vertex labels. As this kernel, as well as a related *edge optimal*



**Figure 3.11:** An illustration of the Weisfeiler-Lehman optimal assignment kernel. Assume a graph with unlabelled nodes, and its subsequent labelling according to the Weisfeiler-Lehman algorithm for iteration  $h = 0$  (a),  $h = 1$  (b), and  $h = 2$  (c). This relabelling process provides a hierarchy (d), where each vertex  $v$  is annotated with  $w(v); \omega(v)$ , representing the weight and additive weight of  $v$  respectively. We assume an additive weight of 0, which provides values for the hierarchy once we assign an initial weight to the root node  $w(j) = 0$ . This hierarchy induces a kernel (e) on the leaf nodes, where  $k(x, y) = w(c)$ , if  $c$  is the lowest common ancestor of  $x$  and  $y$ , shown by the colour in the kernel matrix. (f) shows the feature map for each leaf node, where each element in the feature map for a node  $v$  has a value  $\sqrt{\omega(m)}$  in the feature map if  $m$  is on the path between  $v$  and the root node  $j$ . A graph  $G$  is then represented by the histogram of the sum of the element wise squared feature maps for each node in (c), i.e.  $H(G) = [1 \ 2 \ 2 \ 0 \ 1 \ 1 \ 1 \ 1 \ 4 \ 1 \ 7]$ . Given a second (undepicted) graph  $G'$  with histogram  $H(G')$ , the histogram intersection kernel is then just the sum of the element wise minimum of each component of the two histograms.

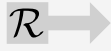
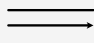

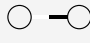
*assignment kernel*, already demonstrate better predictive performance than regular vertex label and edge label kernels, the family of Weisfeiler–Lehman optimal assignment kernels is particularly interesting.

Following the notation for the Weisfeiler–Lehman iteration (see Section 3.2.2.1), the *Weisfeiler–Lehman optimal assignment kernel* is defined on the vertices of a graph while using a base kernel that evaluates the compressed subtree labels. For  $h$  iterations, the kernel between two vertices  $u$  and  $v$  is thus defined as

$$\kappa(u, v) := \sum_{i=0}^h k_{\delta}(\sigma_u^{(i)}, \sigma_v^{(i)}), \quad (3.70)$$

where  $k_{\delta}$  denotes a Dirac delta kernel. We provide an visualisation of the Weisfeiler–Lehman optimal assignment kernel in Figure 3.11.

In addition to its highly favourable predictive performance (Kriege *et al.*, 2016), this kernel is advantageous because its calculation can be done extremely efficiently using histogram intersection. The computational complexity of evaluating the kernel for two graphs is thus asymptotically not larger than that of the Weisfeiler–Lehman labelling operation, leading to  $O(hm)$ , where  $m$  is the maximum number of edges.

	based on	graph type	node type	edge type	complexity
Weisfeiler-Lehman optimal assignment kernel <small>Kriege et al., 2016</small>	 beyond $\mathcal{R}$ -convolutions	 undirected directed	 labelled	 labelled	$\mathcal{O}(hm)$

### 3.3.2.3 Deep graph kernels

Inspired by new models in natural language processing that are capable of generating word embeddings with semantic meanings (Mikolov *et al.*, 2013), Yanardag and Vishwanathan (2015) developed a framework that applies the same reasoning to substructures that arise from graph kernels. More precisely, given a graph kernel representation in terms of an inner product of feature vectors, *i.e.*


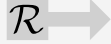


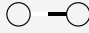
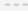
$$k(G, G') = \phi(G)^{\top} \phi(G'), \quad (3.71)$$

where  $G$  and  $G'$  are two graphs, they propose computing a diagonal matrix  $\mathcal{D} = \text{diag}(d_1, d_2, \dots)$ , of an appropriate size. The previous equation is then augmented to include weights of each individual substructure, such that

$$k_{\text{deep}}(G, G') := \phi(G)^\top \mathcal{D} \phi(G'), \quad (3.72)$$

which Yanardag and Vishwanathan (2015) denote as a “deep” variant of the previous kernel (equivalently, the previous equation can be seen as a simple reweighting similar to the kernels in Section 3.3.2.1 on p. 72).

The intuition behind this approach is to consider substructures of a graph kernel as “words” whose contexts can be calculated with standard methods (Mikolov *et al.*, 2013). This requires defining a proper co-occurrence relationship between the substructures of different kernels, and Yanardag and Vishwanathan (2015) define such relationships for some common kernels, namely the shortest-path kernel (Section 3.1.3.1), the graphlet kernel (Section 3.1.4.4), and the Weisfeiler–Lehman subtree kernel (Section 3.2.2.1). While the computational complexity of this approach is higher because of the additional embedding calculation step, the “deep variants” of some kernels are reported to achieve slightly higher classification accuracies.

	based on	graph type	node type	edge type	complexity
	 beyond $\mathcal{R}$ -convolutions	 undirected	 labelled	 labelled	

### 3.3.2.4 Core based kernel framework

Nikolentzos *et al.* (2018a) proposed a new framework of graph kernels by sequentially comparing nested subgraphs formed using a classic graph theoretic decomposition called a  $k$ -core decomposition. They layer such a decomposition with a base kernel, such as the shortest path or Weisfeiler–Lehman to generate a multi-scale view of the base kernel evaluated alongside the decomposition, which they find improves performance compared to the base kernels by providing a more nuanced view of similarity across different scales of the graphs. Before defining the kernel, we must first formally introduce a few concepts.

**DEFINITION 3.38 ( $k$ -core).** A  $k$ -core of graph  $G$ , denoted  $G_k = (V_k, E_k)$ , is the maximal subgraph of  $G$  such that  $\deg(v) \geq k$  for all  $v \in V_k$ , where  $\deg(v)$  is the degree of a vertex  $v$ . The nodes in the  $k$ -core need not all be connected, and thus  $G_k$  may contain multiple disconnected components.

DEFINITION 3.39 (Degeneracy). The *degeneracy* of a graph  $G$ ,  $\delta^*(G)$ , is determined by the largest non-empty  $k$ -core subgraph of  $G$ , i.e.  $\delta^*(G) = \max_k: G_k \neq \emptyset$ .

DEFINITION 3.40 ( $k$ -core decomposition). The  $k$ -core decomposition of  $G$  is the nested sequence of  $k$ -cores from  $k = 0, \dots, \delta^*(G)$ :  $G_0 \subseteq G \subseteq \dots \subseteq G_{\delta^*(G)}$ . We define the set of the  $k$ -core subgraphs of  $G$  as  $\mathcal{K}_G = \{G_0, \dots, G_{\delta^*(G)}\}$ .

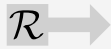


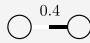
Fortunately,  $\mathcal{K}$  is quite efficient to compute, since one can proceed sequentially, starting with  $G_0$ , for each  $k$  remove any node  $v$  if  $\deg(v) < k$ .

DEFINITION 3.41 (Core based kernel). Given two graphs  $G$  and  $G'$  and their respective  $k$ -core decompositions  $\mathcal{K}$  and  $\mathcal{K}'$ , the *core based kernel* is defined as:

$$k_{\text{core}}(G, G') = \sum_{k=0}^p \kappa(G_k, G'_k), \quad (3.73)$$

where  $\kappa$  can be any valid base kernel, such as the shortest path kernel or Weisfeiler–Lehman kernel, and  $p = \min(\delta^*(G), \delta^*(G'))$ .

Due to the efficiency of the  $k$ -core decomposition, which can be achieved in linear time, the overall complexity for a pair of graphs hinges upon the complexity of the chosen base kernel  $\kappa$ .

	based on	graph type	node type	edge type	complexity
core based kernel framework <small>Nikolentzos et al., 2018</small>	 beyond $\mathcal{R}$ -convolutions	 undirected	 labelled attributed	 labelled attributed	---

### 3.4 Conclusion

This chapter provided an overview of the “zoo” of available graph kernels. It is clear that, due to the closure properties of kernel functions, even more graph kernels can be constructed from the existing ones. Certain overarching themes emerged though, one of the most common being the idea of enumerating certain substructures—such as shortest paths or subgraphs—and determine similarity by means of their co-occurrence in two graphs.

Graph kernels continue to be an active research topic, with recent publications focussing on topological attributes of graphs (Rieck *et al.*, 2019), or using more advanced concepts

from *optimal transport theory*, such as Wasserstein distances (Togninalli *et al.*, [2019](#)). We do not discuss these kernels in detail for reasons of brevity.

Subsequently, we will discuss how to properly *navigate* this zoo, *i.e.* we will discuss similarities in the practical performance of certain graph kernels, which will make it easier to pick a suitable one for a given application.

## 4 Experimental evaluation of graph kernels

While the previous chapters provided a thorough overview of the rich field of graph kernels, this chapter will focus on their practical performance. We are mostly interested in (i) analysing and explaining the empirical behaviour of graph kernels by means of numerous benchmark data sets, (ii) discussing differences and commonalities as well as other properties of the benchmark data sets, and (iii) ultimately providing some much-needed guidance to choose a suitable graph kernel in practice. To this end, we provide a thorough experimental setup for assessing the performance of individual graph kernels in a fair and comparative setup. The insights that we gain along the way will be used to inform our predictions and comments on future directions for (i) potential applications, (ii) the field of graph kernels, and (iii) requirements for benchmark data sets.

### 4.1 Data sets

We use the data sets provided by Kersting *et al.* (2016). They consist of more than 50 different graph data sets of varying sizes and complexity. Table 4.1 lists the data sets, along with some summary statistics. We observe that the graph data sets tend to be very sparse, *i.e.* their number of edges is roughly of the same order as their number of vertices. While this is not a issue per se, it can have an influence on the selection of a graph kernel. Neighbourhood-based approaches, for example, may suffer from reduced performance—both in the computational and in the predictive sense—when dealing with *dense* graphs: as the density of a graph approaches that of a complete graph, differences between individual node neighbourhoods start to become indiscernible. Figure 4.2 depicts the distribution of density values, whereas Figure 4.1 shows the average number of nodes versus the average number of edges of each data set in order to give a visual summary.

Moreover, we can see in the table that graphs with either node or edge attributes are under-represented, as most data sets contain labels but no continuous attributes. Of the 41 data sets in this section, 27 contain node labels while 12 have edge labels. Except for a single case, namely COIL-DEL, there are no data sets that have edge labels but no node labels. If a data set did not have node labels, we generated a node label using the degree of the node. For data sets without edge labels, we generated an edge label as the sorted concatenation of the node labels for the nodes incident to the edge. In the event that the data set has no node labels or edge labels, the edge label is assigned using the node labels that were created based on the node degree. The absence or presence of certain label or attributes might limit the applicability of certain graph kernels and we shall discuss the



implications of this later on when we categorise the data sets according to which labels and attributes each has.

**Excluded data sets** We excluded several data sets—such as the collection of Tox\_21 data sets—that are present in the original repository from the subsequent analysis because their size precludes running a sufficiently large number of graph kernels on them. Moreover, we removed the FIRSTMM\_DB data set because its small size makes it impossible to apply our training procedure that we describe in Section 4.2.3.

#### 4.1.1 Data set categorisation

Before discussing our experimental setup, we will first categorise the data sets we are working with and, where applicable, explain some of their common properties. Following the categorisation of Morris *et al.* (2020), the data sets included can be grouped into five primary groups: (i) social networks, (ii) small molecules, (iii) bioinformatics, (iv) computer vision, and (v) synthetic. We will now introduce each group in turn and indicate which data sets belong in each category.

**Social networks** Several data sets, such as COLLAB, IMDB-BINARY, IMDB-MULTI, REDDIT-BINARY, REDDIT-MULTI-5K and REDDIT-MULTI12K represent a kind of social network. While they often feature large graphs (with many nodes), they tend to have relatively few edges, and therefore low density. COLLAB is a notable exception to this, with a density of 0.51. All the data sets that we used in this category are fully unlabelled, meaning they do not have any node or edge labels or attributes.

**Small molecules** Another important category of the benchmark data sets are small molecules. This group contains the following data sets: AIDS, BZR, BZR\_MD, COX2, COX2\_MD, DHFR, DHFR\_MD, ER\_MD, FRANKENSTEIN, MUTAG, Mutagenicity, NCI1, NCI109, PTC\_FM, PTC\_FR, PTC\_MM, and PTC\_MR. While these graphs are often small (in terms of number of nodes) and often have a similar number of nodes and edges, the data sets BZR\_MD, COX2\_MD, DHFR\_MD and ER\_MD are a notable exception to that, since they are fully connected. This presents a challenge for methods based on neighbourhood aggregation, since each node is connected to all other nodes in the graphs. All the data sets in the small molecules category contain some kind of node or edge labels or attributes.

**Bioinformatics** The third group of data sets falls under the grouping of bioinformatics. Several data sets, such as DD, ENZYMES, PROTEINS, and PROTEINS\_full are data sets of

proteins, whereas KKI, OHSU, and Peking\_1 are representations of a brain. All of these data sets have node labels (ENZYMES and PROTEINS\_full also have node attributes), but all lack any information about their edges.

**Computer vision** The next category falls within the field of computer vision, where the COIL-DEL, COIL-RAG, Letter-high, Letter-low, Letter-med, MSRC\_9, MSRC\_21 and MSRC\_21C data sets represent graphs constructed from images. This group of data sets features a particularly large diversity among the data sets in terms of graph size and which node and label attributes they support, and we therefore refer the reader to Table 4.1.

**Synthetic** Finally, there are a few datasets which were synthetically created, namely SYNTHETIC, SYNTHETICnew, and Synthie. All graphs were endowed with node attributes by design, since there are relatively few data sets containing such attributes.

## 4.2 Experimental setup

Having explained the data sets we use, we now detail our experimental setup, which uses two phases: (i) computation of kernel matrices for each graph kernel, and (ii) classifier training based on the set of kernel matrices. Prior to discussing the details of these two steps, we discuss the included kernels.

### 4.2.1 Inclusion criteria

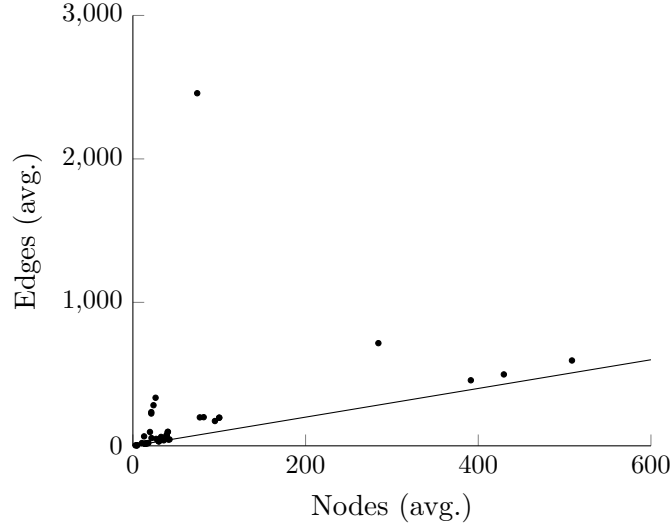
As we have seen in Chapter 3, there is a plethora of graph kernels. To make this review feasible, we had to restrict the computations to a subset of the existing graph kernels literature. In the following set of experiments, we tried to include a representative set of graph kernels from the ones whose code is openly available. Specifically, we made sure to include at least one kernel from each of the categories in Chapter 3. This comprises some graph kernels contained in the `graphkernels` software package for Python (Sugiyama *et al.*, 2017), others from the `graKel` software package for Python (Siglidis *et al.*, 2020) as well as several other kernels for which we were able to obtain an implementation.

**Table 4.1:** Summary statistics of the data sets used for the subsequent experiments. Data set sizes vary but most of the graphs are comparatively small.

Data set	Graphs	Classes	Density	Nodes (avg.)	Edges (avg.)	N. attr.	E. attr.	Node labels	Edge labels
AIDS	2000	2	0.19	15.69	16.20	4		✓	✓
BZR	405	2	0.06	35.75	38.36	3		✓	✓
BZR_MD	306	2	1.00	21.30	225.06		1	✓	✓
COIL-DEL	3900	100	0.33	21.54	54.24	2		✓	✓
COIL-RAG	3900	100	0.92	3.01	3.02	64	1	✓	✓
COLLAB	5000	3	0.51	74.49	2457.78			✓	✓
COX2	467	2	0.05	41.22	43.45	3		✓	✓
COX2_MD	303	2	1.00	26.28	335.12		1	✓	✓
DD	1178	2	0.03	284.32	715.66			✓	✓
DHFR	756	2	0.05	42.43	44.54	3		✓	✓
DHFR_MD	393	2	1.00	23.87	283.02		1	✓	✓
ENZYMES	600	6	0.16	32.63	62.14	18		✓	✓
ER_MD	446	2	1.00	21.33	234.85		1	✓	✓
FRANKENSTEIN	4337	2	0.17	16.90	17.88	780		✓	✓
IMDB-BINARY	1000	2	0.52	19.77	96.53			✓	✓
IMDB-MULTI	1500	3	0.77	13.00	65.94			✓	✓
KKI	83	2	0.18	26.96	48.42			✓	✓
Letter-high	2250	15	0.58	4.67	4.50	2		✓	✓
Letter-low	2250	15	0.42	4.68	3.13	2		✓	✓
Letter-med	2250	15	0.42	4.67	3.21	2		✓	✓
MSRC_21	563	20	0.07	77.52	198.32			✓	✓
MSRC_21C	209	17	0.12	40.28	96.60			✓	✓
MSRC_9	221	8	0.12	40.58	97.94			✓	✓
MUTAG	188	2	0.14	17.93	19.79			✓	✓
Mutagenicity	4337	2	0.09	30.32	30.77			✓	✓
NCI1	4110	2	0.09	29.87	32.30			✓	✓
NCI109	4127	2	0.09	29.68	32.13			✓	✓
OHSU	79	2	0.08	82.01	199.66			✓	✓
PROTEINS	1113	2	0.21	39.06	72.82			✓	✓
PROTEINS_full	1113	2	0.21	39.06	72.82	29		✓	✓
PTC_FM	349	2	0.22	14.11	14.48			✓	✓
PTC_FR	351	2	0.21	14.56	15.00			✓	✓
PTC_MM	336	2	0.22	13.97	14.32			✓	✓

**Table 4.1:** Summary statistics of the data sets used for the subsequent experiments. Data set sizes vary but most of the graphs are comparatively small.

Data set	Graphs	Classes	Density	Nodes (avg.)	Edges (avg.)	N. attr.	E. attr.	Node labels	Edge labels
PTC_MR	344	2	0.21	14.29	14.69			✓	✓
Peking_1	85	2	0.13	39.31	77.35			✓	✗
REDDIT-BINARY	2000	2	0.02	429.63	497.75			✗	✗
REDDIT-MULTI-12K	11929	11	0.02	391.41	456.89			✗	✗
REDDIT-MULTI-5K	4999	5	0.01	508.52	594.87			✗	✗
SYNTHETIC	300	2	0.04	100.00	196.00	1		✓	✗
SYNTHETICnew	300	2	0.04	100.00	196.25	1		✗	✗
Synthetic	400	4	0.04	95.00	172.93	15		✗	✗



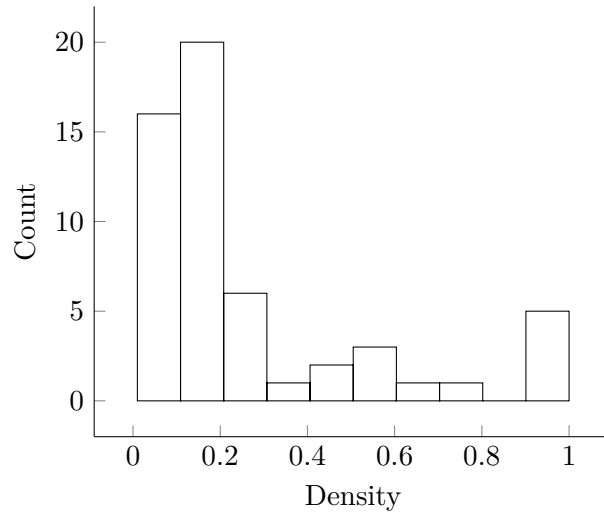
**Figure 4.1:** A visualisation of the average number of nodes and the average number of edges for each data set. Most of the data sets are extremely *sparse*, featuring only a small number of nodes and edges on average.

Specifically, we included the following kernels:

- (i) the GraphHopper kernel (Feragen *et al.*, 2013, GH),
- (ii) the graphlets kernel (Shervashidze *et al.*, 2009, GL),
- (iii) two histogram kernels (based on vertex (V) and edge labels (E), respectively),
- (iv) two instances of the hash graph kernels framework (Morris *et al.*, 2016, HGK-SP, HGK-WL),
- (v) the message passing kernel (Nikolentzos and Vazirgiannis, 2018, MP),
- (vi) the multiscale Laplacian graph kernel (Kondor and Pan, 2016, MLG),
- (vii) the random walk kernel (Vishwanathan *et al.*, 2006, RW),
- (viii) the shortest-path kernel (Borgwardt and Kriegel, 2005, SP),
- (ix) the subgraph matching kernel (Kriege and Mutzel, 2012, CSM),
- (x) the Weisfeiler–Lehman subtree kernel (Shervashidze *et al.*, 2011, WL), and
- (xi) the Weisfeiler–Lehman optimal assignment kernel (Kriege *et al.*, 2016, WL-OA).

#### 4.2.2 Kernel matrix computation

For each of the included graph kernels, we generate a set of full kernel matrices, *i.e.* kernel matrices between all pairs of graphs of the input data set. We account for the parameters of a graph kernel by generating a new matrix for all possible combinations of parameter values. While seemingly wasteful, this ensures that we are able to perform



**Figure 4.2:** A histogram of the density values of the graphs. Few dense or complete graphs can be found among the benchmark data sets.

a proper hyperparameter optimisation of each kernel and select the *best*—in terms of predictive performance—parameter set for each algorithm. As a brief example, consider the Weisfeiler–Lehman subtree kernel. Its single parameter is  $h$ , the subtree depth. In this case, we calculate a collection of kernel matrices that are indexed by the respective value of  $h$ . Table 4.2 lists the parameters used to create the set of kernel matrices and which information from the graph is processed by each kernel. For some of the graph kernels, parameter selection is dictated by computational efficiency (graphlet enumeration does not scale well to higher-order graphlets, for example). For other kernels, we used parameter ranges suggested by the authors. If the parameter ranges suggested by the authors were too expansive to successfully run in 120 hours, we resorted to a subset of the original parameters in order to obtain results. Additionally, some kernels allowed for the specification of additional kernels on node and/or edge attributes. In the GraphHopper kernel, we used a gaussian kernel on the node attributes, with  $\gamma = \frac{1}{d}$ , where  $d$  is the dimension of the node attributes (or one-hot representations of the node labels, if there were no node attributes), as was suggested by the authors. In the subgraph matching kernel, we used the Brownian bridge kernel for node attributes (when present) and the triangular kernel for edge attributes (when present), with the parameters specified in Table 4.2. While some kernels can theoretically incorporate more graph information, we found that many of the available implementations did not allow for it out of the box. Our results accordingly largely reflect what the implementations currently natively support.

**Table 4.2:** Selected parameters for each of the graph kernels. TP refers to the triangular kernel, and BB is the Brownian bridge kernel. Please refer to the indicated page for more details about the parameters. \* indicates that node labels were used if there were no node attributes.

Kernel	Reference	Parameters	Node labels	Node attr.	Edge labels	Edge attr.
GraphHopper	p. 31	$\gamma = \frac{1}{d}$		✓*		
Graphlets	p. 37	$k \in \{3, 4, 5\}$				
HGK-SP	p. 69	$\emptyset$	✓	✓		
HGK-WL	p. 69	$h \in \{0, 1, 2, 3, 4, 5, 6, 7\}$	✓	✓		
Histogram (V)	p. 26	$\emptyset$	✓			
Histogram (E)	p. 28	$\emptyset$			✓	
Message passing	p. 59	$T \in \{1, 2, 3, 4\},$ $\alpha = 0.8, \beta = 0.2$	✓			
Multiscale Laplacian	p. 62	$\eta, \gamma \in \{0.01, 0.1\},$ $r, l \in \{2, 3\}$	✓			
Shortest-path	p. 29	$\emptyset$	✓			
Subgraph matching	p. 66	$k \in \{3, 4, 5\}$ BB: $c = 3$ TP: $c \in \{0.1, 0.5, 1.0\}$	✓	✓	✓	✓
Random walk	p. 43	✓				
WL subtree	p. 47	$h \in \{0, 1, 2, 3, 4, 5, 6, 7\}$	✓			
WL-OA	p. 74	$h \in \{0, 1, 2, 3, 4, 5, 6, 7\}$	✓			

### 4.2.3 Training procedure

Given a set of kernel matrices that belong to a certain graph kernel, we use a nested cross-validation procedure, as this ensures that we obtain a suitable assessment of the generalisation performance of a kernel without risking to suffer from overfitting. Our outer cross-validation loop employs a stratified 10-fold cross-validation (randomly shuffled), while the inner loop uses a 5-fold cross-validated grid search, which is used to determine the *best* parameter set of a kernel. In addition, this procedure is repeated 10 times so that we can report an average performance value and its standard deviation. We use a standard support vector machine (SVM) classifier with a precomputed kernel matrix. The setup and the training times are thus comparable—by contrast, it is possible to use different implementations in different programming languages. The SVM uses  $C \in \{10^{-3}, 10^{-2}, \dots, 10^2, 10^3\}$ . In addition, we consider *normalising* each kernel matrix to be

a trainable hyperparameter. Hence, we make it possible to replace each kernel matrix  $K = (k_{ij})_{i,j \in \{1, \dots, n\}}$  by  $K' = (k'_{ij})_{i,j \in \{1, \dots, n\}}$ , where

$$k'_{ij} = \frac{k_{ij}}{\sqrt{k_{ii}k_{jj}}}, \quad (4.1)$$

which is a non-linear normalisation. Intuitively, this can be seen as the “kernel variant” of restricting  $d$ -dimensional feature vectors to lie on a unit hypersphere; in this case, however, the hypersphere is “measured” via the kernel function, instead of the usual metric of a space. Such a normalisation can have a positive impact on SVM classifiers (Graf and Borer, 2001). Our experiments indicate, however, that normalisation is rarely required to obtain good performance values.

#### 4.2.4 Training environment

Training is performed on a multi-core cluster system. Each kernel is allocated 120 h of multi-core processing time for its graph kernel matrix computation, followed by an additional 120 h to perform hyperparameter search and model fitting. Moreover, we use a maximum of 500 iterations to fit the SVM classifier. Convergence is usually obtained much more rapidly, but the restriction ensures that we are able to train all graph kernels.

Our training environment necessitated the cross-validation setup described above; with a nested 10-fold cross-validation in which both the inner cross-validation loop and the outer loop use 10 folds, some graph kernels would be penalised because their hyperparameter search procedure would not converge. In the interest of fairness, we selected parameters that allowed the majority of graph kernels to be trained, despite some of them—such as the multiscale Laplacian graph kernel—requiring very dense parameter grids. We thus opted for a 5-fold cross-validated grid search, as described above. Moreover, every kernel is allocated a computational budget of 128 GB of RAM, in order to specify a realistic training environment. Any runs that fail to satisfy these requirements have been marked with “OOM” (short for “out-of-memory”). In some cases, the kernel matrices did not finish computing in 120h, and thus have been marked with “OOT” (short for “out of time”). Graph kernels whose implementations preclude handling a certain data set have been marked with “NA” to indicate that results are “not available”. The code used for our experiments can be found at <https://github.com/BorgwardtLab/graphkernels-review/>.



**Table 4.3:** Class ratio of the data sets that we used in the subsequent experiments. For binary classification problems, we provide an (approximate) class ratio, whereas for multi-class problems we either list label counts individually or give the imbalance with respect to the largest class. A value of 1 : 1 means that the data set is (almost) perfectly balanced. Such data sets are printed with an additional asterisk (\*) after their name.

Data set	Graphs	Classes	Class balance
AIDS	2000	2	4 : 1
BZR	405	2	$\approx$ 4 : 1
BZR_MD*	306	2	$\approx$ 1 : 1
COIL-DEL*	3900	100	1 : 1
COIL-RAG*	3900	100	1 : 1
COLLAB	5000	3	2600 : 1625 : 775
COX2	467	2	$\approx$ 4 : 1
COX2_MD*	303	2	$\approx$ 1 : 1
DD	1178	2	$\approx$ 2 : 1
DHFR	756	2	$\approx$ 2 : 1
DHFR_MD	393	2	$\approx$ 2 : 1
ENZYMES*	600	6	1 : 1
ER_MD	446	2	$\approx$ 2 : 1
FRANKENSTEIN*	4337	2	$\approx$ 1 : 1
IMDB-BINARY*	1000	2	1 : 1
IMDB-MULTI*	1500	3	1 : 1
KKI*	83	2	$\approx$ 1 : 1
Letter-high*	2250	15	1 : 1
Letter-low*	2250	15	1 : 1
Letter-med*	2250	15	1 : 1
MSRC_21*	563	20	$\approx$ 1 : 1
MSRC_21C	209	17	$\approx$ 10 : 1
MSRC_9*	221	8	$\approx$ 1 : 1
MUTAG	188	2	$\approx$ 2 : 1
Mutagenicity*	4337	2	$\approx$ 1 : 1
NCI1*	4110	2	$\approx$ 1 : 1
NCI109*	4127	2	$\approx$ 1 : 1
OHSU*	79	2	$\approx$ 1 : 1
PROTEINS	1113	2	$\approx$ 2 : 1
PROTEINS_full	1113	2	$\approx$ 2 : 1
PTC_FM	349	2	$\approx$ 2 : 1
PTC_FR	351	2	$\approx$ 2 : 1
PTC_MM	336	2	$\approx$ 2 : 1
PTC_MR*	344	2	$\approx$ 1 : 1
Peking_1*	85	2	$\approx$ 1 : 1
REDDIT-BINARY*	2000	2	1 : 1
REDDIT-MULTI-12K	11929	11	$\approx$ 3 : 1
REDDIT-MULTI-5K*	4999	5	1 : 1
SYNTHETIC*	300	2	1 : 1
SYNTHETICnew*	300	2	1 : 1
Synthie*	400	4	$\approx$ 1 : 1

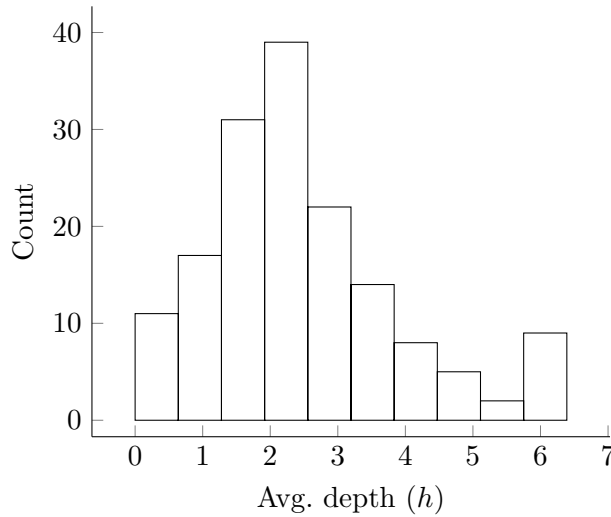
### 4.2.5 Evaluation procedure

As the listing of class ratios in Table 4.3 shows, most of the data sets are balanced and consist of two classes. We thus use *accuracy* as our main evaluation measure. For multi-class data sets, an evaluation in terms of the area under the Receiver Operating Characteristic curve (AUROC). For two classes (which are by custom termed “positive” and “negative”), this measure defines the probability that a randomly-selected positive example is assigned a *higher* score than a randomly-selected negative example. AUROC can therefore be understood as a measure of how well a classifier is able to distinguish between two classes. Being scale-invariant, AUROC is suitable for comparing classifiers *across* data sets. In order to extend this binary measure to a multi-class situation, we calculate AUROC values for all one-versus-rest classification scenarios and calculate their mean. This is also known as “macro averaging” (Yang, 1999). We provide macro-averaged AUROC values in an additional table and for all analyses that compare kernels *across* data sets.

## 4.3 Classification performance

This section details the performance of numerous graph kernels on all data sets. Table 4.4 provides the accuracies and standard deviations of what we consider to be the baseline graph kernels, namely the node and edge label histograms. Table 4.5 summarises the additional, more sophisticated graph kernel results in terms of mean accuracy and standard deviations, calculated over the 10 iterations of our training procedure. In addition, Table 4.6 and Table 4.7 provide a similar summary of the performance in terms of AUROC. Given the density of the tables, we will subsequently discuss the results in more detail and under different aspects, such as a breaking down values by data set type.

**Overall assessment** Before delving into various aspects of the performance of these kernels, we want to briefly comment on some global patterns that are observable in the table. First, in Table 4.5, it is striking to observe that the best-performing algorithms on every data set tend to employ the Weisfeiler–Lehman relabelling procedure, or a variant thereof: out of 41 data sets, MP (the message passing kernel, which is based on the Weisfeiler–Lehman relabelling procedure) exhibits the best performance in 10 data sets. In addition, WL-OA (the optimal assignment variant of the Weisfeiler–Lehman subtree scheme) outperforms all other kernels on 6 data sets, while HGK-WL (the hash graph kernel variant of the Weisfeiler–Lehman subtree kernel) does so on 4 data sets. Last, the Weisfeiler–Lehman subtree kernel leads on a single data set. Consequently, on 21 out of 41 data sets, kernels based on the principles of the Weisfeiler–Lehman relabelling procedure



**Figure 4.3:** A histogram of the average depth, *i.e.* the average number of iterations  $h$  over all folds of the training, of graph kernels that are based on a variant of the Weisfeiler–Lehman framework.

outperform all other kernels. On the outset, it thus seems that higher performance can be achieved by looking at decompositions of the graph—for the Weisfeiler–Lehman procedure, these decompositions are provided by increasing neighbourhoods. In the following, we will look more closely at this aspect.

**The impact of  $h$**  Given that algorithms based on Weisfeiler–Lehman relabelling are among the top performers on the benchmark data sets, we analyse their performance in more detail. Our main question is to what extent a sufficient propagation depth into a graph is required in order to achieve good performance. To this end, Figure 4.3 depicts the mean “depth”—*i.e.* the mean number of iterations  $h$ —over the training process of these graph kernels. A value of  $h = 0$  would be tantamount to *not* using any neighbourhood information at all; higher values indicate that information from more distant neighbourhoods is propagated. Overall, we observe that all graph kernels that are capable of propagating information across neighbourhoods—which can also be seen as diffusing information of the graph over different scales—tend to do so in order to reach their final accuracy values. This demonstrates that graph kernels need to be capable of analysing the graph at multiple scales.

**Table 4.4:** Empirical performance of the baseline graph kernels, the vertex histogram (H(V)) and edge histogram (H(E)) on the benchmark data sets. The mean accuracy over 10 iterations of a nested cross-validation procedure is shown along with its corresponding standard deviation. The highest mean accuracy of each data set across the baseline kernels and the normal kernels is shown in **red**. OOM means “out-of-memory”, OOT means “out-of-time”, and NA indicates that the given implementation could not handle a certain data set.

Data set	H(V)	H(E)
AIDS	<b>99.70±0.00</b>	99.28±0.07
BZR	65.18±0.93	77.36±1.11
BZR_MD	70.44±1.25	65.49±1.76
COIL-DEL	15.03±0.27	7.81±0.28
COIL-RAG	7.79±0.07	NA
COLLAB	31.32±2.53	79.52±0.44
COX2	59.71±0.92	73.89±1.02
COX2_MD	62.80±0.93	60.03±1.16
DD	68.68±3.04	78.52±0.34
DHFR	60.25±0.36	67.55±0.86
DHFR_MD	67.92±0.08	62.24±1.78
ENZYMES	25.20±0.96	27.33±0.80
ER_MD	66.88±1.00	69.79±1.35
FRANKENSTEIN	64.96±0.34	60.33±1.90
IMDB-BINARY	50.58±0.20	73.46±0.60
IMDB-MULTI	34.90±0.31	50.38±0.55
KKI	52.40±2.66	48.97±2.32
Letter-high	36.69±0.52	NA
Letter-low	47.93±0.33	NA
Letter-med	43.93±0.55	NA
MSRC_21	89.45±0.41	90.04±0.84
MSRC_21C	83.36±1.39	84.68±0.77
MSRC_9	89.36±0.84	<b>93.17±1.09</b>
MUTAG	85.98±0.40	85.14±1.03
Mutagenicity	67.01±0.83	49.13±1.75
NCI1	64.66±0.53	51.71±1.45
NCI109	63.24±0.54	51.45±2.06
OHSU	51.86±3.05	54.23±3.59
PROTEINS	70.13±1.61	69.32±0.92
PROTEINS_full	70.13±1.61	69.32±0.92
PTC_FM	58.12±0.85	57.57±1.40
PTC_FR	<b>67.84±0.16</b>	40.26±2.03
PTC_MM	<b>66.55±0.61</b>	41.36±1.13
PTC_MR	58.46±0.27	53.03±2.21
Peking_1	57.75±3.03	55.12±4.12
REDDIT-BINARY	50.03±2.24	78.94±0.60
REDDIT-MULTI-12K	7.34±1.59	31.06±0.31
REDDIT-MULTI-5K	17.86±2.13	45.72±0.22
SYNTHETIC	50.00±0.00	50.00±0.00
SYNTHETICnew	62.30±0.55	71.20±1.69
Synthie	48.78±1.33	47.17±1.81

**Table 4.5:** Empirical performance of graph kernels on the benchmark data sets. The mean accuracy over 10 iterations of a nested cross-validation procedure is shown along with its corresponding standard deviation. The highest mean accuracy of each data set across the baseline kernels and the normal kernels **red**. OOM means “out-of-memory”, OOT means “out-of-time”, and NA indicates that the given implementation could not handle a certain data set.

Data set	CSM	GH	Graphlet	HGK-SP	HGK-WL	MLG	MP	SP	RW	WL	WL-OA
ATDS	99.47±0.05	99.13±0.07	98.05±0.14	99.38±0.02	98.76±0.09	98.38±0.14	99.46±0.06	99.64±0.02	<b>99.70±0.00</b>	99.52±0.10	99.69±0.02
BZR	84.54±0.65	79.32±0.48	79.20±0.65	81.99±0.30	81.42±0.60	88.04±0.70	<b>88.08±0.93</b>	81.58±0.75	76.63±1.76	87.16±0.97	87.43±0.81
BZR_MD	<b>77.63±1.29</b>	51.99±0.25	52.71±0.24	60.08±0.88	52.64±1.20	51.46±0.61	65.11±1.59	68.90±1.61	68.98±1.28	67.45±1.20	68.19±1.09
COIL-DEL	OOT	OOM	NA	66.19±0.20	61.39±0.29	3.90±0.19	<b>80.94±0.49</b>	17.32±0.23	OOT	16.68±0.29	16.56±0.31
COIL-RAG	NA	OOM	4.91±0.10	91.65±0.26	<b>91.11±0.47</b>	OOM	83.50±0.39	NA	NA	7.83±0.08	7.90±0.10
COLLAB	OOT	OOM	NA	77.15±0.15	OOM	OOM	<b>80.93±0.28</b>	79.92±0.37	OOM	68.25±1.50	80.18±0.25
COX2	79.78±1.04	78.16±0.00	49.90±0.00	78.16±0.00	78.16±0.00	76.76±0.87	80.76±0.78	78.03±1.10	63.21±5.27	79.67±1.32	<b>81.08±0.89</b>
COX2_MD	OOT	60.99±1.06	51.15±0.00	59.92±0.66	57.15±1.20	51.15±0.00	61.81±1.51	<b>64.95±1.09</b>	63.14±1.57	60.07±2.22	62.37±2.11
DD	OOM	OOM	NA	OOM	75.35±0.94	75.68±0.84	79.02±0.25	<b>80.22±0.51</b>	OOM	77.73±1.97	77.78±1.22
DHFR	77.99±0.96	68.70±0.86	60.98±0.00	72.48±0.65	75.35±0.66	<b>83.22±0.94</b>	80.47±0.92	79.35±1.55	OOT	81.72±0.80	82.40±0.97
DHFR_MD	OOT	<b>67.95±0.00</b>	<b>67.95±0.00</b>	<b>67.95±0.00</b>	66.08±1.02	<b>67.95±0.00</b>	66.07±0.88	63.76±2.15	64.35±1.43	62.56±1.51	64.10±1.70
ENZYMES	<b>66.38±1.14</b>	46.53±1.26	NA	63.07±0.69	54.53±1.34	51.17±1.59	60.02±0.75	41.27±1.18	26.10±1.15	54.27±0.94	58.88±0.85
ER_MD	OOT	59.42±0.00	59.42±0.00	59.42±0.00	66.72±1.28	60.72±0.69	<b>71.62±1.20</b>	70.55±0.86	NA	70.35±1.01	70.96±0.75
FRANKENSTEIN	OOT	OOM	56.28±0.19	56.05±0.10	63.69±0.51	<b>72.36±0.22</b>	57.01±0.66	58.85±1.96	OOT	71.81±0.31	72.02±0.30
IMDB-BINARY	OOT	OOM	NA	73.34±0.47	72.75±1.02	52.56±0.42	72.28±0.75	72.23±0.78	<b>74.20±0.76</b>	71.15±0.47	74.01±0.66
IMDB-MULTI	OOT	OOM	NA	<b>51.58±0.42</b>	50.73±0.63	34.27±0.33	49.55±0.68	51.31±0.28	50.13±0.50	50.25±0.72	49.95±0.46
KKI	49.56±3.50	<b>55.22±0.75</b>	NA	53.07±2.52	52.64±1.67	53.59±3.44	46.53±5.95	47.21±3.05	48.26±4.51	53.90±2.42	54.05±2.27
Letter-high	NA	OOM	33.64±0.91	87.96±0.31	<b>90.54±0.32</b>	16.08±1.18	86.07±0.50	NA	NA	37.56±0.26	37.41±0.39
Letter-low	NA	OOM	45.94±0.54	99.29±0.04	<b>99.66±0.03</b>	22.01±0.35	99.52±0.12	NA	NA	49.94±0.31	49.89±0.22
Letter-med	NA	OOM	41.31±0.38	92.25±0.19	93.82±0.17	19.03±1.16	<b>94.56±0.27</b>	NA	NA	45.47±0.28	45.84±0.39
MSRC_21	OOT	86.66±0.57	NA	84.36±0.41	78.18±0.54	67.67±0.67	<b>90.47±0.75</b>	90.04±0.74	OOT	89.19±0.63	89.42±0.55
MSRC_21C	83.24±0.80	81.35±1.32	NA	81.21±0.76	75.18±0.99	60.56±2.13	84.55±0.45	84.49±0.90	82.13±1.33	82.96±1.45	<b>85.70±1.56</b>
MSRC_9	92.50±1.30	89.85±0.65	NA	89.26±0.80	88.46±0.57	79.74±2.51	90.21±0.67	92.59±0.67	91.18±1.18	89.87±1.07	91.16±1.07
MUTAG	<b>87.29±1.25</b>	81.07±0.45	67.38±0.45	80.90±0.48	75.51±1.34	78.53±2.25	86.98±1.09	85.06±1.28	85.62±1.84	85.75±1.96	86.10±1.95
Mutagenicity	OOT	OOM	55.31±0.03	71.83±0.15	80.12±0.39	OOM	79.03±0.32	50.75±2.50	OOT	82.03±0.44	<b>83.24±0.65</b>
NCI1	OOT	OOM	50.98±0.47	69.55±0.16	81.26±0.21	78.17±0.33	78.05±0.76	55.76±1.68	OOT	85.60±0.36	<b>85.95±0.23</b>
NCI109	OOT	OOM	50.55±0.07	69.56±0.19	80.69±0.19	78.01±0.58	76.75±0.39	55.78±2.01	OOT	85.76±0.22	<b>86.17±0.19</b>
OH5U	52.66±3.37	<b>55.79±0.00</b>	NA	50.74±1.73	55.40±0.64	54.80±3.18	54.63±2.22	52.16±2.81	OOT	52.36±3.08	52.36±3.08
PROTEINS	OOT	75.08±0.29	NA	74.53±0.35	73.65±0.72	75.55±0.71	73.30±0.64	<b>75.72±0.42</b>	OOM	73.06±0.47	73.50±0.87
PROTEINS_full	69.35±0.25	OOM	NA	<b>75.92±0.49</b>	75.57±0.48	75.55±0.71	73.86±0.83	75.72±0.42	OOM	73.06±0.47	73.50±0.87

**Table 4.5:** Empirical performance of graph kernels on the benchmark data sets. The mean accuracy over 10 iterations of a nested cross-validation procedure is shown along with its corresponding standard deviation. The highest mean accuracy of each data set across the baseline kernels and the normal kernels **red**. OOM means “out-of-memory”, OOT means “out-of-time”, and NA indicates that the given implementation could not handle a certain data set.

Data set	CSM	GH	Graphlet	HGK-SP	HGK-WL	MLG	MP	SP	RW	WL	WL-OA
PTC_FM	59.75±1.90	63.63±0.62	58.59±0.50	63.78±0.33	<b>64.38±0.71</b>	59.87±1.64	63.09±1.97	62.44±0.84	62.35±1.00	61.77±1.92	61.98±2.22
PTC_FR	59.97±2.57	66.53±0.31	65.53±0.00	67.50±0.25	67.81±0.24	66.25±0.72	64.76±1.70	64.56±1.57	39.10±2.76	65.68±1.59	65.17±1.41
PTC_MM	62.34±0.90	64.23±0.60	60.02±0.40	64.71±0.78	65.69±0.97	60.71±0.80	65.19±1.68	64.23±0.64	56.22±1.53	64.36±2.36	64.18±1.18
PTC_MR	59.40±1.88	57.76±1.44	54.45±0.37	57.48±1.14	59.87±1.00	60.37±1.57	<b>61.24±2.21</b>	57.26±2.43	53.25±1.63	59.97±1.95	60.38±1.40
Peking_1	55.86±3.49	OOM	NA	<b>58.74±2.11</b>	56.13±2.39	53.82±2.79	57.70±4.04	54.79±2.42	OOT	56.90±2.02	56.22±2.52
REDDIT-BINARY	OOM	OOM	NA	OOM	OOM	OOM	<b>89.24±0.48</b>	89.20±0.37	OOM	77.95±0.60	87.60±0.33
REDDIT-MULTI-12K	OOM	OOM	NA	OOM	OOM	OOM	<b>42.09±0.31</b>	31.06±0.63	OOM	26.88±0.62	OOM
REDDIT-MULTI-5K	OOM	OOM	NA	OOM	OOM	OOM	50.85±0.47	45.54±0.75	OOM	<b>51.63±0.37</b>	OOM
SYNTHETIC	66.27±1.71	58.83±0.98	50.00±0.00	59.93±1.24	<b>74.07±1.13</b>	50.00±0.00	50.00±0.00	50.00±0.00	OOT	50.00±0.00	50.00±0.00
SYNTHETICnew	94.47±0.50	58.73±0.93	NA	63.73±1.59	71.60±1.94	82.97±2.06	62.00±2.38	82.97±1.07	OOT	97.87±0.61	<b>98.10±0.39</b>
Synthetic	51.05±1.70	68.07±0.79	NA	82.38±0.63	50.04±0.69	50.26±2.83	<b>96.57±0.50</b>	47.38±2.23	OOT	48.53±2.01	48.88±2.40

**Table 4.6:** Empirical performance of the baseline graph kernels on the benchmark data sets. The mean area under the Receiver Operating Characteristic curve (AUROC) over 10 iterations of a nested cross-validation procedure is shown along with its corresponding standard deviation. The highest AUROC value for each data set (considering the baseline kernels and normal kernels) is shown in **red**. OOM means “out-of-memory”, OOT means “out-of-time”, and NA indicates that the given implementation could not handle a certain data set.

Dataset	H(V)	H(E)
AIDS	99.62±0.02	99.64±0.02
BZR	72.85±0.60	57.29±2.23
BZR_MD	75.86±0.94	67.83±1.36
COIL-DEL	88.82±0.05	82.94±0.08
COIL-RAG	76.40±0.12	NA
COLLAB	50.29±2.37	90.78±0.17
COX2	64.65±0.71	69.86±2.16
COX2_MD	67.54±0.66	57.94±1.68
DD	76.40±4.99	84.87±0.25
DHFR	42.49±2.50	72.41±0.70
DHFR_MD	47.11±2.92	52.50±2.63
ENZYMES	59.47±0.32	62.36±0.67
ER_MD	75.17±0.53	<b>79.10±0.73</b>
FRANKENSTEIN	71.23±0.11	38.01±3.41
IMDB-BINARY	49.62±0.41	81.25±0.57
IMDB-MULTI	50.66±0.84	<b>67.26±0.51</b>
KKI	47.48±5.02	50.41±4.20
Letter-high	87.13±0.03	NA
Letter-low	93.55±0.05	NA
Letter-med	91.55±0.04	NA
MSRC_21	99.22±0.05	99.14±0.07
MSRC_21C	95.22±1.27	94.63±0.58
MSRC_9	98.58±0.18	99.05±0.14
MUTAG	89.80±1.05	89.20±0.79
Mutagenicity	73.70±0.37	50.80±2.40
NCI1	70.38±0.25	50.78±4.44
NCI109	69.19±0.68	49.40±3.44
OHSU	48.28±5.97	41.45±3.81
PROTEINS	77.68±0.37	75.46±0.29
PROTEINS_full	77.68±0.37	75.46±0.29
PTC_FM	50.02±4.26	44.69±2.42
PTC_FR	53.48±1.81	55.91±2.99
PTC_MM	63.53±1.71	47.29±2.98
PTC_MR	50.46±2.95	45.86±2.93
Peking_1	40.85±5.02	46.89±7.56
REDDIT-BINARY	49.12±6.96	84.81±0.31
REDDIT-MULTI-12K	44.52±1.75	77.65±0.08
REDDIT-MULTI-5K	44.78±4.14	78.01±0.14
SYNTHETIC	50.00±0.00	50.00±0.00
SYNTHETICnew	62.78±0.52	76.18±0.64
Synthie	83.20±0.82	82.97±0.76

**Table 4.7:** Empirical performance of graph kernels on the benchmark data sets. The mean area under the Receiver Operating Characteristic curve (AUROC) over 10 iterations of a nested cross-validation procedure is shown along with its corresponding standard deviation. The highest AUROC value for each data set (considering the baseline kernels and normal kernels) is shown in **red** OOM means “out-of-memory”, OOT means “out-of-time”, and NA indicates that the given implementation could not handle a certain data set.

Data set	CSM	GH	Graphlet	HGK-SP	HGK-WL	MLG	MP	SP	RW	WL	WL-OA
ATDS	99.64±0.04	99.57±0.02	99.56±0.06	99.61±0.02	99.25±0.05	98.57±0.10	99.64±0.02	99.64±0.02	<b>99.67±0.01</b>	99.61±0.04	99.63±0.03
BZR	85.17±1.14	73.06±1.20	49.81±3.39	79.45±0.80	83.77±0.88	<b>89.49±1.14</b>	89.03±1.07	76.05±3.13	60.53±1.43	87.16±0.89	87.77±1.36
BZR_MD	<b>85.53±1.05</b>	48.40±7.05	35.35±3.32	68.96±2.09	48.14±8.64	35.11±2.89	67.41±1.41	75.37±1.69	75.70±1.05	70.24±1.00	73.13±1.45
COIL-DEL	OOT	OOM	NA	98.93±0.02	98.13±0.03	53.91±5.43	<b>99.43±0.02</b>	89.34±0.07	OOT	88.34±0.14	87.85±0.12
COIL-RAG	NA	OOM	73.16±0.15	<b>99.85±0.01</b>	99.83±0.01	OOM	99.36±0.02	NA	NA	76.57±0.14	76.73±0.14
COLLAB	OOT	OOM	NA	91.17±0.21	OOM	OOM	<b>92.97±0.20</b>	91.87±0.20	OOM	81.48±1.66	92.70±0.09
COX2	81.63±1.00	69.65±0.79	44.98±0.43	73.47±1.00	73.19±1.32	74.32±0.93	<b>81.82±1.50</b>	75.70±4.88	55.10±3.68	79.87±1.01	79.96±0.51
COX2_MD	OOT	59.61±3.86	48.76±2.05	64.54±0.65	53.29±2.53	48.54±1.17	63.78±1.32	<b>69.12±0.78</b>	68.57±1.64	63.37±2.87	65.38±2.59
DD	OOM	OOM	NA	OOM	84.51±0.48	82.16±0.39	85.51±0.44	<b>87.44±0.38</b>	OOM	83.93±1.90	84.75±1.41
DHFR	85.40±0.80	76.21±0.46	45.44±1.47	77.95±0.48	80.39±0.66	88.66±0.71	88.41±0.58	85.79±0.94	OOT	89.49±0.65	<b>90.17±0.74</b>
DHFR_MD	OOT	54.50±2.69	47.62±4.04	<b>62.65±4.39</b>	56.66±1.79	54.69±1.85	60.05±2.21	54.37±2.82	57.92±2.96	55.72±2.46	61.84±1.44
ENZYMES	<b>91.73±0.47</b>	78.97±0.41	NA	87.97±0.36	84.00±0.39	79.79±0.82	85.37±0.57	74.67±0.53	62.56±0.93	80.45±0.46	84.86±0.48
ER_MD	OOT	72.86±0.28	70.39±0.35	72.58±0.34	71.13±1.10	61.42±1.16	73.28±1.17	76.18±0.91	NA	73.28±1.16	75.84±0.98
FRANKENSTEIN	OOT	OOM	60.09±2.41	65.14±1.21	<b>77.25±0.26</b>	77.22±0.19	59.83±0.61	52.10±4.09	OOT	76.58±0.35	77.09±0.50
IMDB-BINARY	OOT	OOM	NA	80.88±0.25	80.08±0.54	44.32±2.69	77.07±1.29	80.21±0.61	<b>81.87±0.46</b>	78.74±0.99	80.08±0.89
IMDB-MULTI	OOT	OOM	NA	66.92±0.29	66.24±0.46	44.93±0.72	65.41±0.46	66.95±0.38	62.37±0.40	65.87±0.70	65.78±0.50
KKI	48.72±6.41	<b>59.90±4.85</b>	NA	52.49±4.29	42.33±4.20	48.41±6.48	53.22±7.32	56.60±4.98	54.61±5.11	51.20±6.00	49.31±6.26
Letter-high	NA	OOM	84.96±0.71	99.39±0.02	<b>99.49±0.02</b>	73.36±0.50	99.28±0.05	NA	NA	86.78±0.08	86.86±0.13
Letter-low	NA	OOM	93.21±0.01	<b>100.00±0.00</b>	<b>100.00±0.00</b>	78.12±0.42	<b>100.00±0.00</b>	NA	NA	93.63±0.05	93.61±0.05
Letter-med	NA	OOM	90.91±0.04	99.72±0.02	99.78±0.01	74.46±1.20	<b>99.85±0.01</b>	NA	NA	91.77±0.06	91.72±0.11
MSRC_21	OOT	99.38±0.05	NA	99.16±0.05	98.75±0.06	95.75±0.10	99.45±0.05	99.31±0.07	OOT	99.20±0.06	<b>99.47±0.04</b>
MSRC_21C	94.04±0.69	94.96±1.30	NA	95.40±1.03	94.63±0.99	90.63±1.03	94.55±1.38	95.06±0.42	94.37±0.65	95.19±1.43	<b>95.55±1.23</b>
MSRC_9	99.03±0.27	<b>99.13±0.08</b>	NA	98.64±0.29	98.51±0.22	98.21±0.39	98.84±0.09	<b>99.13±0.13</b>	98.81±0.10	98.71±0.11	98.93±0.16
MUTAG	<b>93.64±0.95</b>	83.62±0.85	85.72±0.81	87.87±0.79	88.11±0.52	86.43±1.29	92.65±1.26	91.16±0.93	91.62±1.09	91.54±1.46	90.03±2.56
Mutagenicity	OOT	OOM	46.84±2.78	79.93±0.05	87.34±0.33	OOM	86.12±0.29	56.35±2.93	OOT	88.93±0.34	<b>90.12±0.46</b>
NCI1	OOT	OOM	49.98±4.29	76.31±0.08	87.19±0.13	84.41±0.35	85.27±0.66	58.33±3.49	OOT	91.02±0.22	<b>92.14±0.17</b>
NCI109	OOT	OOM	51.74±0.26	76.65±0.06	86.72±0.14	83.98±0.38	83.96±0.39	57.50±4.18	OOT	91.19±0.16	<b>91.76±0.07</b>
OH5U	41.51±8.60	<b>58.75±4.30</b>	NA	47.59±5.34	47.70±7.30	45.34±6.36	47.78±7.08	45.62±2.65	OOT	44.25±4.75	42.41±4.92
PROTEINS	OOT	80.82±0.07	NA	79.65±0.16	80.78±0.37	80.67±0.47	78.33±0.54	<b>82.20±0.25</b>	OOM	79.37±0.77	78.96±0.93
PROTEINS_full	70.67±0.45	OOM	NA	81.18±0.15	81.76±0.24	80.67±0.47	78.99±0.59	<b>82.20±0.25</b>	OOM	79.38±0.77	78.97±0.93



**Table 4.7:** Empirical performance of graph kernels on the benchmark data sets. The mean area under the Receiver Operating Characteristic curve (AUROC) over 10 iterations of a nested cross-validation procedure is shown along with its corresponding standard deviation. The highest AUROC value for each data set (considering the baseline kernels and normal kernels) is shown in **red** OOM means “out-of-memory”, OOT means “out-of-time”, and NA indicates that the given implementation could not handle a certain data set.

Data set	CSM	GH	Graphlet	HGK-SP	HGK-WL	MLG	MP	SP	RW	WL	WL-OA
PTC_FM	51.98±3.51	61.00±0.75	53.14±2.44	61.75±1.21	64.06±1.68	54.77±4.33	<b>66.27±1.94</b>	57.40±4.02	52.70±3.10	62.41±2.47	64.44±2.46
PTC_FR	59.43±3.24	62.00±1.39	51.12±2.18	63.04±0.92	64.04±2.03	50.60±2.90	65.28±1.64	<b>66.00±1.75</b>	49.06±1.81	63.05±2.99	63.65±1.62
PTC_MM	53.62±3.23	65.17±1.39	47.43±2.79	63.71±0.97	<b>68.12±1.30</b>	49.60±4.29	66.16±1.32	63.38±3.64	61.47±2.12	63.56±2.24	61.79±2.34
PTC_MR	62.14±2.36	61.32±1.35	48.44±3.79	61.54±1.04	63.29±1.80	63.40±3.31	<b>64.90±1.26</b>	61.68±1.97	53.17±3.13	63.07±1.27	64.33±2.06
Peking_1	45.34±5.56	OOM	NA	<b>54.80±7.22</b>	49.78±7.76	46.47±5.09	52.99±6.60	42.86±6.70	OOT	49.86±7.52	49.99±6.37
REDDIT-BINARY	OOM	OOM	NA	OOM	OOM	OOM	<b>95.54±0.26</b>	95.22±0.15	OOM	83.51±2.72	94.62±0.13
REDDIT-MULTI-12K	OOM	OOM	NA	OOM	OOM	OOM	<b>85.66±0.09</b>	80.78±0.30	OOM	75.36±0.32	OOM
REDDIT-MULTI-5K	OOM	OOM	NA	OOM	OOM	OOM	<b>81.77±0.16</b>	79.80±0.22	OOM	81.59±0.13	OOM
SYNTHETIC	<b>71.96±1.30</b>	39.20±1.81	50.00±0.00	39.27±3.08	27.86±5.01	50.00±0.00	50.00±0.00	50.00±0.00	OOM	50.00±0.00	50.00±0.00
SYNTHETICnew	98.69±0.30	38.00±1.86	NA	33.72±2.60	29.92±6.00	90.91±1.26	68.43±2.23	91.19±1.09	OOM	<b>99.90±0.11</b>	99.87±0.13
Synthetic	82.64±0.80	91.43±0.21	NA	97.08±0.08	86.60±0.36	83.11±0.99	<b>99.74±0.10</b>	82.95±1.07	OOM	82.56±0.80	82.93±0.96

**Table 4.8:** Mean rank (and standard deviation) for each graph kernel. The ranking has been obtained by simulating accuracy distributions. Methods based on the Weisfeiler–Lehman relabelling scheme or one of its variants are printed with an additional asterisk (\*) after their name.

Kernel	Rank
Message passing*	$4.27 \pm 2.49$
Weisfeiler–Lehman (optimal assignment)*	$4.51 \pm 2.34$
Weisfeiler–Lehman*	$5.04 \pm 2.05$
HGK-WL*	$5.85 \pm 3.26$
HGK-SP	$5.85 \pm 3.02$
Shortest-path	$5.89 \pm 3.02$
Histogram ( $V$ )	$6.74 \pm 2.87$
Multiscale Laplacian	$7.57 \pm 3.30$
Histogram ( $E$ )	$7.74 \pm 3.20$
Subgraph Matching	$8.48 \pm 3.69$
GraphHopper	$8.67 \pm 3.18$
Random Walk	$9.88 \pm 3.20$
Graphlet	$10.49 \pm 2.30$

**Ranking** As an additional simple summary of Table 4.5, we also calculate the *ranks* of individual algorithms. To make proper use of the standard deviation, we consider each kernel’s accuracy values to be normally distributed, which is a standard assumption when employing a cross-validation setup. Using the corresponding mean accuracy and standard deviation as the respective mean and standard deviation of such a normal distribution, we simulate 10,000 independent “draws” of accuracy values from these distributions. Ultimately, this will permit us to calculate a mean rank and standard deviation for each kernel. The results of this Monte Carlo simulation are shown in Table 4.8. In some sense, the table confirms our observation from above: approaches based on the Weisfeiler–Lehman relabelling scheme tend to outperform other kernels. Somewhat surprisingly, the vertex histogram kernel is not among the worst-performing kernels—we would expect that this kernel, which after all is not using *any* connectivity information of a graph, cannot reach a competitive performance. As this kernel, and edge histogram kernels, are often used as a baseline kernel, we consider it necessary to perform a more detailed analysis here. Hence, after giving a breakdown by graph data set type for each kernel in Section 4.3.1, we will assess the performance of histogram kernels in a more detailed manner in Section 4.3.2.

### 4.3.1 Breakdown of results per data set type

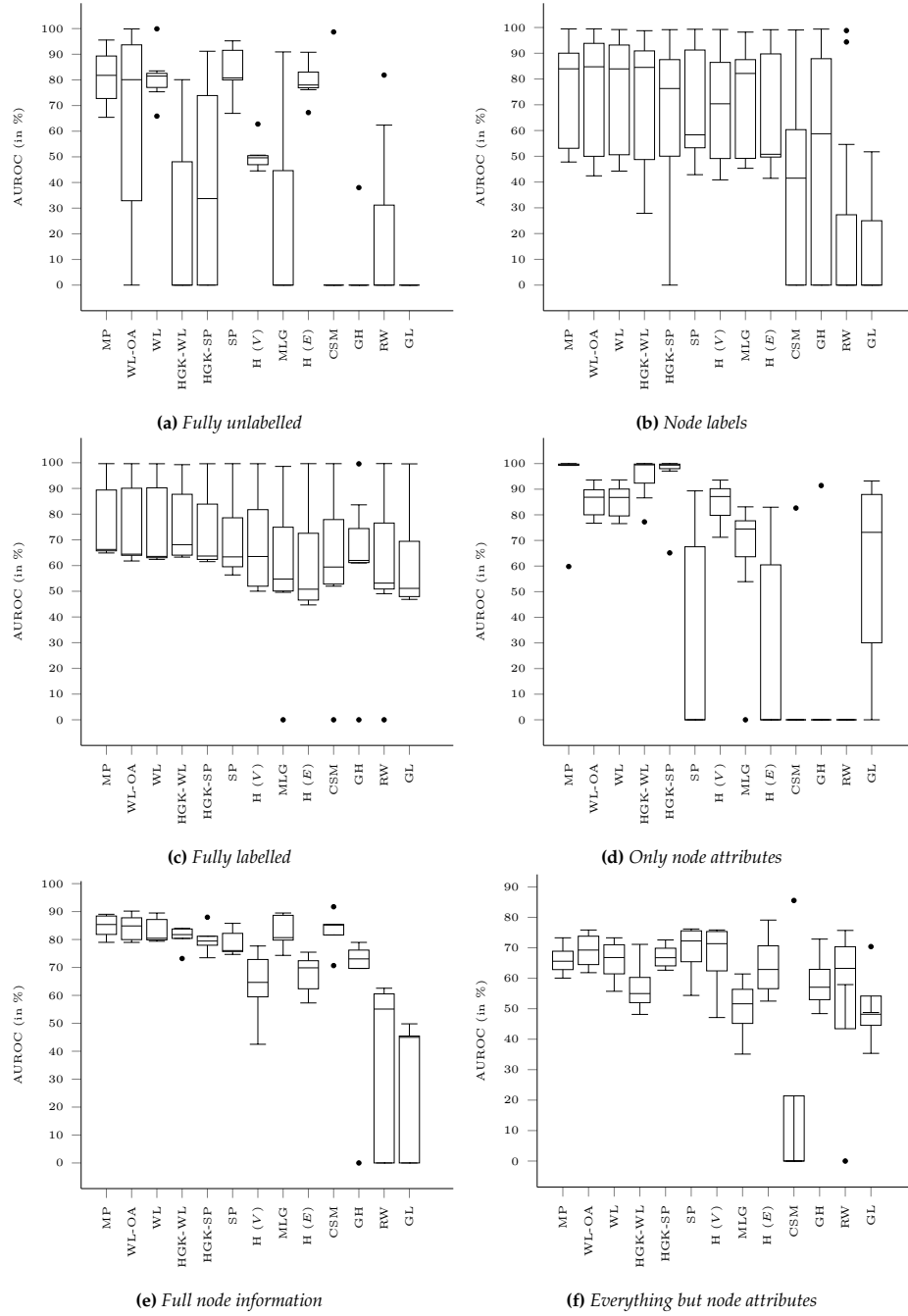
As a precursor to deciding which kernel to apply for a *new* data set, we first use Table 4.1 to perform a coarse type assessment. Looking at the presence and absence of either node or edge labels or attributes, we create the following classes of data sets:

- (i) *fully unlabelled*: data sets that do not have *any* attributes or labels
- (ii) *node labels*: data sets that *only* have node labels
- (iii) *fully labelled*: data sets that have node labels and edge labels but no other information
- (iv) *only node attributes*: data sets that contain node attributes and nothing else; for reasons of simplicity, we also include COIL-DEL in this category because said data set would otherwise constitute a category of its own.
- (v) *full node information*: data sets that contain node labels and node attributes, but nothing else.
- (vi) *everything but node attributes*: data sets that *lack* node attributes, but feature edge attributes as well as node labels and edge labels.

This list is exhaustive concerning the benchmark data sets. Technically, other categories are possible—such as data sets that only contain edge labels and nothing else—but there are no examples of such data sets in the repository at present.

We provide a ranking based on the *average* performance of a graph kernel on some data set—this will promote graph kernels whose performance on the data set is *consistent*, *i.e.* that are capable of classifying graphs from that data set to a similar extent. Table 4.9 depicts the resulting table. The dominance of Weisfeiler–Lehman approaches is now even more evident—these types of graph kernels perform consistently well for several types of data sets. Class vi (*everything but node attributes*) of data sets is special and surprising in the sense that vertex histogram kernels exhibit suitable overall performance here. In total, the table seems to suggest that, at least for data sets of types i, ii, and iii, the Weisfeiler–Lehman subtree kernel or its optimal assignment variant are most suitable; alternatively, the message passing (MP) kernel, with a somewhat higher complexity, can be used to achieve a good performance.

Finally, Figure 4.4 provides a visual depiction of the accuracies of each kernel, broken down by the classes defined above. To provide a consistent visual design, the graph kernels have been sorted by their ranking according to Table 4.8. Boxplots are generated using the AUROC of a specific graph kernel on a data set in order to ensure comparability. If all graph kernels would deal with all types of data sets in a consistent manner, the *mean* of every boxplot should reflect this trend for each class, and we would be able to observe similar boxplots across all classes. As the figure demonstrates, this is not the case—the



**Figure 4.4:** Accuracy values achieved by each kernel on data sets of a specific class. The  $x$ -axis is ordered according to the average accuracy on the complete data set.

**Table 4.9:** A ranking of graph kernels based on their mean accuracy achieved on a specific type of data set.

Type	1 <sup>st</sup>	2 <sup>nd</sup>	3 <sup>rd</sup>
i	SP	MP	WL
ii	WL-OA	WL	HGK-WL
iii	WL-OA	MP	WL
iv	MP	HGK-SP	HGK-WL
v	WL-OA	MP	CSM
vi	SP	VH	WL-OA

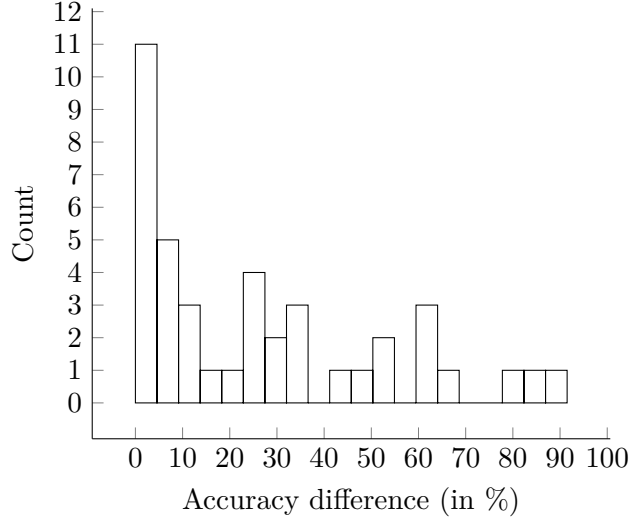
performance of graph kernels varies depending on the type of data set. There are several other interesting patterns that emerge from the plot, though:

1. The performance of all graph kernels for the *fully labelled* graphs is much more consistent than on other types of data sets.
2. For graphs with *full node information*, there is a clear division between the graph kernels in terms of their classification accuracy.
3. A similar observation holds for the *node-labelled* graphs, even though this type of data set exhibits large variances in AUROC.
4. In general, the *overall* ranking—which was calculated in terms of mean accuracy—is not evident in the mean AUROC distributions over different data sets.

We will return to this discussion later on when we give suggestions for *choosing* a suitable graph kernel. Prior to that, we first discuss the performance of baseline kernels, as well as the data set difficulty in general.

#### 4.3.2 Performance of histogram kernels

The performance of pure label histogram kernels, either based on vertex labels ( $V$ ) or on edge labels ( $E$ ) is noteworthy because they outperform *all* remaining kernels on 4 data sets out of the 41 (out of these, the vertex histogram kernel performs best for 3 of them). The performance seems to suggest that for some of the benchmark data sets, the underlying structure of the graph is *irrelevant*, at least insofar as it is not required to obtain good predictive performance. This raises the issue of assessing the overall difficulty of the benchmark data sets; we will discuss it further in Section 4.4, whereas this section will focus on a comparison of histogram kernels with other graph kernels.



**Figure 4.5:** A distribution of the relative differences in mean accuracy of the vertex histogram kernel and the corresponding best-performing graph kernel.

#### 4.3.2.1 Distribution analysis

As a first analysis, we look at the vertex histogram kernels. Figure 4.5 depicts the *relative* accuracy differences of the vertex histogram kernel, with respect to the best-performing graph kernel for each data set. To this end, letting  $x_b$  refer to the accuracy of the best-performing graph kernel on a data set, and  $x_v$  refer to the accuracy of the vertex histogram graph kernel, we calculate

$$\Delta = \frac{100(x_b - x_v)}{x_b} \quad (4.2)$$

and plot it in a histogram. We observe that for 16 out of the 41 of the data sets, the relative differences are below 10%. This suggests that a more complex method that takes edges, nodes, and their connectivity—as well as their labels or attributes—into account does not necessarily yield a classification accuracy that is higher by a large margin. Moreover, this indicates that some data sets do *not* require the usage of a complex graph kernel, because they do not contain graphs whose structure needs to be exploited in order to obtain good classification results.

#### 4.3.2.2 Visual analysis

To analyse this situation from a more detailed perspective, we need a more detailed visualisation that is capable of showing individual data sets. Hence, Figure 4.6 depicts

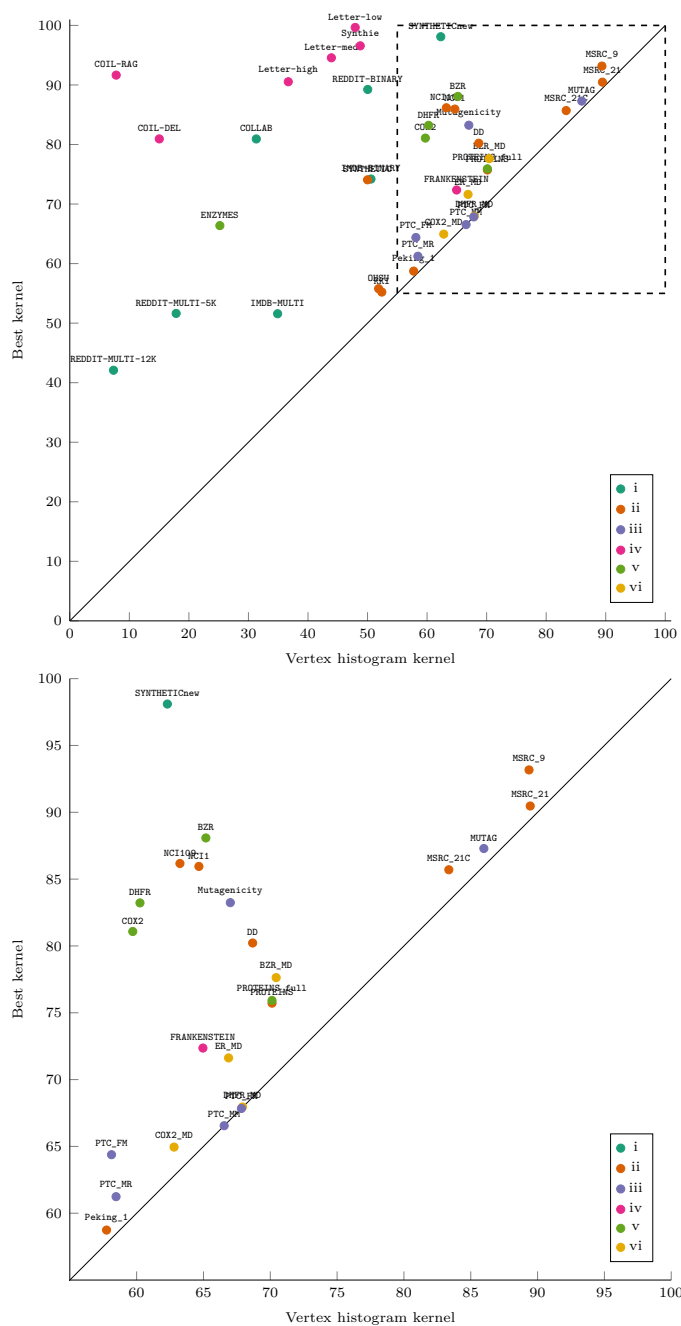
these data from another perspective: it shows a scatterplot with the vertex histogram kernel performance on the  $x$ -axis and the performance of the respective *best* graph kernel on the  $y$ -axis. Furthermore, data sets have been colour-coded according to the types introduced in Section 4.3.1. In this plot, the distance to the diagonal can thus be seen as indicating to what extent a data set is “graphical,” meaning that there is a gap in classification performance between simple histogram-based methods and more complex graph kernels. Since accuracy was used to measure performance, the relative distance between data sets has no meaning in this plot and should not be taken to indicate similarities between data sets. A second variant of this plot is shown in Figure 4.7; since it uses AUROC as the main comparison measure, relative differences can be compared more easily. Even though the placement of several data sets is slightly different in comparison to Figure 4.6, the same observations as for Figure 4.6 apply.

The scatterplot visualisation gives rise to several interesting observations. First of all, we see that several data sets are situated well above the diagonal. This includes data sets of class i and class iv that miss node labels—in which case the histogram kernel boils down to comparing node degrees—but also more “rich” (in terms of features) data sets such as ENZYMEs or the Letter-\* data sets. The other classes are closer to the diagonal, though. A “zoomed-in” version of the plot shows a portion of them in greater detail. In general, the vertex histogram kernel provides a useful baseline for them, and provides a surprisingly competitive performance for several data sets. This makes it clear that the performance of the vertex histogram kernel is caused by selecting data sets that do not feature any “graphical” structure; we will get back to this point in a subsequent section, when we discuss the suitability of some benchmark data sets.

#### 4.3.2.3 Histogram kernels compared to other kernels

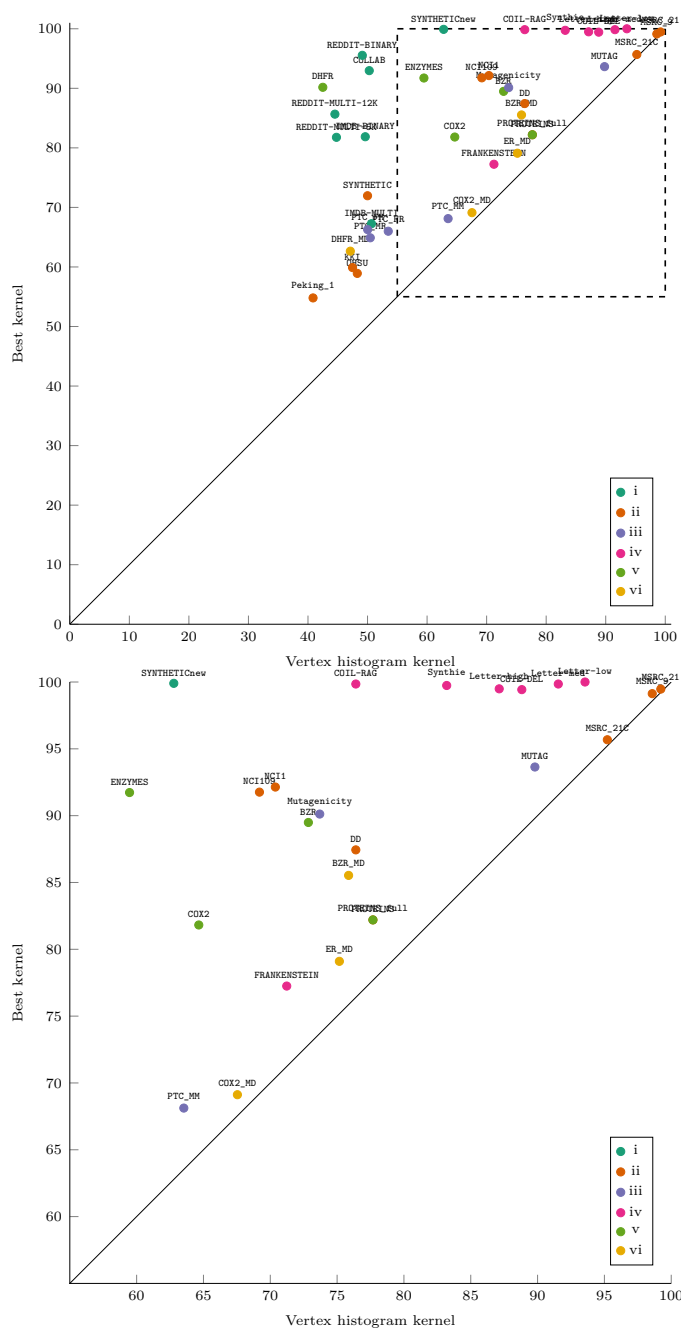
As a last item in our analysis of histogram kernels, we observe to what extent it is possible to distinguish histogram-based kernels from other graph kernels. This is demonstrated in Figure 4.8, which provides a dense visualisation of the accuracies (including standard deviations) of all data sets, while highlighting the histogram kernels. For most of the data sets, there is a clear gap between the performance of histogram-based kernels and other kernels, with the other kernels typically outperforming the histogram-based ones.

To summarise our analysis so far: we have seen that the performance of graph kernels hinges largely on the type of data set. For some of the data sets, simple histogram-based kernels, which are incapable of exploiting any structures of a graph beyond vertex/edge labels, are sufficient to obtain suitable—and in some cases even competitive—performance values. Considering that these histogram-based graph kernels represent a *baseline* and not

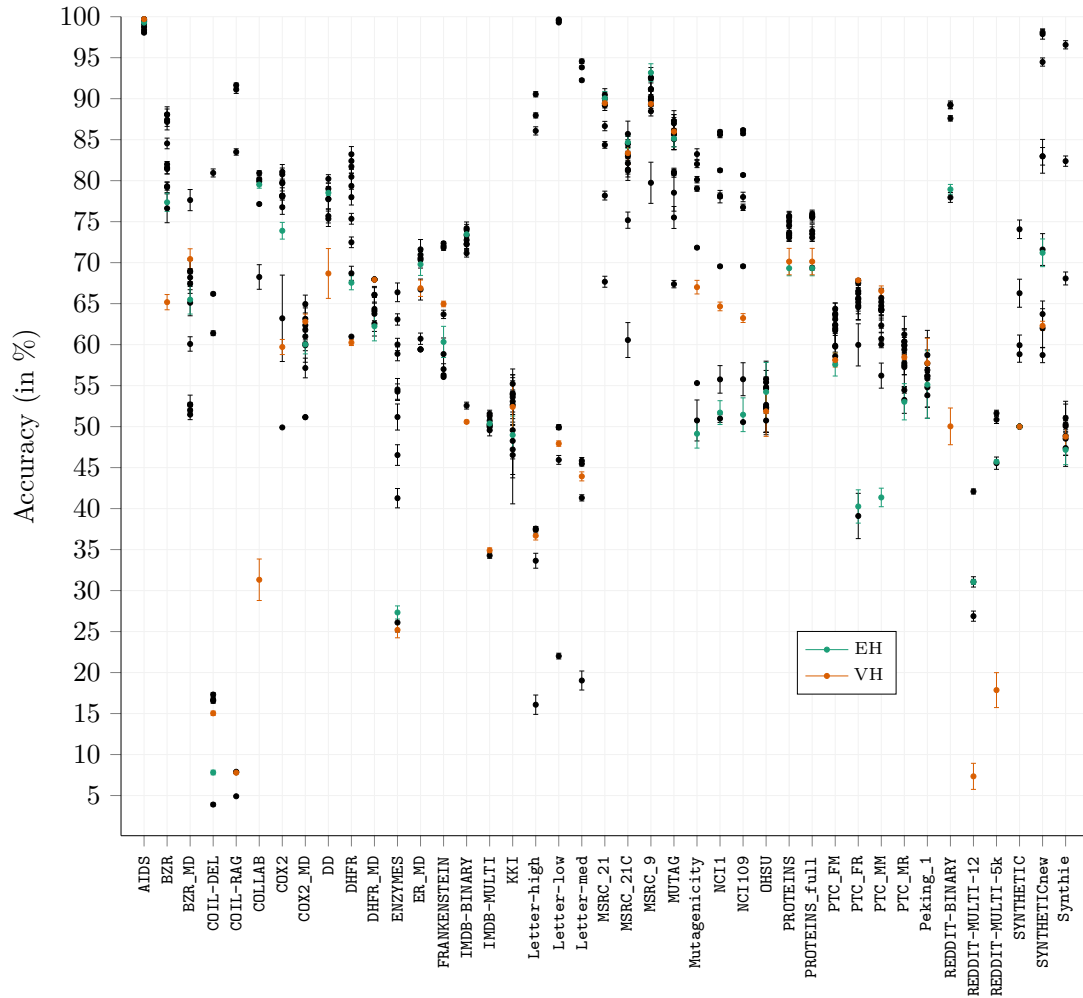


**Figure 4.6:** The performance of the vertex histogram kernel plotted against the respective *best* kernel on every benchmark data set. We also provide a second plot that “zooms” into the marked region to decrease the clutter. Points have been coloured according to the data set type introduced in Section 4.3.1.





**Figure 4.7:** Similar to Figure 4.6, we depict the performance of the vertex histogram kernel compared to the respective *best* kernel on every benchmark data set. Here, classification performance is measured in terms of AUROC.



**Figure 4.8:** A visualisation of *all* accuracies (including the standard deviation) on all benchmark data sets. Each individual kernel is represented by a “dot” that includes error bars. The histogram kernels are highlighted in this visualisation; they can be clearly distinguished from the remaining data sets through their performance.

a regular choice of algorithm to be used in practice, the preceding discussion raises the question of the *difficulty* of the benchmark data sets. We will discuss this in the next section.

## 4.4 Analysing the difficulty of data sets

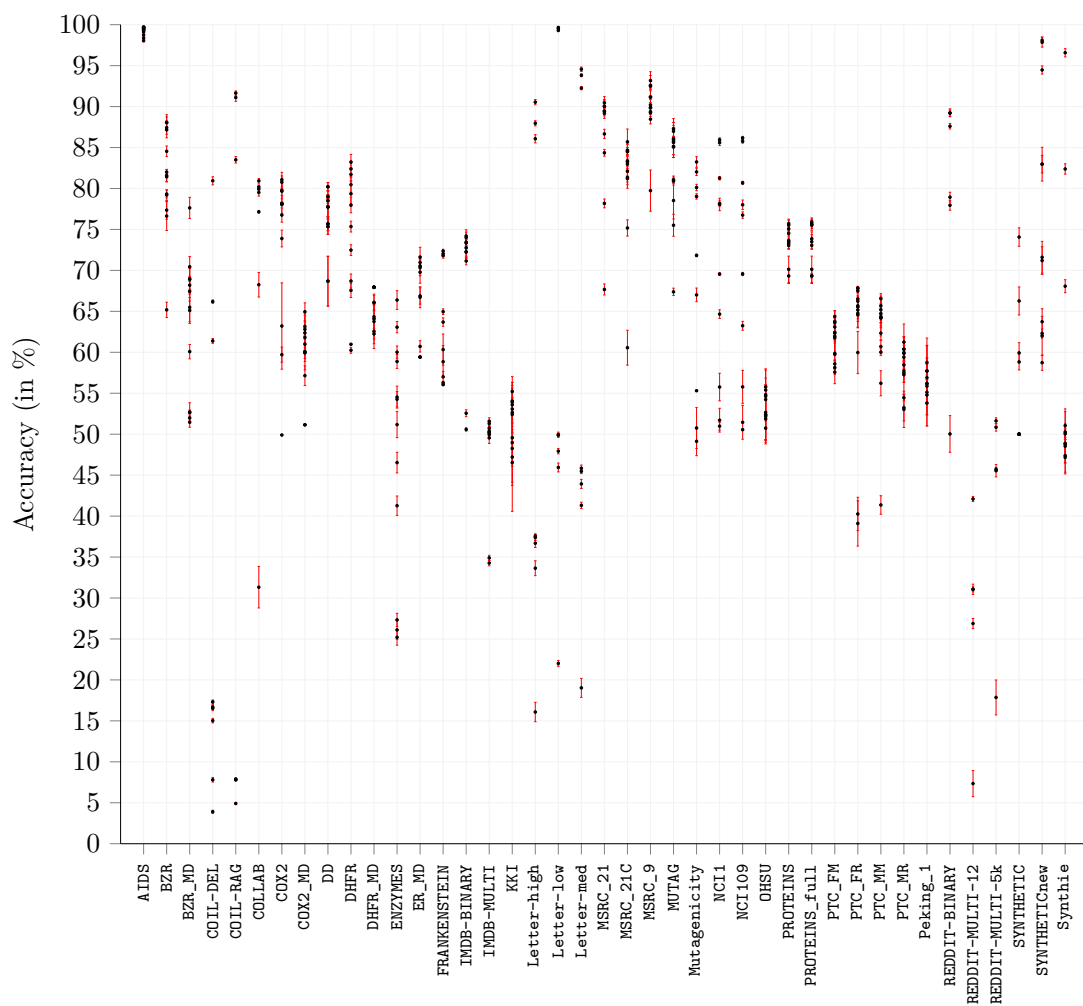
To further examine the behaviour of *all* kernels—not only the histogram-based ones—we now turn to analysing the *difficulty* of available graph benchmark data sets. We will present multiple ways of depicting the difficulty, starting with a high-level discussion of accuracy distributions, which is followed by increasingly detailed discussions on optimal classification accuracy estimates.

### 4.4.1 Accuracies and standard deviations

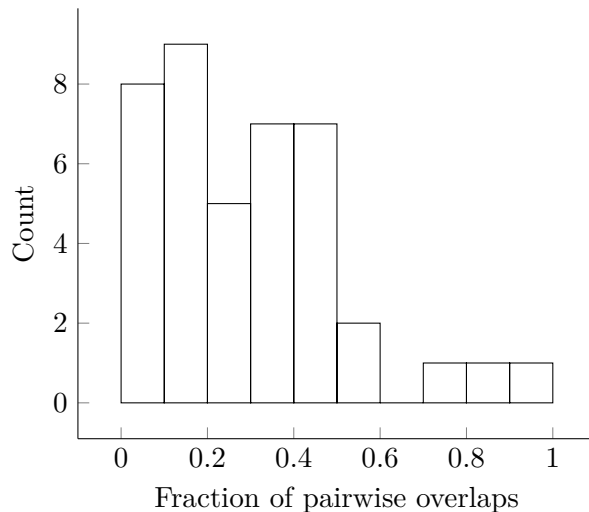
We begin our analysis with a visualisation in the style of Figure 4.8. However, instead of highlighting histogram-based kernels, we show the accuracies and standard deviations of all kernels without labels. This will make it easier to see to what extent there are different groups of kernels for specific data sets. Moreover, including the standard deviation also provides us with information about the performance across different iterations of the cross-validation training procedure.

Figure 4.9 depicts the resulting visualisation. Each point corresponds to the mean accuracy of a specific graph kernel, whereas each bar indicates its standard deviation across the different repetitions of the cross-validation process. Intuitively, this bar can also be seen as an *uncertainty* of the “true” performance on an unseen part of a specific data set. This data-rich visualisation depicts certain idiosyncrasies of the data sets in an intuitive manner: for each data set, the presence of a *single* region, *i.e.* a region of—either pairwise or mutually—overlapping error bars, indicates that the performance of a specific graph kernel varies too much between folds and thus cannot be easily distinguished from the remaining kernels. By contrast, a *gap* indicates that there is a subset of kernels that exhibits a markedly different performance over all iterations.

**Visual analysis of overlaps** Out of all the data sets described here, REDDIT-MULTI-12K is the only one for which we observe *no* overlaps at all—different graph kernels are thus perfectly separable from each other. Similarly, for the data sets (i) REDDIT-BINARY, and (ii) COIL-DEL, only a single overlap occurs. For all of these data sets, different graph kernels can be easily separated from each other in terms of their performance. By contrast, Peking\_1 exhibits the largest number of pairwise overlaps; here, almost *all* standard deviation intervals exhibit a mutual overlap. We will subsequently quantify these observations.



**Figure 4.9:** Mean accuracy values along with their standard deviations (plotted as error bars) over the different iterations of cross-validation for all graphs, separated by data set. A gap indicates that performance values do not overlap for different repetitions of the training.



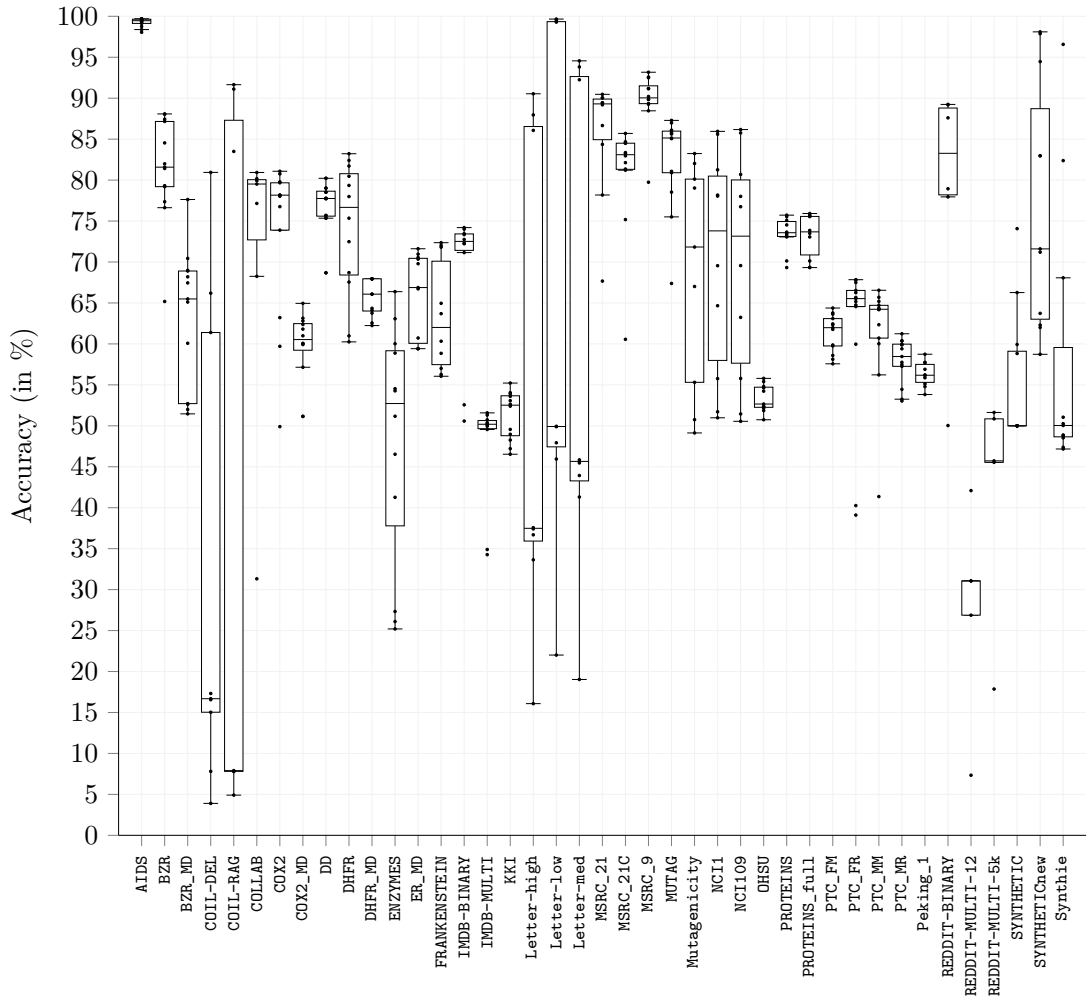
**Figure 4.10:** A histogram of the fraction of pairwise overlaps between the mean accuracies and standard deviations shown in Figure 4.9. A small fraction of pairwise overlaps is desirable because it simplifies comparing the performance of different graph kernels.

**Histogram analysis of overlaps** As a histogram of all pairwise overlaps in Figure 4.10 shows, most of the data sets exhibit a fraction of 0 % to 50 % of pairwise overlaps. This is not necessarily problematic, but as we will see in Section 4.5.1 on p. 119, it will slightly decrease statistical power if the *full* data set is selected to make claims on the statistical superiority of specific graph kernels.

**Discussion** In general, care must be taken when considering these analyses; a low number of overlaps can have multiple causes, among them being (i) the data set could be too easy, making it impossible to distinguish between different graph kernels in terms of their predictive performance, or (ii) the data set could be too small, making predictive performance highly vary depending on the training procedure and the fold assignment, or (iii) the data set could be too hard to classify in general, leading to a high variance of predictive values. Hence, we will subsequently discuss the difficulty and general suitability of the benchmark data sets under different perspectives, before giving our recommendations.

#### 4.4.2 Boxplot analysis

The preceding visualisations are very “dense” in the sense that they show all data at the same time. To assess the difficulty of data sets, a coarse perspective is sufficient. Figure 4.11



**Figure 4.11:** Boxplots of the accuracy distribution of all graph kernels, separated by data set. A high spread indicates that a data set poses difficulties for a certain class of graph kernels.

depicts boxplots of the accuracy distributions of kernels, grouped by data set (kernels that did not finish computing were *not* included; thus, the number of accuracy values for each data set might vary). The underlying idea of such a visualisation is to show whether *all* kernels behave similarly on a specific data set or not. Even though one might be tempted to compare different data sets via their boxplots, only the variance of kernels on each data set should be considered—this visualisation cannot be used to assess whether a certain graph kernel is suitable for classification because no baselines for a random classifier are shown.

#### 4.4.2.1 High-variance data sets

We first observe that some of the data sets exhibit a large spread in their accuracies. The list of high-variance data sets includes

- (1) COIL-RAG,
- (2) COIL-DEL,
- (3) ENZYMES,
- (4) Letter-high,
- (5) Letter-low,
- (6) Letter-med,
- (7) Mutagenicity,
- (8) NCI1,
- (9) NCI109,
- (10) SYNTHETICnew.

Out of those, only COIL-DEL, ENZYMES, Mutagenicity, NCI1, and NCI109 have node or edge labels. The remaining data sets either feature node or edge attributes. If we link this back to Figure 4.6, which depicted the differences in performance with respect to the vertex histogram kernel here, we see that this list comprises data sets in which the vertex histogram kernel did not perform as well as other types of kernels. Thus, these data sets can be considered “hard” to classify accurately, but the performance also highlights the need for developing (more) graph kernels that (i) are capable of handling graphs with node or edge attributes, and (ii) scale well. Such graph kernels have the potential to significantly improve classification performance here.

#### 4.4.2.2 Low-variance data sets

By contrast, there are also data sets that can be considered to be “solved” in the sense that most graph kernels perform extremely similarly (such as for the AIDS data set, which *every* kernel can classify very well). This does *not* necessarily imply that all such data sets are solved. For example, for the PTC-\* data sets, it is unclear whether performance can be

significantly improved with, for example, a new technique that is better able to exploit structural information, or whether the best performance on this data set has already been reached. Prior to discussing how to estimate the difficulty of a data set in a more principled manner, we first provide a numerical view on the accuracies of all data sets.

#### 4.4.2.3 Summarising differences in accuracy

Table 4.10 summarises the performance measures that we extracted in the previous plots by showing the performance gap between the worst-performing method and the best-performing method, as well as the average accuracy obtained on a given data set. Using an arbitrary cut-off of 10 % accuracy difference, we have the following data sets:

- (1) AIDS,
- (2) DHFR\_MD,
- (3) KKI,
- (4) OHSU,
- (5) PROTEINS,
- (6) PROTEINS\_full,
- (7) PTC\_FM,
- (8) PTC\_MR, and
- (9) Peking\_1.

All of these data sets also exhibit small standard deviations in their accuracy distributions. This suggests that *all* graph kernels are performing almost equally and none of them have a clear advantage over the other.

Again, this does not necessarily imply that these data sets are too easy: while AIDS can be considered as “solved”, the performance in the remaining data sets could be improved. However, the list shows that these data sets appear to contain a sufficient amount of structural information that can be exploited to some extent by all graph kernels. This makes these data sets beneficial for comparing different types of graph kernels. Any analysis that claims the superiority of a specific graph kernel should nonetheless employ other data sets that provide more information about its generalisation performance.

#### 4.4.3 Estimating maximum predictive performance

So far, we have analysed all data sets from different perspectives, focusing on how “easy” they make classification for different graph kernels. Now we want to assess their difficulty in a more principled manner. To this end, we estimate the *maximum* predictive performance that can be achieved on a given data set for the considered graph kernels. We follow a very conservative procedure here: we first take the predictions of all graph kernels over all folds



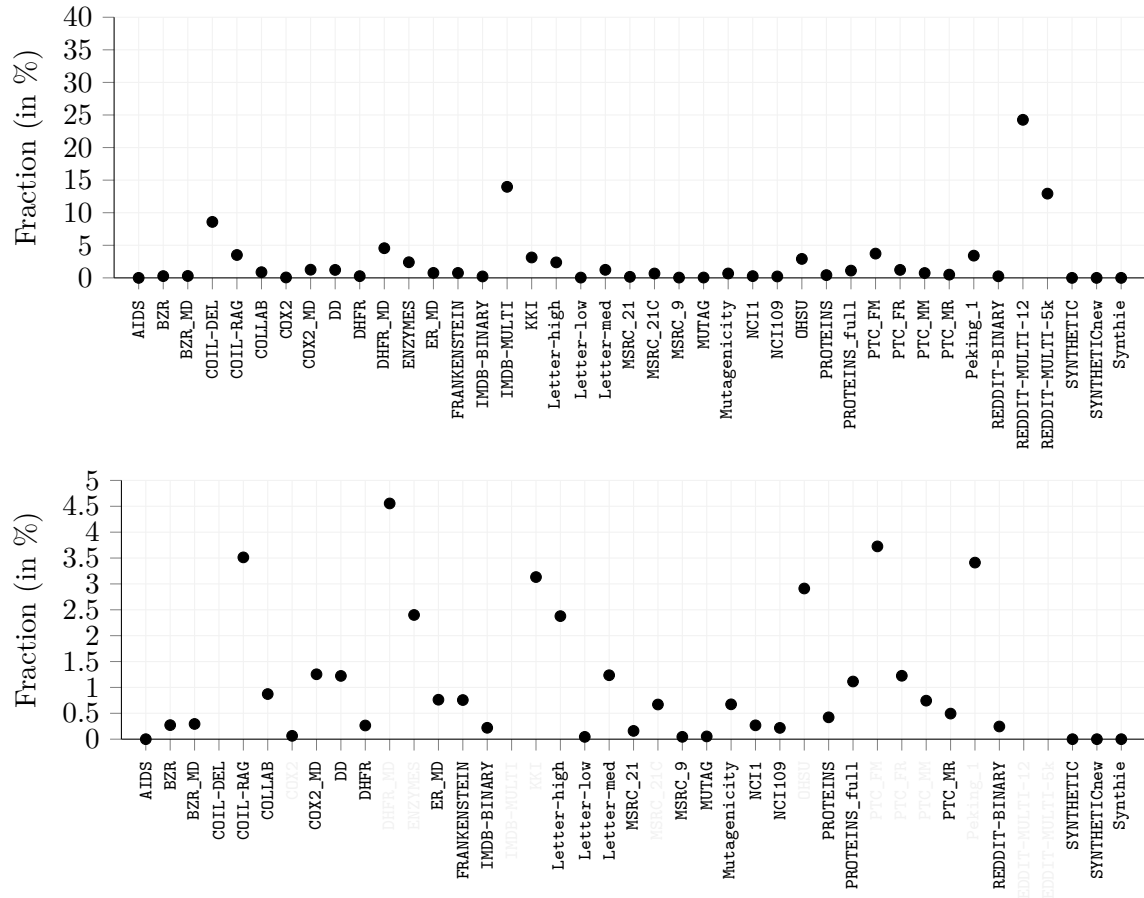
**Table 4.10:** An overview of the performance values of all graph kernels on the benchmark data sets. Data sets whose performance difference is less than 10 % have been highlighted.

Data set	min	max	Avg.	% $\Delta$
AIDS	98.05	99.70	99.24 $\pm$ 0.53	1.65
BZR	65.18	88.08	81.38 $\pm$ 6.32	22.90
BZR_MD	51.46	77.63	63.16 $\pm$ 8.53	26.17
COIL-DEL	3.90	80.94	31.76 $\pm$ 29.11	77.04
COIL-RAG	4.91	91.65	30.42 $\pm$ 37.69	86.74
COLLAB	31.32	80.93	71.04 $\pm$ 18.05	49.61
COX2	49.90	81.08	73.64 $\pm$ 9.73	31.18
COX2_MD	51.15	64.95	59.63 $\pm$ 4.42	13.80
DD	68.68	80.22	76.62 $\pm$ 3.59	11.54
DHFR	60.25	83.22	74.20 $\pm$ 8.17	22.97
DHFR_MD	62.24	67.95	65.74 $\pm$ 2.24	5.71
ENZYMES	25.20	66.38	47.90 $\pm$ 14.75	41.18
ER_MD	59.42	71.62	65.99 $\pm$ 5.19	12.20
FRANKENSTEIN	56.05	72.36	63.34 $\pm$ 6.70	16.31
IMDB-BINARY	50.58	74.20	68.66 $\pm$ 9.06	23.62
IMDB-MULTI	34.27	51.58	47.30 $\pm$ 6.73	17.31
KKI	46.53	55.22	51.28 $\pm$ 2.99	8.69
Letter-high	16.08	90.54	51.37 $\pm$ 26.20	74.46
Letter-low	22.01	99.66	63.19 $\pm$ 27.49	77.65
Letter-med	19.03	94.56	58.21 $\pm$ 26.16	75.53
MSRC_21	67.67	90.47	85.55 $\pm$ 7.34	22.80
MSRC_21C	60.56	85.70	80.78 $\pm$ 6.92	25.14
MSRC_9	79.74	93.17	89.78 $\pm$ 3.49	13.43
MUTAG	67.38	87.29	82.41 $\pm$ 5.77	19.91
Mutagenicity	49.13	83.24	68.72 $\pm$ 13.80	34.11
NCI1	50.98	85.95	70.17 $\pm$ 13.68	34.97
NCI109	50.55	86.17	69.80 $\pm$ 13.76	35.62
OHSU	50.74	55.79	53.36 $\pm$ 1.66	5.05
PROTEINS	69.32	75.72	73.38 $\pm$ 2.15	6.40
PROTEINS_full	69.32	75.92	73.20 $\pm$ 2.68	6.60
PTC_FM	57.57	64.38	61.33 $\pm$ 2.29	6.81
PTC_FR	39.10	67.84	61.61 $\pm$ 9.94	28.74
PTC_MM	41.36	66.55	61.52 $\pm$ 6.67	25.19
PTC_MR	53.03	61.24	57.92 $\pm$ 2.77	8.21
Peking_1	53.82	58.74	56.30 $\pm$ 1.51	4.92
REDDIT-BINARY	50.03	89.24	78.83 $\pm$ 14.99	39.21
REDDIT-MULTI-12K	7.34	42.09	27.69 $\pm$ 12.70	34.75
REDDIT-MULTI-5K	17.86	51.63	42.32 $\pm$ 13.96	33.77
SYNTHETIC	50.00	74.07	54.93 $\pm$ 8.14	24.07
SYNTHETICnew	58.73	98.10	76.90 $\pm$ 15.07	39.37
Synthetic	47.17	96.57	58.10 $\pm$ 16.86	49.40

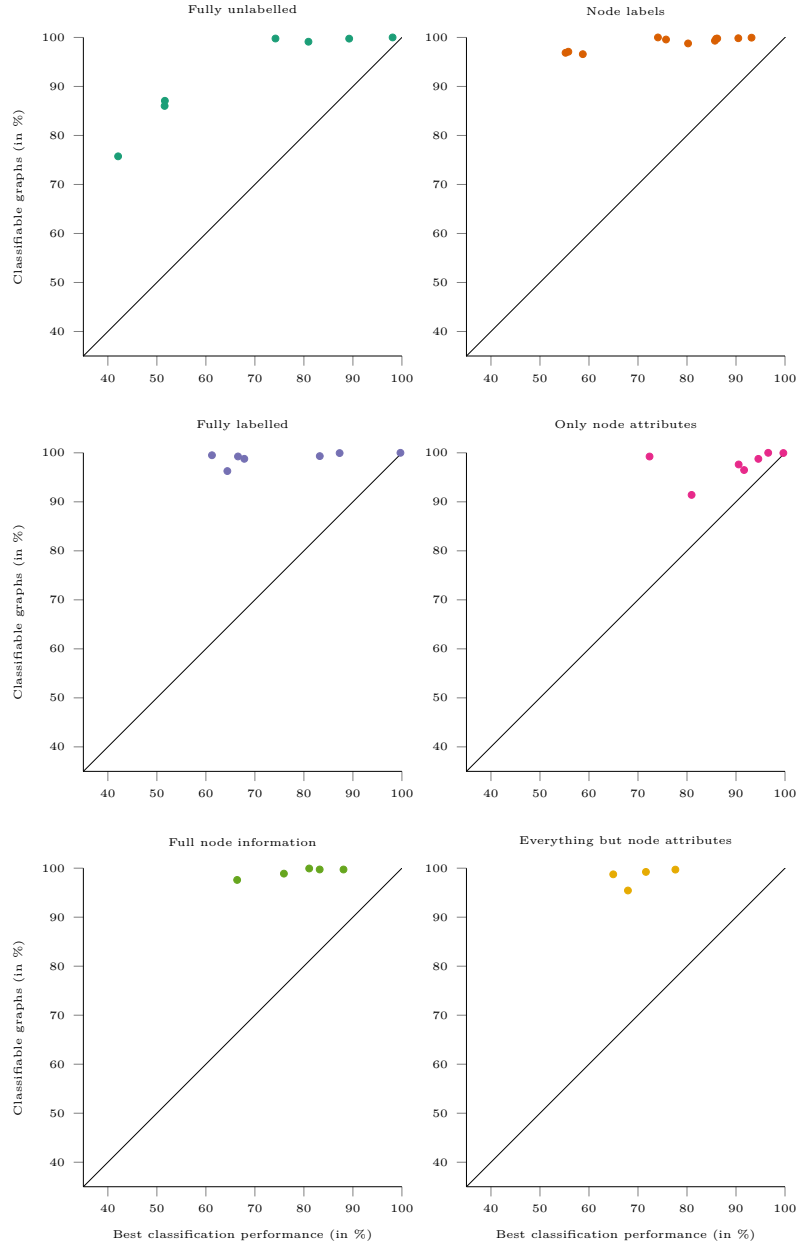
and all repetitions of the training process. Following our cross-validation procedure, we will thus be able to collect predictions of all graphs in every data set. For each data set and each of its graphs, we now count how many kernels exist that are capable of classifying a graph correctly. For example, assume we observe graph  $i$  at fold  $j$  and some kernel  $k$  is predicting the correct label. We then add  $k$  to a set  $K_{ij}$  that contains all graph kernels that are capable of classifying graph  $i$  in this fold. This information can now be summarised in multiple ways. We opt for the most conservative one, which involves counting all matrices for which  $K_{ij} = \emptyset$ , *i.e.* all graphs over all folds that cannot be classified by *any* of the graph kernels we considered. Letting  $N$  refer to the number of all graphs over all folds and  $N'$  to the number of matrices with  $K_{ij} = \emptyset$ , the fraction  $N'/N$  can thus serve as an indicator of the difficulty of a benchmark data set. We call graphs that were unable to be correctly classified on any split of the data and by any of the included graph kernels *generally misclassified*.

#### 4.4.3.1 Depicting generally misclassified graphs

Figure 4.12 depicts the fraction of generally misclassified graphs over all data sets—once for *all* fractions, and once for only those data sets whose fraction of generally misclassified graphs is below 5%. We observe that numerous data sets remain. The implications of this plot are positive: the fact that there are few generally misclassified graphs in all data sets means that the data sets are *highly consistent* in the sense that they contain few graphs that were always misclassified in our experiments (for example, because their label is inconsistent, or their representation is non-unique and overlaps with another graph that contains a different label). The obvious exceptions from this are the unlabelled data sets IMDB-MULTI, REDDIT-MULTI-12, and REDDIT-MULTI-5k. We conjecture that these data sets suffer from graphs that are either duplicates or quasi-isomorphic but with different labels. Given the provenance of these data sets, *i.e.* their generation based on online forums without the inclusion of labels (Yanardag and Vishwanathan, 2015), care needs to be taken in assessing classification results here. Having generally misclassified graphs in a data set poses two plausible interpretations. On the one hand, it is possible that these graphs are unclassifiable, perhaps due to non-unique representation or mistaken labels, as mentioned above. On the other hand, it is also possible that the graph kernels considered are simply not powerful enough to differentiate these challenging graphs. Since our experiments considered a broad array of graph kernels across nearly all categories defined in Chapter 3, we suspect these graphs are indeed quite often generally misclassified, which therefore would represent an upper limit on the classification performance we would expect any graph kernel to achieve.



**Figure 4.12:** A depiction of the fraction of *generally misclassified* graphs in each data set, *i.e.* graphs that were not classified correctly on any split of the data for any graph kernel in our experiments. The upper part of the figure shows *all* fractions, whereas in the lower part, only those data sets whose fraction of generally misclassified graphs is below 5 % are shown.



**Figure 4.13:** A visualisation of the difficulty of each data set, grouped by data set type, by plotting the fraction of graphs that were correctly classified on at least one fold of one kernel against the best performance achieved by some kernel. The further away from the diagonal, the more difficult a data set is. By contrast, data sets that are situated close to the diagonal may have reached their upper limit of performance, since the best performance of the included graph kernels is roughly similar to the fraction of graphs in the data set that at least one graph kernel can identify correctly. On the other hand, it could also indicate the need for a more powerful kernel in order to classify these *generally misclassified* graphs. The colour-coding follows the classes described in Section 4.3.1.

#### 4.4.3.2 Gauging the difficulty of all data sets

Having seen that most of the data sets are highly consistent, we now finally gauge their difficulty. This requires making use of the best classification accuracy that we obtained for them. Before we depict the resulting visualisations, we want to motivate the subsequent assessment by the following observation: if a data set poses a *simple* classification task, we would expect that the fraction of graphs that cannot be classified by *any* considered graph kernel could be approximately ascertained from the best performance on the data set. Specifically, if  $x$  is the fraction of generally misclassified graphs, the performance of the best graph kernel should be  $\approx 1 - x$ , the fraction of graphs that were successfully classified at least once. In other words, the best graph kernel should be able to classify a simple data set *up to* its subset of generally misclassified graphs. This gives us a separate axis, namely the best classification performance for each data set. Figure 4.13 depicts the resulting plot, grouped by data set type. Each dot represents a benchmark data set; the  $x$ -axis depicts the best classification performance, while the  $y$ -axis depicts the percentage of graphs that were successfully classified at least once in our experiments. In the interest of readability, we removed the data set labels from the plot and will only refer to them in the subsequent analysis.

This figure lends itself to numerous insights: we first observe that there are several data sets whose fraction of graphs that were correctly classified at least once is approached by the best performance of some graph kernel (within less than 0.5 %), namely (i) AIDS, (ii) Letter-low, (iii) Synthie, and (iv) SYNTHETICnew. We therefore state that these data sets have reached their upper limit of performance with respect to the graph kernels considered. Any additional kernel comparisons should therefore take care to ensure that the performance surpasses the percent of graphs that are currently classified correctly, because otherwise they might inadvertently conclude that the performance of a new graph kernel surpasses existing graph kernels, when in reality, the performance benefits are minuscule (or in the worst case, are just caused by fold variations).

If we extend the threshold between the fraction of the graphs that were correctly classified at least once versus the best performance of a graph kernel to 5 %, the list of simple data sets starts to include COIL-RAG and Letter-med. Their optimal classification performance, according to these considerations, should be larger than 95 %. As the values in Table 4.5 demonstrate, there is still a gap that cannot be fully explained by the standard deviation. Hence, it is likely that the classification performance of these data sets may yet be increased by a few performance points by some future graph kernel.

By contrast, it is interesting to see that the challenging data sets—according to this metric—are the *unlabelled* data sets of class i, which can be clearly seen as outliers in the

aforementioned plot. Data sets of class vi, containing everything *but* node attributes also appear to have a hidden complexity that is yet to be overcome. On the other hand, data sets from class ii (only node labels) and class iii (node and edge labels), are distributed in the plot. Some of these data sets hence appear to be more difficult than others of the same type, which is generally preferable for a collection of benchmark data sets.

#### 4.4.4 Consequences

We conclude this analysis by discussing the consequences of the preceding analyses. Our recommendations vary in terms of their epistemic status between “authoritative”, implying that we consider our claim to be strong, and “exploratory”, which we consider to be *suggestions* for the community.

##### 4.4.4.1 Exclusion of easy data sets

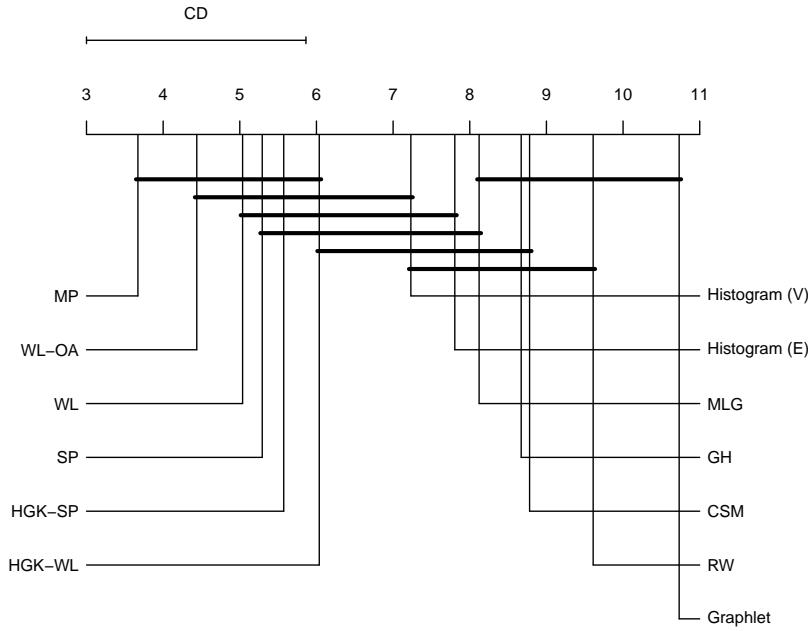
We consider this to be an authoritative claim that is backed up very well by the previous analyses: given their simplicity, the data sets (i) AIDS, (ii) Letter-low, (iii) Synthie, and (iv) SYNTHETICnew should *not* be considered in any formal comparison of graph kernels any more.

##### 4.4.4.2 Exclusion of node-attributed data sets

As Figure 4.13 demonstrates, the performance of many data sets of type iv, *i.e.* containing node attributes and no labels (except for COIL-DEL, which we included in this category for reasons of simplicity), is already *close* to optimal. As an exploratory suggestion, to guard against picking up a wrong signal when discussing the merits of a specific graph kernel, we suggest to consider excluding at least (i) Letter-low, (ii) Letter-med, and (iii) Letter-high from an analysis (please note that Synthie, as suggested above, should *always* be removed because we consider it to be solved). The other data sets of this type, *i.e.* COIL-DEL and FRANKENSTEIN, can be kept, but we suggest caution when basing any performance claims on these data sets alone.

## 4.5 Grouping graph kernels

Despite classification accuracy being the primary metric of interest, we nonetheless require tools to select a graph kernel in practice. Thus, we discuss multiple methods for *grouping* graph kernels before providing a flowchart to *choose* them.



**Figure 4.14:** A *critical difference plot* of the graph kernels at the  $\alpha = 0.05$  level. Any two kernels that are part of the same interval do *not* exhibit a statistically significantly different classification performance.

#### 4.5.1 Critical difference analysis

Prior to employing methods that focus on individual predictions or kernel matrices, we perform a statistical analysis of the AUROC values and the ranks of individual graph kernels. Our goal is to assess to what extent different graph kernels are statistically significantly different from each other. We then calculate a *critical difference plot* (Calvo and Santafé, 2016; Demšar, 2006). Originally developed for the comparison of classification algorithms (Demšar, 2006), the critical difference plot is now commonly employed in large-scale surveys of classifiers (Bagnall *et al.*, 2017). Briefly put, a critical difference plot employs a Nemenyi test to obtain a critical difference value. If the performance difference between two algorithms *exceeds* said value, the algorithms are considered to be statistically significantly different. This can be visualised in a corresponding diagram, in which algorithms whose performance is not statistically significantly different are connected by a line—thus immediately grouping pairs of available algorithms in terms of their differences. However, it needs to be stressed that the test analyses *pairwise* differences, so the plot should only be used to make claims about *pairs* of classifiers; it is not to be seen as a “clustering” method.

Figure 4.14 depicts the critical difference plot for different graph kernels, at a significance level of  $\alpha = 0.05$ . We can see that, despite the better average rank of the graph kernels based on the Weisfeiler–Lehman relabelling scheme, the performance of a group of graph kernels is statistically not significantly different. These kernels include (i) MP, (ii) WL-OA, (iii) WL, and (iv) the two Hash Graph Kernel variants. Each pair of these graph kernels is *not* statistically significantly different from each other in terms of their performance on the whole benchmark data set. As the test is very conservative, we can only claim statistical significance of differences between several pairs of other graph kernels. For example, from the group of kernels mentioned above, there is only a statistically significant difference between MP and the vertex histogram kernel or between WL-OA and the vertex histogram kernel. For *all* other pairs of graph kernels of the same group, the test lacks statistical power to claim a statistically significant difference. Hence, these results need to be taken with a grain of salt. At the very least, given the large number of pairwise comparisons, the benchmark data set repository does not seem to be entirely suitable to make claims about the statistical significance of large groups of graph kernels.

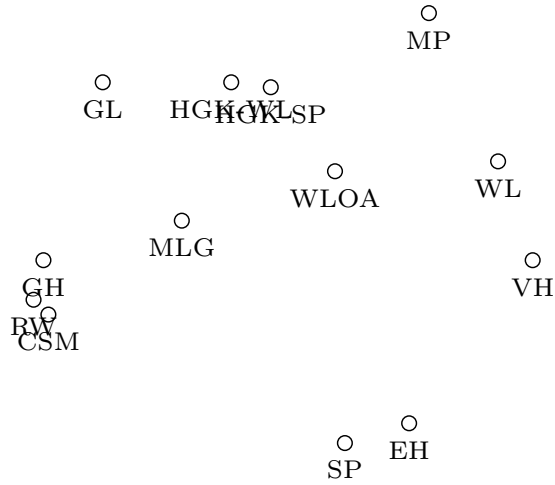
#### 4.5.2 Grouping based on predictions

Next to the critical difference analysis, a straightforward way of grouping graph kernels involves their *predictions* on the benchmark data sets. To this end, we aggregate all predictions (on all folds) of a graph kernel into a high-dimensional label vector  $\mathbf{y}$ . Given another such vector  $\mathbf{y}'$  created from the predictions of another graph kernel, we calculate their *Hamming distance* to see how similar their predictions are. We are *not* interested in knowing whether these predictions are correct; we are merely interested in knowing to what extent they agree. Since the Hamming distance is a metric, we can collect the pairwise dissimilarity scores in a quadratic matrix and use *metric multidimensional scaling* (Borg and Groenen, 2005, Chapter 9) to obtain a two-dimensional embedding.

Figure 4.15 depicts the resulting embedding. The distances in this plot correspond to the differences in predictions between the individual graph kernels. Contrary to our intuition, there are no direct “obvious” groups in the embedding. While HGK-WL and HGK-SP are put relatively close to each other, there is no group of methods based on Weisfeiler–Lehman propagations, for example. Nevertheless, there are some noteworthy aspects in this plot: we observe that the message passing kernel (MP), which employs additional approximation schemes, is predicting labels differently than other kernels.

All in all, this plot is *not* sufficient to “pick” a graph kernel to use, though, so we require a more involved method.





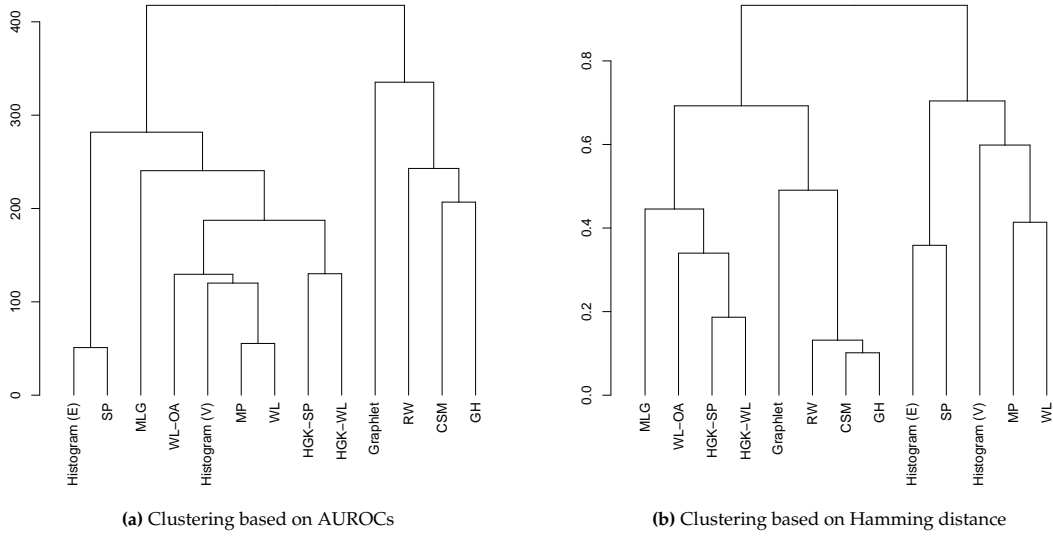
**Figure 4.15:** An embedding of the graph kernels of this section in terms of their actual predictions. Distances in the plot correspond to how similar the prediction profile of two kernels is.

### 4.5.3 Grouping based on hierarchical clustering

In a manner similar to the grouping presented in Section 4.5.2, we can also employ hierarchical clustering to obtain different views on all graph kernels. Such a hierarchy will be useful because it makes it easier to assess the differences in graph kernels at multiple levels. In the following, we will describe two different hierarchies, one based on the *accuracies*, the other one based on the predicted labels.

#### 4.5.3.1 Clustering based on AUROC values

For this clustering, we treat each graph kernel as a “sample” of data set and each benchmark data set as a “feature”, yielding an  $n \times m$  matrix with  $n$  graph kernels in the rows and  $m$  data sets in the columns. We take each entry of the matrix to be an AUROC such that the values are comparable across multiple data sets. Calculating the pairwise Euclidean distance then results in an  $n \times n$  matrix, which we can cluster using *complete linkage hierarchical clustering* (Müllner, 2011). Figure 4.16a depicts the resulting dendrogram. Interestingly, Weisfeiler–Lehman approaches are clustered together here; there is a cluster containing WL-OA, MP, and WL, and HGK-WL suggesting that the performance of these kernels across all data sets is extremely similar. While this can be used to make a coarse pre-selection of a graph kernel in practice, a more precise analysis would also include the actual predictions of each method. Hence, we will now define a more-detailed variant of this plot.



**Figure 4.16:** Dendrograms obtained from performing hierarchical clustering on the graph kernels and their predictions.

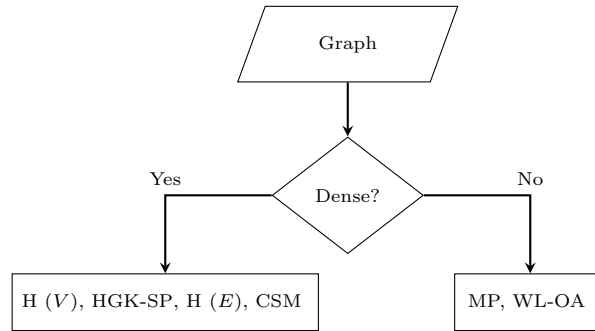
#### 4.5.3.2 Clustering based on Hamming distance

To have a more in-depth analysis of the differences and similarities between the graph kernels, we once again use the Hamming distance between their individual predictions, as described in Section 4.5.2. Thus, two algorithms will be considered *similar* or *related* if their predictions are similar over all data sets and all folds.

Figure 4.16b shows the corresponding dendrogram (which in turn should correspond to Figure 4.15, as this plot shows a two-dimensional embedding based on the same distances). Here, WL and MP form one cluster, as do HGK-SP and HGK-WL. However, the higher level clusters are not as informative.

## 4.6 Choosing a graph kernel

Having analysed graph kernels and the benchmark data sets at length and under different perspectives, we now provide guidelines for choosing a graph kernel *in practice*. The recommendations we give in this section are informed mainly by the per-type ranking shown in Table 4.9, p. 101, as well as on the different groupings we developed in Section 4.5, p. 118. We distinguish two different scenarios: first, a scenario with unlimited computational

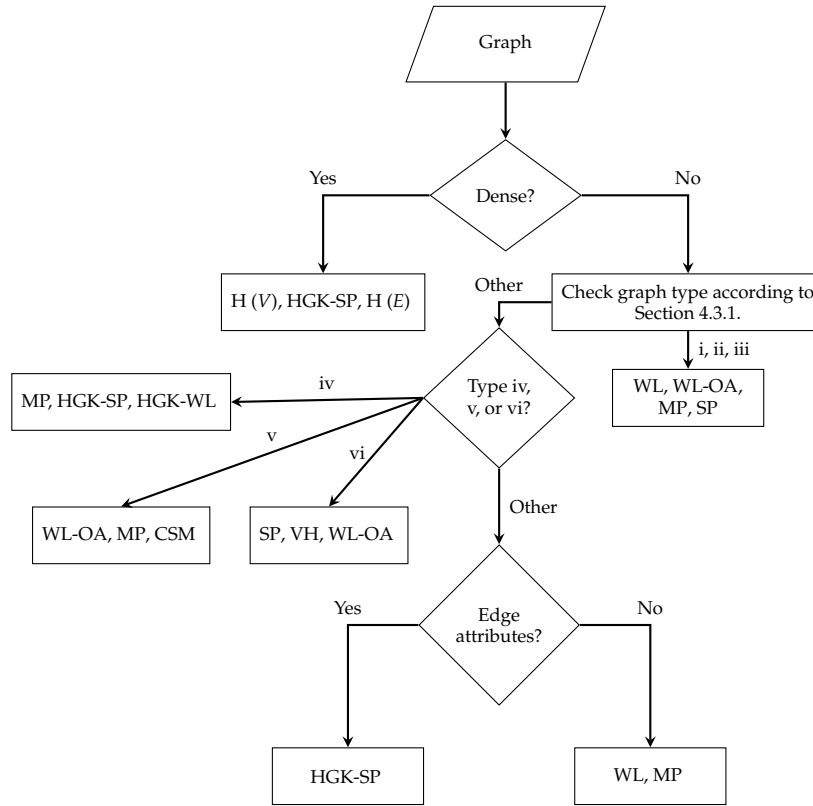


**Figure 4.17:** Selection process for a graph kernel in a scenario with no restrictions on computational resources.

resources; second, a scenario in which computational resources are more limited. Since the graph kernels are implemented using different programming languages, we cannot provide a fair comparison in terms of runtime. We can, however, discuss the extent to which parameter tuning is required in order to obtain good predictive performance.

#### 4.6.1 Scenario 1: unlimited computational resources

In this scenario, runtime and memory does not matter—we assume that one is only interested in classification performance. Suitable candidates are thus those graph kernels that outperform all other kernels on a specific type of data set. Using the ranking from Table 4.9 on p. 101, we suggest to follow the flowchart in Figure 4.17 in order to choose a suitable graph kernel. The only decision a user needs to take here is to check the *density* of the graphs data set beforehand. We purposefully leave the definition of what constitutes a dense graph open—a straightforward threshold would be to define graphs with a density of  $> 0.5$  to be dense, as opposed to sparse. For complete graphs, *i.e.* graphs with a density of 1, all schemes based on a Weisfeiler–Lehman propagation of label information are not applicable any more because all neighbourhoods will be essentially the same. In such a case, histogram-based kernels or a Hash graph kernel based on shortest paths can be more suitable. The former group of kernels has computational advantages—which are not relevant in this scenario—while the latter graph kernel has the advantage of being flexible in terms of how to use label or attribute information (recall that the shortest-path graph kernel family can handle arbitrary node/edge information; since in complete graphs, the shortest path between two vertices typically degenerates to an edge, this remains computationally feasible).



**Figure 4.18:** Selection process for a graph kernel in a scenario where only restricted computational resources are available.

#### 4.6.2 Scenario 2: limited computational resources

In this scenario, computational resources are *limited*, either in the sense of having large-scale data sets, limited storage, or limited CPU time. In this case, the selection process has to be a little bit more measured and also depend on the data set type. Figure 4.18 presents the flowchart that we recommend to follow in this situation. It is informed by Table 4.9 on p. 101, but also by the clustering of graph kernels in Figure 4.16b.

This flowchart is more detailed because it takes into the different data set types as well as potential runtime requirements and parameter choices. Whenever multiple kernels are listed in a field of the chart, our ordering goes from kernels that feature few hyperparameters to kernels that feature more. This is motivated by the observation that more hyperparameters require more complex search strategies, which may quickly become infeasible in case resources are restricted.

## 4.7 Conclusion

This chapter presented a comprehensive empirical analysis of a variety of graph kernels. We discussed the difficulty and suitability of the benchmark data sets and gave recommendations about their usage. A comprehensive comparison of predictive performance showed that graph kernels that are based on some form of the Weisfeiler–Lehman algorithm are among the best-performing graph kernels. After discussing several strategies for grouping them, either based on statistical measures or based on clustering, we closed this chapter with suggestions on how to choose a graph kernel for handling new data sets. In the next and final chapter, we will discuss novel research directions for this field but also some necessary actions that result from our analyses.

## 5 Discussion & future directions

In this final section, we will discuss actionable items that arise from the preceding analyses. We will also describe future directions, extensions, and emerging topics in the field of graph kernels.

### 5.1 Current limitations in graph kernels research

As our discussion in the preceding sections demonstrated, the current benchmark data sets and methods suffer from several limitations. We consider the crucial issues to be (i) limitations of benchmark data sets, (ii) challenges in kernel usage, (iii) reproducibility and software availability, and (iv) scalability. In the following, we will briefly comment on each of these issues and give our recommendations on how to address them.

#### 5.1.1 Limitations of benchmark data sets

Overall, as emerged from our experimental evaluation, we consider many of the current benchmark data sets to be insufficient to assess whether graph kernels possess expressivity. First, the lack of information in their topological structure is a major issue. We already observed that the topological structure of graphs only partially contributes to the information gain, as we can infer from the histogram kernels being good predictors (see Section 4.3.2). This aspect has been previously discussed by Sugiyama and Borgwardt (2015), who showed that histograms of node and edge labels, combined with a Gaussian kernel, can be extremely competitive.

Second, tightly linked to the first point, our analysis also uncovered the issue of missing *provenance information*, *i.e.* information about the construction process, for the data sets: some of the graph data sets contain “derived” or “constructed” graphs—graphs that involved user-defined choices in their creation. The repository does not provide sufficient provenance information to understand or reproduce these graphs. For example, if a data set of sparse graphs has been created by thresholding a set of dense graphs, information about this thresholding should be added to the data set or, even better, the *original* data set should be provided as well. This will make it possible to develop graph kernels that take structural information at multiple scales into account—but it will also make the creation process of the data sets more transparent. In light of the performance of histogram kernels, which we analysed in Section 4.3.2 on p. 4.3.2, we conjecture that the creation process of the data sets contributes to their performance, which is sometimes surprisingly competitive, as we would expect graph data sets to require structural information for correct classification.

Third, another limitation of the current benchmark data sets, analysed in Section 4.4, is the general lack of “difficulty”. Our discussion suggested that the current graph benchmark repository contains data sets that can and should be excluded due to being *too easy*, i.e. classifiable by a simple vertex histogram kernel, or *already solvable*. We recall that a data set was considered as already solvable if the overlap of correctly-classified graphs among the different methods was sufficiently large. Intuitively, this implies that the achievable performance has already been reached, and the remaining non-classifiable graphs are either noisy or outliers, and in conclusion too “tricky” to classify.

Fourth, current benchmark data sets are not sufficiently *diverse*. In Section 4.3.1 on p. 99, we partitioned the benchmark repository into six different types. Considering the presence or absence of the four individual types of information (node labels, edge labels, node attributes, and edge attributes) to be binary variables, there are 16 possible data set types—with the repository containing no examples for some of them. While it is theoretically possible to remove or mask certain types of features, this is not necessarily the same as lacking a given type of feature, such as a node label; this is particularly problematic because some types of graph features can be derived from another type, thus potentially leaking information. This lack of diversity is also expressed in other ways, such as the density of data sets—see Figure 4.2 on p. 86—and their size.

**Recommendation** Clearly, there is a strong need for new graph benchmark data sets, given the lack of topological information, diversity and difficulty in the current ones. Two strategies appear to be paramount to achieve this: first, to develop new methods for generating graph classification benchmark data sets that overcome these shortcomings. Second, to define and explore new application domains of graph kernels that result in a larger variety of real-world data sets for graph classification (see also Section 5.2.3). When including new—either synthetic or real-world—data sets into the collection of benchmark data sets, provenance information should be provided, including (i) information about parameters (if any) that were used to create the data set, as well as (ii) choices in pre-selecting edges or vertices. This information will help to decide whether one can expect the topology of a graph to positively influence classification in a data set, and whether a particular graph kernel has an advantage because its features mirror important parameters in the data set generation.

While a priori it is not possible to define the difficulty of a *new* graph data set, being able to assess it is crucial in order to choose the most suitable graph kernel approach. It is particularly relevant to evaluate and compare the performance of a vertex histogram kernel to other—more complex—methods. On the one hand, if the vertex histogram kernel outperforms the others, one might conclude that the data set is *too easy* and no information

about graph topology is required to classify it. On the other hand, if most of the methods perform the same or similarly, one should precisely analyse *which* graphs are classified incorrectly by each kernel. Following the logical flow analysis conducted in Section 4.4, one can then conclude whether to consider the data as already “solved”, and therefore not requiring the development of additional more advanced methods for it.

Once these issues are addressed, a future wealth of diverse graph benchmark data sets can then be utilised to conduct a fairer empirical comparison of graph kernels, and for a targeted design of novel graph kernels for particular types of graphs, *e.g.* graphs with high-dimensional node attributes. We support the recent efforts of Hu *et al.* (2020) and Morris *et al.* (2020), who each created repositories of new benchmark data sets. The latter is in fact an updated version of the repository of data sets we used in this review, and now encompasses over 120 different benchmark data sets.

### 5.1.2 Challenges in graph kernels usage

Another challenge in graph kernel research arises from how graph kernels are compared. With more and more kernels being defined in the literature, more and more empirical comparisons between them will be conducted. It is important to be aware of stumbling blocks in these comparisons.

First, one should be aware that most graph kernels do not define *one* single way of comparing graphs to each other, but rather a *family* of methods. This property is often under-utilised in comparisons or applications, leading to an unnecessarily low predictive performance that is not competitive. For instance, there is a whole family of random walk kernels, which differ by the way they weigh steps in the walks: geometric random walk kernels, for example, use exponentially decaying weights for subsequent steps, whereas random walks of a fixed length  $k$  give the *same* weight to all  $k$  steps. This difference can have drastic effects: in fact, Sugiyama and Borgwardt (2015) showed that the decaying factor in the geometric random walk kernel often has to be chosen so small that it degenerates to a simple edge comparison between two graphs, resulting in poor classification accuracy. Still, the fixed-length random walk is reported to achieve results that are competitive with the state of the art. It is therefore important to not falsely generalise empirical findings across all instances of family of graph kernels, but to select a competitive instance.

Second, our empirical results indicate that node and edge label histograms information is extremely beneficial for good classification. Several graph kernels can capture this type of information: for example, Weisfeiler–Lehman kernels with  $h = 0$  iterations are already equivalent to a comparison of node histograms. Nevertheless, some publications inadvertently use a parameter grid that excludes  $h = 0$ , thereby preventing only original



label information from being used. As another example, graphlet kernels that consider graphlets of size 1 and 2 count nodes and edges, respectively, whereas fixed-length random walk kernels with  $k = 1$  count edges in a graph. A way to severely hurt the performance of a graph kernel is to *exclude* these simple graph properties from kernel computation by not considering such simple kernel instances in the hyperparameter search of the kernels.

**Recommendation** Kernel choice and hyperparameter tuning should be performed for all the competitive methods, in order to guarantee the best performance of the state-of-the-art methods. Hyperparameters should be chosen such that they also allow for inclusion of simple graph statistics such as node and edge histograms. Moreover, the choice of kernel as well as all hyperparameters should be clearly reported, at least in the appendix of published manuscripts, and ideally be reproducible with published code. Furthermore, as Sugiyama and Borgwardt (2015) pointed out, we again emphasise the crucial importance of using histogram kernels as baselines when developing and benchmarking new graph kernels.

### 5.1.3 Reproducibility and software availability

Aside from an appropriate choice of graph kernel comparison partners, the growing number of empirical graph kernel comparisons above also creates an enormous need for reproducibility and, in particular, necessitates the availability of open source software to reproduce results.

**Reproducibility** The lack of reproducibility in the graph kernel community is largely due to the lack of a “common agreement” concerning the experimental setup and its parameters, such as the number of folds, or the number of splits to employ for a given data set. A lack of code and information about the experimental setup may cause the accuracy on a certain data set to differ from one publication to another one, thereby leading to inconclusive results and, in the worst case, incorrect claims about kernel performance. The comparability of graph kernels is further exacerbated by a non-uniform selection of benchmark data sets when it comes to evaluating prediction performance.

**Software availability** There are also cases in which the code for kernel computation is not published; even if it is available, there is still the issue of heterogeneity between programming languages. To address this problem, public software packages that facilitate the application and implementation of graph kernels in popular and uniform coding languages have recently been developed.

The `graphkernels` (Sugiyama *et al.*, 2017) package is a Python and R wrapper that relies on a C++ backend implementation. The advantage of C++ can certainly be found in the high speed and the efficiency of the code. Furthermore, the user-friendly interface permits computing all the individual graph kernel matrices with similar steps. The analogous interface between Python and R contributes to the versatility of the two languages.

The `GraKeL` (Siglidis *et al.*, 2020) package was entirely developed in Python, is compatible with `scikit-learn`, and exploits the `Cython` extension to benefit from a fast implementation in C. At present, `GraKeL` supports a larger spectrum of graph kernel methods than `graphkernels`. Its compatibility with the popular `scikit-learn` library simplifies the integration into a classification pipeline.

**Recommendation** We strongly encourage researchers to always provide code as well as pre-compiled data set splits when publishing a new graph kernel. It is crucial to also report experimental setup information for the competitor methods in order to guarantee a fair and complete assessment. Furthermore, it would be extremely beneficial for the community to define standard splits on the benchmark data sets, provide results with the existing methods, and always use them when a new approach is developed. We welcome the recent efforts of Hu *et al.* (2020), Morris *et al.* (2020), and Dwivedi *et al.* (2020) in this direction.

#### 5.1.4 Scalability

Lastly, scalability remains a key challenge in graph kernel computation. As Table 4.5 on p. 94 demonstrates, some graph kernels cannot be trained efficiently even on a high-performance computing cluster architecture. While a lot of past graph kernel research was motivated by the need to develop faster graph kernels, there may still be room to find strategies how to speed up existing kernels.

**Recommendation** We think that the community should continue to focus on computational efficiency. In addition to parallelising some calculations, we suggest investigating *approximation strategies* to speed up the computation of kernel matrices. Classical examples of this are the Nyström method (Nyström, 1930), which was successfully used to speed up calculations of the message passing graph kernel (Nikolentzos and Vazirgiannis, 2018). Similarly, the use of less restrictive, *i.e. non-perfect*, hashing functions was instrumental in speeding up the family of hash graph kernels (Morris *et al.*, 2016). We also envision that progress could be made by employing probabilistic data structures such as *bloom filters* (Bloom, 1970). These data structures could be used to replace traditional data structures

such as *sets* to improve computational efficiency, at the expense of correctness in certain queries, making the method approximative.

## 5.2 Emerging topics and future challenges

Despite these limitations, there are many different exciting new lines of research. In this section, we elaborate on emerging topics from which the field of graph kernels could benefit. Our discussion is structured as follows: (i) we discuss the idea of building more complex graph kernels, (ii) we outline the link between graph kernels and graph neural networks while paying particular attention to the Weisfeiler–Lehman framework and the theoretical link to the graph isomorphism problem, and (iii) we describe new application domains for graph kernels.

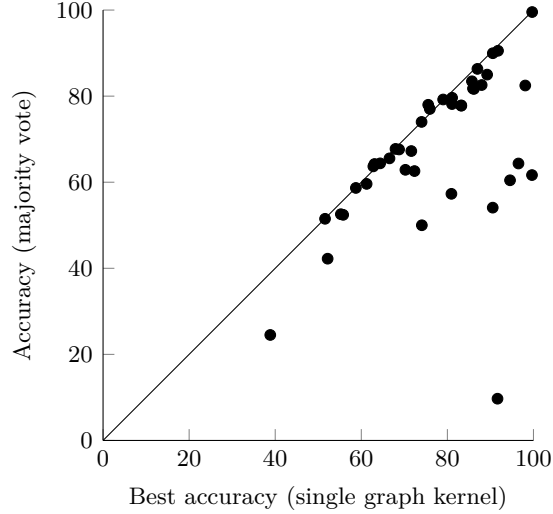
### 5.2.1 Increased complexity for graph kernels

A natural path forward is to consider more complex graph kernels. We will focus on a few initial efforts in this area, beginning with the idea of building *hybrid graph kernels*, i.e. ensembles of graph kernels. We then describe the limitations of the popular  $\mathcal{R}$ -convolution framework and present ideas how to overcome them.

#### 5.2.1.1 Ensembles of graph kernels

Given the wealth of graph kernels in the literature, an exciting question to explore is whether superior kernels could be built by combining existing ones. This could result in *graph kernel ensembles* that are capable of exploiting different sets of structural elements of graphs, thereby surpassing any individual graph kernel on certain data sets.

Such an endeavour is fraught with obstacles, though. As a simple experiment, we use the results from the preceding chapter to create a simple graph kernel ensemble. Specifically, we collate all predictions of all graph kernels and use a majority vote to predict the label. Figure 5.1 depicts the performance of this simplistic combination and compares its performance to that of the best graph kernel on the corresponding data set. We observe that in most of the cases, the predictive performance of the ensemble graph kernel is lower than that of the best-performing individual one. In fact, there are only five data sets for which this ensemble kernel improves predictive performance, namely (i) COX2\_MD, (ii) DD, (iii) ENZYMES, (iv) PROTEINS, and (v) PROTEINS\_full. Next to the computational challenges inherent in any ensemble method, this experiment also demonstrates the difficulty of creating useful ensembles—more involved methods are required; in our simple experiment,



**Figure 5.1:** A comparison of the best performance of a single graph kernel and the ensemble performance obtained via a majority vote.

the predictor does not benefit from the fact that different graph kernels are capable of capturing different characteristics of a data set. By only following the majority vote, the resulting ensemble cannot exploit the specialisation of individual graph kernels, as different features are not weighted according to their relevance to the task at hand.

One promising direction for future research is therefore the integration of confidence information; in the simplest case, such information could be used to predict according to the most *confident* graph kernel. However, it would also be possible to create a hierarchy of graph kernel predictors that are activated “on demand” whenever the confidence drops below a certain threshold. We also suggest that, according to the priority of the user, one can restrict the ensemble to only a subclass of kernels, such as propagation-based or Weisfeiler–Lehman based schemes. Additionally, more complex ensemble approaches than a simple majority vote could be employed. Furthermore, we speculate that multiple kernel learning (Lanckriet *et al.*, 2004; Sonnenburg *et al.*, 2006) could be used to effectively learn an optimal way to combine different substructures into a more powerful graph kernel, an avenue that has already begun to be explored (Aioli *et al.*, 2015). Nevertheless, the major limitation of ensemble approaches is obviously their high computational complexity.

### 5.2.1.2 Alternatives to the $\mathcal{R}$ -convolution framework

Another direction of graph kernel research reconsiders the foundation of how most graph kernels are designed, with the goal of finding alternatives that can improve performance.

Most graph kernels have been developed based on a simple instance of the  $\mathcal{R}$ -convolution framework (see Section 2.3.4), which decomposes two structured objects into their sets of substructures, to then aggregate the pairwise similarities of these substructures via a naïve sum or average. Recent efforts have been made to overcome the limitations arising from this aggregation step, which might possibly disregard complex interactions between substructures. Originally, a kernel based on an optimal assignment of node labels was proposed Fröhlich *et al.* (2005); while being empirically successful, this kernel has been later shown to be non positive definite (Vert, 2008). Recently, Kriege *et al.* (2016) extended these ideas by developing a Weisfeiler–Lehman based optimal assignment kernel (WL-OA). Successively, Togninalli *et al.* (2019) also proposed an extension of the original Weisfeiler–Lehman kernel, which is especially designed for continuously attributed graphs (WWL). This method employs the Wasserstein distance (Villani, 2008) to capture more complex similarities between substructures, computing a graph level representation from node features obtained via a multi iteration Weisfeiler–Lehman inspired scheme. The WL-OA and WWL kernels for graphs with categorical node labels have been shown to be positive semi-definite; assessing the positive definiteness of WWL on continuous node attributed graphs is still an open problem. These approaches open the door to a new line of research, connecting the emerging field of *optimal transport* (Villani, 2008), which has recently gained considerable interest in the community, to graph kernels. Challenging theoretical problems, such as assessing positive definiteness of existing methods, and theoretical contributions, including the design of new kernels based on optimal transport theory, will be of interest in the future.

The field of topological data analysis, focusing on connectivity properties of structured objects in general, has recently started to demonstrate its capabilities in graph classification, constituting a somewhat complementary view to existing methods. Topological features, such as connected components and cycles, have shown their capabilities for improving existing graph kernels (Rieck *et al.*, 2019), but they can also “hold their own” upon being combined with appropriate machine learning architectures (Hofer *et al.*, 2017; Zhao and Wang, 2019). With recent work establishing a framework for *learning* topological descriptors in an end-to-end fashion to improve classification performance (Hofer *et al.*, 2020), we envision that this topic will be of increasing relevance in the future.

We conclude this section by pointing out that the last step in kernel computation on structured objects, *i.e.* the aggregation of node representations, is also a limitation in the field of graph neural networks (Xu *et al.*, 2019), where it is commonly referred to as a READOUT layer. Most GNNs approaches use a mean, sum, max or a combination of these functions to generate the graph-level representations from the node features (as obtained via Equations 5.1 and 5.2). Extensions of the current scheme, based for instance on

attention mechanisms (Gilmer *et al.*, 2017), pooling strategies (Ying *et al.*, 2018), or network architectures (Schütt *et al.*, 2017), have yet to be fully explored and certainly represent an interesting direction to pursue in graph neural networks and graph kernel research. We proceed now to a larger discussion of graph neural networks, and explore their connection to graph kernels.

### 5.2.2 Link between graph kernels and graph neural networks

Graph Neural Networks (GNNs) have emerged in recent years and established a successful line of research, achieving state-of-the-art performance in both graph classification and regression tasks (see Wu *et al.* (2019) for a recent survey). We will first provide a definition and brief overview of GNNs, and will later discuss how this procedure is related to the Weisfeiler–Lehman labelling scheme (see Section 3.2.2.1).

The main idea underlying GNNs is to propagate the initial feature representation of the nodes and edges across the graph, thereby exploiting a multi-iterative scheme that at each step updates the current state by looking at the neighbourhood information of a node. In the following, the term *node feature* refers to the node representation at a given iteration, which can be either the original node label or attribute, or an update of it obtained after one or more steps.

Graph Neural Networks employ an affine transformation followed by a pointwise non-linear activation function to update the node or edge information, which encourages *smooth* information propagation on the graph. We will follow the structure and notation introduced in Xu *et al.* (2019). Given a graph  $G = (V, E)$  and a set of node features  $X_G \in \mathbb{R}^{|V| \times p}$ , most GNNs employ a neighbourhood aggregation strategy. Such a strategy updates the node feature of the current iteration by *aggregating* the representations of the neighbours using, for example, the calculation of a mean. The aggregation function is crucial because it makes all learned representations invariant with respect to permutations; a GNN is therefore impervious to changing the indices of nodes. Let  $x_v^0 \in \mathbb{R}^p$  be the initial node feature (*i.e.* either attributes or a label) of node  $v$  in graph  $G$ . We recursively define

$$z_v^{(h)} := \text{AGGREGATE}\{x_{v'}^{(h-1)} \mid v' \in N(v)\}, \quad (5.1)$$

and update the node feature of  $v$  as

$$x_v^{(h)} := \text{COMBINE}(x_v^{(h-1)}, z_v^{(h)}). \quad (5.2)$$

for up to  $h_{\max}$  rounds of propagation. Finally, the collection of all node feature vectors obtained during the iteration process can be summarised into a *single* vectorial representation for the graph by

$$\phi(G) = \text{READOUT}\left(\left\{x_v^{(h)} \mid v \in V, h = \{0, \dots, h_{\max}\}\right\}\right). \quad (5.3)$$

Multiple possibilities exist for defining the COMBINE, AGGREGATE, and READOUT functions, leading to different approaches as described by Duvenaud *et al.* (2015), Kipf and Welling (2017), and Hamilton *et al.* (2017a), for example.

**Weisfeiler–Lehman versus GNNs** We note that the idea behind GNNs follows the Weisfeiler–Lehman propagation scheme, as highlighted by Xu *et al.* (2019). Recalling the terminology and notation introduced in Section 3.2.2.1, we defined the Weisfeiler–Lehman node feature update as

$$l_V(v)_{\text{WL}}^{(h+1)} := f\left(l_V(v)_{\text{WL}}^{(h)}, \{l_V(v')_{\text{WL}}^{(h)} \mid v' \in N(v)\}\right), \quad (5.4)$$

where  $f(\cdot)$  represents a *perfect hashing* scheme that uniquely maps tuples formed by the node label of the current vertex,  $l_V(v)_{\text{WL}}^{(h)}$ , and the multiset of node labels of all neighbours of the current vertex,  $\{l_V(v')_{\text{WL}}^{(h)} \mid v' \in N(v)\}$ , to a new categorical label. Denoting by  $\phi_V(v)_{\text{WL}}^{(h)}$  the one-hot vector corresponding to  $l_V(v)_{\text{WL}}^{(h)}$ , the simplest instance of the Weisfeiler–Lehman framework would then aggregate these node representations across all propagation steps  $h = 0, 1, \dots, h_{\max}$  as

$$\phi_{\text{WL}}(G) = \text{concat}\left(\sum_{v \in V} l_V(v)_{\text{WL}}^{(0)}, \dots, \sum_{v \in V} l_V(v)_{\text{WL}}^{(h_{\max})}\right), \quad (5.5)$$

to obtain a single vectorial embedding for the graph.

Thus, the main difference between the Weisfeiler–Lehman scheme and GNN approaches boils down to the definition of the COMBINE, AGGREGATE, and READOUT functions. Perhaps the most crucial distinction is that while graph neural networks typically implement the AGGREGATE and COMBINE steps as smooth functions with learnable parameters, the Weisfeiler–Lehman uses instead a perfect hash. Theoretically, despite being virtually parameter-free, the Weisfeiler–Lehman implementation of information propagation is at least as expressive as that of graph neural networks due to the use of perfect hashing. However, it lacks the ability to be “tuned” end-to-end to a specific task if a sufficiently large data set is available. Similarly, the READOUT phase of the simplest instance of the Weisfeiler–Lehman framework can be understood as forming an (unnormalised) node label histogram for each step  $h$  and then concatenating these histograms. In contrast, graph neural networks use a wide range of alternatives, some being virtually equivalent to that of the Weisfeiler–Lehman framework, while others implement complex smooth functions with a large number of learnable parameters.



### 5.2.2.1 Link to the graph isomorphism problem

Having established the connection between the Weisfeiler–Lehman scheme and GNNs, we now want to understand how expressive GNNs can be. To do so, we will return to the graph isomorphism problem introduced in Section 2.2.1. In general, determining whether two graphs are isomorphic is so far a problem that is not known to be solvable in polynomial time. In practice, the WL test works for the majority of all cases, though it is possible to find—or construct—pairs and families of non-isomorphic graphs that the WL test cannot distinguish. Recently, it has been investigated whether graph neural networks are more powerful than the WL test and can succeed in distinguishing these graphs (Xu *et al.*, 2019). Xu *et al.* (2019) concluded that GNNs are *at most* as powerful as the WL test in distinguishing graph structures. The authors further commented that certain requirements in the scheme of GNNs need to be satisfied in order to *achieve* such power, and they propose a novel Graph Isomorphism Network (GIN) architecture, which is capable of reaching a discriminative power comparable to that of the Weisfeiler–Lehman isomorphism test for distinguishing graph structures. Xu *et al.* (2019) argue that the READOUT function in a GNN needs to be injective, to guarantee that two *non-isomorphic* graphs will be mapped to different graph embeddings, thereby being correctly identified as *non-isomorphic*.

### 5.2.2.2 Learning node representations with GNNs & graph kernels

Finally, we would like to highlight an additional use case for GNNs and graph kernels which is of increasing interest to the community: learning representations of nodes. While this review has been centered primarily around graph classification, many graph neural networks are often used for the purpose of node classification (Kipf and Welling, 2017) or the related task of learning representations of nodes in a graph (Dai *et al.*, 2016; Hamilton *et al.*, 2017b). While the graph kernels we described have been primarily used for classification or regression tasks, for most of the existing approaches, an explicit feature vector representation of a graph can be derived, or an approximation of it can be computed (Kriege *et al.*, 2019). Due to most current graph kernels being instances of the  $\mathcal{R}$ -convolution framework, in which a graph is represented as a set of nodes, graph kernels indirectly also provide a vectorial representation of each node in the graph. While there is long-standing interest in kernels between nodes in one graph (Kondor and Lafferty, 2002; Smola and Kondor, 2003), these efficient-to-compute node representations based on graph kernels have not been studied in any detail. At the very least, they will offer a baseline that node kernel and deep learning approaches need to improve over in order to prove the merits of their representation learning.



As we’ve seen in this section, graph neural networks have emerged alongside graph kernels as a state-of-the-art approach to solve graph classification tasks. We conclude by highlighting an exciting line of future research that explores the relative benefits of graph kernels and GNNs and exploits them in hybrid approaches. Initial research (Nikolentzos *et al.*, 2018b; Du *et al.*, 2019) demonstrated that such *hybrid* approaches, which combine the “best of both worlds”, can indeed achieve good predictive performance. Du *et al.* (2019), for instance, introduce the *graph neural tangent kernel*, which under certain assumptions can be shown to be equivalent to an infinitely wide neural network trained by gradient descent. This therefore promises to have the expansive expressivity of a neural network, while still maintaining the benefits of a convex optimization objective. Given the distinct strengths of graph kernels and graph neural networks, developing methods that can fuse components of the two presents an promising new direction in the field of graph classification.

### 5.2.3 New application domains

While GNNs represent a new suite of methods applicable to the task of graph classification, another promising direction for future research is the exploration of new application domains. Structural biology and chemoinformatics will remain a primary application domain of graph kernels and graph learning, but we predict that emerging application domains will increase the variety of the data sets and the number and type of learning tasks on graphs. In light of the issues that we discussed in the preceding sections, we consider multiple domains to be promising for the future, particularly within new medical and mathematical applications. Each of these fields, which we will subsequently discuss, has their own idiosyncratic data set types, which will enrich future research.

#### 5.2.3.1 Medical applications

One of the most promising new application domains is within medical applications. We will now introduce two specific areas where graph-based approaches are starting to take hold, namely with (i) electronic health records and (ii) brain connectivity networks.

**Electronic health records** Electronic health records refer to the ensemble of all records of a patient in a hospital. Their multi-modal nature makes them hard to use in classification scenarios. Recent advances in machine learning show that the inclusion of structural, *i.e.* *graphical*, information can be used for medical purposes, such as mortality or medications prediction (Choi *et al.*, 2019). Similarly, there are ambitious projects to learn knowledge graphs from such records (Rotmensch *et al.*, 2017). The future of graph kernels research

should embrace this domain because of its challenges (large, multi-modal, noisy graphs) and its potential to improve patient welfare.

**Brain connectivity networks** In a similar fashion, magnetic resonance imaging (MRI) data have started to become ubiquitous over recent years and various analysis methods have been proposed. MRI data can be subject to thresholding (representing an uncertainty, or a certain noise level) to yield functional connectivity networks of the human brain. There are numerous publications discussing network extraction and network analysis techniques (see Ktena *et al.* (2018) and Wang *et al.* (2010) for two randomly-selected examples), making them prime examples for the development of graph kernels that can handle heterogeneous data sets at multiple scales or different “resolution” levels. The relevance of the topology, *i.e.* the definition of connectivity to extract such a graph, is known to be one of the recurring problems of the field (Expert *et al.*, 2019), and we are convinced that graph kernels could provide solutions. Pioneering studies by Vega-Pons and Avesani (2013) and Gkirtzou *et al.* (2013) exploited Weisfeiler–Lehman based techniques to analyse the fMRI graphs, and their results are encouraging for the further development of the field.

### 5.2.3.2 Mathematical applications

A second area where there is potential for graph-based methods is within more theoretical mathematical applications. We now highlight two such areas, namely (i) geometric graphs and (ii) the planted clique problem, where we anticipate that graph-based methods can progress the field.

**Geometric graphs** Moving to a somewhat more unorthodox domain, geometric graphs refer to graphs that are constructed on point cloud data—that is to say, sets of unstructured points in a  $d$ -dimensional real-valued vector space—by a *proximity operator* that uses different geometric properties to define edges between individual points. The *Gabriel graph* (Gabriel and Sokal, 1969), for example, creates an edge between two points  $p$  and  $q$  if and only if their diameter circle (or diameter sphere in higher dimensions) contains no other points. Several variants of such graphs exist (Correa and Lindstrom, 2011; Jaromczyk and Toussaint, 1992) and their construction can be shown to have interesting geometric properties. Since point cloud data occur in different domains, we consider them to be an interesting example for further research in graph kernels. Given the existence of some previous work (Bach, 2008), we are convinced that the principled construction process of these graphs yields an interesting starting point for the development of new “geometric” graph kernels.

**The planted clique problem** Adopting a more theoretical perspective, we briefly discuss how graph kernels can be of interest to solve optimisation problems on graphs, thereby helping discover new theorems in complexity theory. While many of these problems exist (Arora and Barak, 2009), we focus on a specific instance, namely the *planted clique problem* (Alon *et al.*, 1998). A clique is defined as a subset of vertices in an undirected graph whose induced subgraph is complete, *i.e.* every pair of vertices is connected by an edge. A planted clique in a graph is a clique that has been added to the graph by selecting a subset of vertices at random and turning them into a clique. In combinatorial optimisation, the planted clique problem consists of distinguishing random graphs from graphs with a planted clique; the probability of adding such a planted clique is typically taken to be  $p = 0.5$ . This problem can be solved in polynomial time only for specific sufficiently large values of  $k$ , with  $k$  being the size of a clique. In practice, this problem can be turned into a binary classification problem on graphs, thus permitting the use of graph kernels (since  $p = 0.5$ , the classification problem does not suffer from class imbalance). We see a great potential in this application, which to the best of our knowledge is yet unexplored. In this domain—and potentially for related tasks—graph kernels could provide major benefits and speed-ups for solving the planted clique problem from a classification perspective with high accuracy.

## 5.3 Conclusion

This survey showed that the field of graph kernels is a vibrant and rich domain of machine learning research. Being well-grounded in the theory of reproducing kernel Hilbert spaces, the field permits contributions on various levels, ranging from the theoretical assessment of kernel properties to the empirical assessment of the integration of new graph features. Given the numerous challenges, open problems and emerging topics around graph kernels, we are convinced that there are plenty of opportunities for future work. We therefore hope that this review provides a stimulus for novel graph kernel research.

## References

- Aggarwal, C. and H. Wang. 2010. "A Survey of Clustering Algorithms for Graph Data". In: *Managing and Mining Graph Data*. Vol. 40. Springer. 275–301.
- Aioli, F., M. Donini, N. Navarin, and A. Sperduti. 2015. "Multiple Graph-Kernel Learning". In: *IEEE Symposium Series on Computational Intelligence*. 1607–1614.
- Alon, N., M. Krivelevich, and B. Sudakov. 1998. "Finding a large hidden clique in a random graph". *Random Structures & Algorithms*. 13(3–4): 457–466.
- Aronszajn, N. 1950. "Theory of Reproducing Kernels". *Transactions of the American Mathematical Society*. 68(3): 337–404.
- Arora, S. and B. Barak. 2009. *Computational complexity: A Modern Approach*. Cambridge, United Kingdom: Cambridge University Press.
- Babai, L. and L. Kucera. 1979. "Canonical labelling of graphs in linear average time". In: *20th Annual Symposium on Foundations of Computer Science*. 39–46.
- Babai, L. 2015. "Graph Isomorphism in Quasipolynomial Time". *arXiv e-prints*. arXiv: [1512.03547](https://arxiv.org/abs/1512.03547) [cs.DS].
- Bach, F. R. 2008. "Graph Kernels between Point Clouds". In: *Proceedings of the 25th International Conference on Machine Learning*. 25–32.
- Bagnall, A., J. Lines, A. Bostrom, J. Large, and E. Keogh. 2017. "The great time series classification bake off: a review and experimental evaluation of recent algorithmic advances". *Data Mining and Knowledge Discovery*. 31(3): 606–660.
- Bai, L., E. R. Hancock, A. Torsello, and L. Rossi. 2013. "A Quantum Jensen–Shannon Graph Kernel Using the Continuous-time Quantum Walk". In: *Graph-Based Representations in Pattern Recognition*. Ed. by W. G. Kropatsch, N. M. Artner, Y. Haxhimusa, and X. Jiang. Heidelberg, Germany: Springer. 121–131.
- Bai, L., L. Rossi, H. Bunke, and E. R. Hancock. 2014. "Attributed Graph Kernels Using the Jensen–Tsallis  $q$ -Differences". In: *Machine Learning and Knowledge Discovery in Databases*. Ed. by T. Calders, F. Esposito, E. Hüllermeier, and R. Meo. Heidelberg, Germany: Springer. 99–114.
- Bai, L., Z. Zhang, P. Ren, L. Rossi, and E. R. Hancock. 2015. "An Edge-based Matching Kernel through Discrete-time Quantum Walks". In: *Image Analysis and Processing – ICIAP*. Ed. by V. Murino and E. Puppo. Cham, Switzerland: Springer. 27–38.
- Bai, Y., H. Ding, S. Bian, T. Chen, Y. Sun, and W. Wang. 2018. "Graph Edit Distance Computation via Graph Neural Networks". *arXiv e-prints*. arXiv: [1808.05689](https://arxiv.org/abs/1808.05689) [cs.LG].

- Berger, F., P. Gritzmann, and S. de Vries. 2009. "Minimum Cycle Bases and Their Applications". In: *Algorithmics of Large and Complex Networks: Design, Analysis, and Simulation*. Ed. by J. Lerner, D. Wagner, and K. A. Zweig. Heidelberg, Germany: Springer. 34–49.
- Bernstein, M., V. De Silva, J. C. Langford, and J. B. Tenenbaum. 2000. "Graph approximations to geodesics on embedded manifolds". *Tech. rep.* Stanford University.
- Blizard, W. D. 1988. "Multiset Theory". *Notre Dame Journal of Formal Logic*. 30(1): 36–66.
- Bloom, B. H. 1970. "Space/Time Trade-offs in Hash Coding with Allowable Errors". *Communications of the ACM*. 13(7): 422–426.
- Borg, I. and P. J. F. Groenen. 2005. *Modern Multidimensional Scaling. Theory and Applications*. 2nd ed. New York, NY, USA: Springer.
- Borgwardt, K. M., C. S. Ong, S. Schönauer, S. Vishwanathan, A. J. Smola, and H.-P. Kriegel. 2005. "Protein function prediction via graph kernels". *Bioinformatics*. 21(suppl\_1): i47–i56.
- Borgwardt, K. and H.-P. Kriegel. 2005. "Shortest-path kernels on graphs". In: *Proceedings of the Fifth IEEE International Conference on Data Mining*. Washington, DC, USA: IEEE Computer Society. 74–81.
- Boser, B. E., I. M. Guyon, and V. N. Vapnik. 1992. "A Training Algorithm for Optimal Margin Classifiers". In: *Proceedings of the Fifth Annual Workshop on Computational Learning Theory*. ACM. New York, NY, USA. 144–152.
- Brouwer, A. E. and W. H. Haemers. 2012. *Spectra of Graphs*. New York, NY, USA: Springer.
- Bunke, H. and K. Riesen. 2007. "A Family of Novel Graph Kernels for Structural Pattern Recognition". In: *Progress in Pattern Recognition, Image Analysis and Applications*. Ed. by L. Rueda, D. Mery, and J. Kittler. Heidelberg, Germany: Springer. 20–31.
- Calvo, B. and G. Santafé. 2016. "scmamp: Statistical Comparison of Multiple Algorithms in Multiple Problems". *The R Journal*. 8(1): 248–256.
- Ceroni, A., F. Costa, and P. Frasconi. 2007. "Classification of small molecules by two- and three-dimensional decomposition kernels". *Bioinformatics*. 23(16): 2038–2045.
- Choi, E., M. T. Bahadori, L. Song, W. F. Stewart, and J. Sun. 2017. "GRAM: Graph-based Attention Model for Healthcare Representation Learning". In: *Proceedings of the 23rd ACM SIGKDD International Conference on Knowledge Discovery and Data Mining*. ACM. New York, NY, USA. 787–795.
- Choi, E., M. W. Dusenberry, G. Flores, Z. Xu, Y. Li, Y. Xue, and A. M. Dai. 2019. "Learning Graphical Structure of Electronic Health Records with Transformer for Predictive Healthcare". In: *ICML Workshop on Learning and Reasoning with Graph-Structured Data*.
- Chung, F. R. K. 1997. *Spectral Graph Theory*. Providence, RI, USA: American Mathematical Society.

- Correa, C. D. and P. Lindstrom. 2011. "Towards Robust Topology of Sparsely Sampled Data". *IEEE Transactions on Visualization and Computer Graphics*. 17(12): 1852–1861.
- Costa, F. and K. De Grave. 2010. "Fast neighborhood subgraph pairwise distance kernel". In: *Proceedings of the 26th International Conference on Machine Learning*. 255–262.
- Curado, M., F. Escolano, E. R. Hancock, F. Nourbakhsh, and M. Pelillo. 2015. "Similarity Analysis from Limiting Quantum Walks". In: *Similarity-Based Pattern Recognition – SIMBAD*. Ed. by A. Feragen, M. Pelillo, and M. Loog. Cham, Switzerland: Springer. 38–53.
- Dai, H., B. Dai, and L. Song. 2016. "Discriminative embeddings of latent variable models for structured data". In: *International Conference on Machine Learning*. 2702–2711.
- Datar, M., N. Immorlica, P. Indyk, and V. S. Mirrokni. 2004. "Locality-Sensitive Hashing Scheme Based on  $p$ -stable Distributions". In: *Proceedings of the 20th Annual Symposium on Computational Geometry*. New York, NY, USA: ACM. 253–262.
- Demšar, J. 2006. "Statistical Comparisons of Classifiers Over Multiple Data Sets". *Journal of Machine Learning Research*. 7: 1–30.
- Dijkstra, E. W. 1959. "A Note on Two Problems in Connexion with Graphs". *Numerische Mathematik*. 1(1): 269–271.
- Du, N., L. Song, M. G. Rodriguez, and H. Zha. 2013. "Scalable Influence Estimation in Continuous-time Diffusion Networks". In: *Advances in Neural Information Processing Systems 26*. Ed. by C. J. C. Burges, L. Bottou, M. Welling, Z. Ghahramani, and K. Q. Weinberger. 3147–3155.
- Du, N., B. Wu, X. Pei, B. Wang, and L. Xu. 2007. "Community Detection in Large-scale Social Networks". In: *Proceedings of the 9th WebKDD and 1st SNA-KDD 2007 Workshop on Web Mining and Social Network Analysis*. ACM. New York, NY, USA. 16–25.
- Du, S. S., K. Hou, B. Póczos, R. Salakhutdinov, R. Wang, and K. Xu. 2019. "Graph Neural Tangent Kernel: Fusing Graph Neural Networks with Graph Kernels". *arXiv e-prints*: 2224–2232. arXiv: [1905.13192](https://arxiv.org/abs/1905.13192) [cs.LG].
- Duvenaud, D. K., D. Maclaurin, J. Iparraguirre, R. Bombarell, T. Hirzel, A. Aspuru-Guzik, and R. P. Adams. 2015. "Convolutional Networks on Graphs for Learning Molecular Fingerprints". In: *Advances in Neural Information Processing Systems 28*. 2224–2232.
- Dwivedi, V. P., C. K. Joshi, T. Laurent, Y. Bengio, and X. Bresson. 2020. "Benchmarking Graph Neural Networks". eprint: [2003.00982](https://arxiv.org/abs/2003.00982).
- Expert, P., L.-D. Lord, M. L. Kringelbach, and G. Petri. 2019. "Editorial: Topological Neuroscience". *Network Neuroscience*. 3(3): 653–655.

- Feragen, A., N. Kasenburg, J. Petersen, M. de Bruijne, and K. Borgwardt. 2013. "Scalable kernels for graphs with continuous attributes". In: *Advances in Neural Information Processing Systems* 26. Ed. by C. J. C. Burges, L. Bottou, M. Welling, Z. Ghahramani, and K. Q. Weinberger. 216–224.
- Floyd, R. W. 1962. "Algorithm 97: Shortest Path". *Communications of the ACM*. 5(6): 345.
- Fröhlich, H., J. K. Wegner, F. Sieker, and A. Zell. 2005. "Optimal Assignment Kernels for Attributed Molecular Graphs". In: *Proceedings of the 22nd International Conference on Machine Learning*. ACM. New York, NY, USA. 225–232.
- Gabriel, K. R. and R. R. Sokal. 1969. "A new statistical approach to geographic variation analysis". *Systematic Biology*. 18(3): 259–278.
- Gärtner, T., P. Flach, and S. Wrobel. 2003. "On Graph Kernels: Hardness Results and Efficient Alternatives". In: *Learning Theory and Kernel Machines*. Ed. by B. Schölkopf and M. K. Warmuth. Heidelberg, Germany: Springer. 129–143.
- Gilmer, J., S. S. Schoenholz, P. F. Riley, O. Vinyals, and G. E. Dahl. 2017. "Neural Message Passing for Quantum Chemistry". In: *Proceedings of the 34th International Conference on Machine Learning*. Ed. by D. Precup and Y. W. Teh. *Proceedings of Machine Learning Research*. PMLR. 1263–1272.
- Gkirtzou, K., J. Honorio, D. Samaras, R. Goldstein, and M. Blaschko. 2013. "fMRI Analysis with Sparse Weisfeiler–Lehman Graph Statistics". In: *Machine Learning in Medical Imaging*. Ed. by G. Wu, D. Zhang, D. Shen, P. Yan, K. Suzuki, and F. Wang. Cham, Switzerland: Springer. 90–97.
- Glem, R., A. Bender, C. Hasselgren, L. Carlsson, S. Boyer, and J. Smith. 2006. "Circular fingerprints: Flexible molecular descriptors with applications from physical chemistry to ADME". *IDrugs : the investigational drugs journal*. 9: 199–204.
- Goh, K.-I., M. E. Cusick, D. Valle, B. Childs, M. Vidal, and A.-L. Barabási. 2007. "The human disease network". *Proceedings of the National Academy of Sciences*. 104(21): 8685–8690.
- Graf, A. B. A. and S. Borer. 2001. "Normalization in Support Vector Machines". In: *Pattern Recognition*. Ed. by B. Radig and S. Florczyk. Heidelberg, Germany: Springer. 277–282. ISBN: 978-3-540-45404-5.
- Greene, D. and P. Cunningham. 2006. "Practical Solutions to the Problem of Diagonal Dominance in Kernel Document Clustering". In: *Proceedings of the 23rd International Conference on Machine Learning (ICML)*. New York, NY, USA: Association for Computing Machinery. 377–384. doi: [10.1145/1143844.1143892](https://doi.org/10.1145/1143844.1143892).
- Hamilton, W. L., R. Ying, and J. Leskovec. 2017a. "Inductive Representation Learning on Large Graphs". In: *Advances in Neural Information Processing Systems* 30. 1024–1034.
- Hamilton, W. L., R. Ying, and J. Leskovec. 2017b. "Representation Learning on Graphs: Methods and Applications". *arXiv e-prints*. arXiv: [1709.05584](https://arxiv.org/abs/1709.05584) [cs. SI].



- Haussler, D. 1999. "Convolution kernels on discrete structures". *Tech. rep.* University of California at Santa Cruz.
- He, Y. and A. Evans. 2010. "Graph theoretical modeling of brain connectivity". *Current Opinion in Neurology*. 23(4): 341–350.
- Hido, S. and H. Kashima. 2009. "A Linear-Time Graph Kernel". In: *Proceedings of the Ninth IEEE International Conference on Data Mining*. Washington, DC, USA: IEEE Computer Society. 179–188.
- Hoerl, A. E. and R. W. Kennard. 1970. "Ridge Regression: Biased Estimation for Nonorthogonal Problems". *Technometrics*. 12(1): 55–67.
- Hofer, C. D., F. Graf, B. Rieck, M. Niethammer, and R. Kwitt. 2020. "Graph Filtration Learning". In: *Proceedings of the 37th International Conference on Machine Learning (ICML). Proceedings of Machine Learning Research*. arXiv: [1905.10996 \[cs.LG\]](https://arxiv.org/abs/1905.10996). In press.
- Hofer, C., R. Kwitt, M. Niethammer, and A. Uhl. 2017. "Deep Learning with Topological Signatures". In: *Advances in Neural Information Processing Systems 30 (NeurIPS)*. Ed. by I. Guyon, U. V. Luxburg, S. Bengio, H. Wallach, R. Fergus, S. Vishwanathan, and R. Garnett. Red Hook, NY, USA: Curran Associates, Inc. 1634–1644.
- Hofmann, T., B. Schölkopf, and A. J. Smola. 2008. "Kernel Methods in Machine Learning". *The Annals of Statistics*. 36(3): 1171–1220.
- Horváth, T., T. Gärtner, and S. Wrobel. 2004. "Cyclic Pattern Kernels for Predictive Graph Mining". In: *Proceedings of the Tenth ACM SIGKDD International Conference on Knowledge Discovery and Data Mining*. New York, NY, USA: Association for Computing Machinery. 158–167.
- Hotelling, H. 1933. "Analysis of a Complex of Statistical Variables into Principal Components". *Journal of Educational Psychology*. 24(6): 417.
- Hsieh, C.-J., S. Si, and I. S. Dhillon. 2014. "Fast Prediction for Large-Scale Kernel Machines". In: *Advances in Neural Information Processing Systems 27*. Ed. by Z. Ghahramani, M. Welling, C. Cortes, N. D. Lawrence, and K. Q. Weinberger. Curran Associates, Inc. 3689–3697.
- Hu, W., M. Fey, M. Zitnik, Y. Dong, H. Ren, B. Liu, M. Catasta, and J. Leskovec. 2020. "Open Graph Benchmark: Datasets for Machine Learning on Graphs". arXiv: [2005.00687](https://arxiv.org/abs/2005.00687).
- Huson, D. H. and D. Bryant. 2005. "Application of Phylogenetic Networks in Evolutionary Studies". *Molecular Biology and Evolution*. 23(2): 254–267.
- Jaromczyk, J. W. and G. T. Toussaint. 1992. "Relative Neighborhood Graphs and Their Relatives". *Proceedings of the IEEE*. 80(9): 1502–1517.
- Jebara, T. and R. Kondor. 2003. "Bhattacharyya and Expected Likelihood Kernels". In: *Learning Theory and Kernel Machines*. Ed. by B. Schölkopf and M. K. Warmuth. Heidelberg, Germany: Springer. 57–71.



- Jebara, T., R. Kondor, and A. Howard. 2004. "Probability Product Kernels". *Journal of Machine Learning Research*. 5: 819–844.
- Kanehisa, M. and S. Goto. 2000. "KEGG: Kyoto Encyclopedia of Genes and Genomes". *Nucleic Acids Research*. 28(1): 27–30.
- Kanungo, T., D. M. Mount, N. S. Netanyahu, C. D. Piatko, R. Silverman, and A. Y. Wu. 2002. "An Efficient  $k$ -Means Clustering Algorithm: Analysis and Implementation". *IEEE Transactions on Pattern Analysis and Machine Intelligence*. 24(7): 881–892.
- Karlebach, G. and R. Shamir. 2008. "Modelling and analysis of gene regulatory networks". *Nature Reviews Molecular Cell Biology*. 9(10): 770.
- Karp, R. M. 1972. "Reducibility among Combinatorial Problems". In: *Complexity of Computer Computations*. Ed. by R. E. Miller, J. W. Thatcher, and J. D. Bohlinger. Boston, MA, USA: Springer. 85–103.
- Kashima, H., K. Tsuda, and A. Inokuchi. 2003. "Marginalized Kernels between Labeled Graphs". In: *Proceedings of the 20th International Conference on Machine Learning*. 321–328.
- Kataoka, T. and A. Inokuchi. 2016. "Hadamard Code Graph Kernels for Classifying Graphs". In: *Proceedings of the 5th International Conference on Pattern Recognition Applications and Methods (ICPRAM)*. 24–32.
- Kersting, K., N. M. Kriege, C. Morris, P. Mutzel, and M. Neumann. 2016. "Benchmark Data Sets for Graph Kernels". URL: <http://graphkernels.cs.tu-dortmund.de>.
- Kipf, T. N. and M. Welling. 2017. "Semi-Supervised Classification with Graph Convolutional Networks". In: *International Conference on Learning Representations (ICLR)*.
- Köbler, J. and O. Verbitsky. 2008. "From Invariants to Canonization in Parallel". In: *Computer Science – Theory and Applications*. Ed. by E. A. Hirsch, A. A. Razborov, A. Semenov, and A. Slissenko. Heidelberg, Germany: Springer. 216–227. ISBN: 978-3-540-79709-8.
- Koller, D. and N. Friedman. 2009. *Probabilistic Graphical Models: Principles and Techniques*. Cambridge, MA, USA: MIT press.
- Kondor, R. I. and J. Lafferty. 2002. "Diffusion Kernels on Graphs and Other Discrete Structures". In: *Proceedings of the 19th International Conference on Machine Learning*. Vol. 2002. 315–322.
- Kondor, R. and H. Pan. 2016. "The Multiscale Laplacian Graph Kernel". In: *Advances in Neural Information Processing Systems* 29. Ed. by D. D. Lee, M. Sugiyama, U. V. Luxburg, I. Guyon, and R. Garnett. 2990–2998.
- Kondor, R., N. Shervashidze, and K. M. Borgwardt. 2009. "The Graphlet Spectrum". In: *Proceedings of the 26th Annual International Conference on Machine Learning*. ACM. New York, NY, USA. 529–536.

- Kriege, N. M., P.-L. Giscard, and R. C. Wilson. 2016. "On Valid Optimal Assignment Kernels and Applications to Graph Classification". In: *Advances in Neural Processing Systems 29*. 1623–1631.
- Kriege, N. M., F. D. Johansson, and C. Morris. 2020. "A survey on graph kernels". *Applied Network Science*. 5(1): 6.
- Kriege, N. M., M. Neumann, C. Morris, K. Kersting, and P. Mutzel. 2019. "A unifying view of explicit and implicit feature maps of graph kernels". *Data Mining and Knowledge Discovery*. 33(6): 1505–1547.
- Kriege, N. and P. Mutzel. 2012. "Subgraph matching kernels for attributed graphs". *Proceedings of the 29th International Conference on Machine Learning*.
- Ktena, S. I., S. Parisot, E. Ferrante, M. Rajchl, M. Lee, B. Glocker, and D. Rueckert. 2018. "Metric learning with spectral graph convolutions on brain connectivity networks". *NeuroImage*. 169: 431–442.
- Lanckriet, G. R. G., N. Cristianini, P. Bartlett, L. E. Ghaoui, and M. I. Jordan. 2004. "Learning the Kernel Matrix with Semidefinite Programming". *Journal of Machine Learning Research*. 5: 27–72.
- Lee, J. A. and M. Verleysen. 2012. "Graph-based dimensionality reduction". In: *Image Processing and Analysis with Graphs: Theory and Practice*. 351–382.
- Leskovec, J., L. A. Adamic, and B. A. Huberman. 2007. "The Dynamics of Viral Marketing". *ACM Transactions on the Web*. 1(1): 5:1–5:39.
- Levi, G. 1973. "A note on the derivation of maximal common subgraphs of two directed or undirected graphs". *Calcolo*. 9(4): 341.
- Lloyd, S. 1982. "Least Squares Quantization in PCM". *IEEE Transactions on Information Theory*. 28(2): 129–137.
- Lonsdale, J., J. Thomas, M. Salvatore, R. Phillips, E. Lo, S. Shad, R. Hasz, G. Walters, F. Garcia, N. Young, *et al.* 2013. "The Genotype-Tissue Expression (GTEx) project". *Nature Genetics*. 45(6): 580–585.
- Mahé, P., N. Ueda, T. Akutsu, J.-L. Perret, and J.-P. Vert. 2004. "Extensions of Marginalized Graph Kernels". In: *Proceedings of the 21st Conference on Machine learning*. New York, NY, USA: ACM. 70–78.
- Mahé, P. and J.-P. Vert. 2009. "Graph kernels based on tree patterns for molecules". *Machine learning*. 75(1): 3–35.
- Menchetti, S., F. Costa, and P. Frasconi. 2005. "Weighted Decomposition Kernels". In: *Proceedings of the 22nd International Conference on Machine Learning*. New York, NY, USA: ACM. 585–592.
- Mikolov, T., K. Chen, G. Corrado, and J. Dean. 2013. "Efficient Estimation of Word Representations in Vector Space". *arXiv e-prints*. arXiv: [1301.3781](https://arxiv.org/abs/1301.3781) [cs.CL].

- Morris, C., N. M. Kriege, F. Bause, K. Kersting, P. Mutzel, and M. Neumann. 2020. "TU-Dataset: A collection of benchmark datasets for learning with graphs". In: *ICML 2020 Workshop on Graph Representation Learning and Beyond (GRL+ 2020)*. arXiv: [2007.08663](https://arxiv.org/abs/2007.08663). URL: [www.graphlearning.io](http://www.graphlearning.io).
- Morris, C., N. M. Kriege, K. Kersting, and P. Mutzel. 2016. "Faster Kernels for Graphs with Continuous Attributes via Hashing". In: *Proceedings of the 16th IEEE International Conference on Data Mining*. 1095–1100.
- Müllner, D. 2011. "Modern hierarchical, agglomerative clustering algorithms". *arXiv e-prints*. arXiv: [1109.2378](https://arxiv.org/abs/1109.2378) [stat.ML].
- Neumann, M., R. Garnett, C. Bauckhage, and K. Kersting. 2016. "Propagation kernels: efficient graph kernels from propagated information". *Machine Learning*. 102(2): 209–245.
- Nikolentzos, G., P. Meladianos, S. Limnios, and M. Vazirgiannis. 2018a. "A Degeneracy Framework for Graph Similarity". In: *Proceedings of the Twenty-Seventh International Joint Conference on Artificial Intelligence, IJCAI-18*. International Joint Conferences on Artificial Intelligence Organization. 2595–2601.
- Nikolentzos, G., P. Meladianos, A. J.-P. Tixier, K. Skianis, and M. Vazirgiannis. 2018b. "Kernel Graph Convolutional Neural Networks". In: *Artificial Neural Networks and Machine Learning – ICANN 2018*. Ed. by V. Kůrková, Y. Manolopoulos, B. Hammer, L. Iliadis, and I. Maglogiannis. Cham, Switzerland: Springer. 22–32.
- Nikolentzos, G., G. Siglidis, and M. Vazirgiannis. 2019. "Graph Kernels: A Survey". arXiv: [1904.12218](https://arxiv.org/abs/1904.12218) [stat.ML].
- Nikolentzos, G. and M. Vazirgiannis. 2018. "Message Passing Graph Kernels". *arXiv e-prints*. arXiv: [1808.02510](https://arxiv.org/abs/1808.02510) [stat.ML].
- Nyström, E. J. 1930. "Über die praktische Auflösung von Integralgleichungen mit Anwendungen auf Randwertaufgaben". *Acta Mathematica*. 54: 185–204.
- Ó Searcóid, M. 2007. *Metric Spaces*. London, England: Springer.
- Orsini, F., P. Frasconi, and L. De Raedt. 2015. "Graph Invariant Kernels". In: *Proceedings of the 24th International Conference on Artificial Intelligence*. Palo Alto, CA, USA: AAAI Press. 3756–3762.
- Paulevé, L., H. Jégou, and L. Amsaleg. 2010. "Locality sensitive hashing: A comparison of hash function types and querying mechanisms". *Pattern Recognition Letters*. 31(11): 1348–1358.
- Pearson, K. 1901. "LIII. On Lines and Planes of Closest Fit to Systems of Points in Space". *The London, Edinburgh, and Dublin Philosophical Magazine and Journal of Science*. 2(11): 559–572.
- Pržulj, N., D. G. Corneil, and I. Jurisica. 2004. "Modeling interactome: scale-free or geometric?" *Bioinformatics*. 20(18): 3508–3515.

- Pržulj, N., D. G. Corneil, and I. Jurisica. 2006. "Efficient estimation of graphlet frequency distributions in protein–protein interaction networks". *Bioinformatics*. 22(8): 974–980.
- Ramon, J. and T. Gärtner. 2003. "Expressivity versus efficiency of graph kernels". In: *Proceedings of the 1st International Workshop on Mining Graphs, Trees and Sequences*. 65–74.
- Read, R. C. and D. G. Corneil. 1977. "The Graph Isomorphism Disease". *Journal of Graph Theory*. 1(4): 339–363.
- Rieck, B., C. Bock, and K. Borgwardt. 2019. "A Persistent Weisfeiler–Lehman Procedure for Graph Classification". In: *Proceedings of the 36th International Conference on Machine Learning*. Ed. by K. Chaudhuri and R. Salakhutdinov. Vol. 97. *Proceedings of Machine Learning Research*. PMLR. 5448–5458.
- Riesen, K. 2015. *Structural Pattern Recognition with Graph Edit Distance*. Cham, Switzerland: Springer.
- Rotmensch, M., Y. Halpern, A. Tlimat, S. Horng, and D. Sontag. 2017. "Learning a Health Knowledge Graph from Electronic Medical Records". *Scientific Reports*. 7(1): 5994.
- Schölkopf, B. and A. J. Smola. 2002. *Learning with Kernels: Support Vector Machines, Regularization, Optimization, and Beyond*. Cambridge, MA, USA: MIT Press.
- Schütt, K. T., F. Arbabzadah, S. Chmiela, K. R. Müller, and A. Tkatchenko. 2017. "Quantum-chemical insights from deep tensor neural networks". *Nature Communications*. 8.
- Scott, J. 2011. "Social network analysis: developments, advances, and prospects". *Social Network Analysis and Mining*. 1(1): 21–26.
- Shawe-Taylor, J. and N. Cristianini. 2004. *Kernel Methods for Pattern Analysis*. Cambridge, United Kingdom: Cambridge University Press.
- Shervashidze, N., P. Schweitzer, E. J. van Leeuwen, K. Mehlhorn, and K. M. Borgwardt. 2011. "Weisfeiler–Lehman Graph Kernels". *Journal of Machine Learning Research*. (12): 2539–2561.
- Shervashidze, N. and K. Borgwardt. 2009. "Fast subtree kernels on graphs". In: *Advances in Neural Information Processing Systems* 22. 1660–1668.
- Shervashidze, N., S. Vishwanathan, T. Petri, K. Mehlhorn, and K. Borgwardt. 2009. "Efficient graphlet kernels for large graph comparison". In: *Proceedings of the 12th International Conference on Artificial Intelligence and Statistics*. 488–495.
- Siglidis, G., G. Nikolettos, S. Limnios, C. Giatsidis, K. Skianis, and M. Vazirgiannis. 2020. "GraKeL: A Graph Kernel Library in Python". *Journal of Machine Learning Research*. 21(54): 1–5.
- Silva, V. de and G. Carlsson. 2004. "Topological estimation using witness complexes". In: *Symposium on Point-Based Graphics*. Ed. by M. Gross, H. Pfister, M. Alexa, and S. Rusinkiewicz. The Eurographics Association.

- Smola, A. J. and I. Kondor. 2003. “Kernels and Regularization on Graphs”. In: *Learning Theory and Kernel Machines*. Ed. by B. Schölkopf and M. K. Warmuth. Heidelberg, Germany: Springer. 144–158.
- Sonnenburg, S., G. Rätsch, C. Schäfer, and B. Schölkopf. 2006. “Large Scale Multiple Kernel Learning”. *Journal of Machine Learning Research*. 7: 1531–1565.
- Sugiyama, M. and K. Borgwardt. 2015. “Halting in Random Walk Kernels”. In: *Advances in Neural Information Processing Systems 28*. Ed. by C. Cortes, N. D. Lawrence, D. D. Lee, M. Sugiyama, and R. Garnett. 1639–1647.
- Sugiyama, M., M. E. Ghisu, F. Llinares-López, and K. Borgwardt. 2017. “graphkernels: R and Python packages for graph comparison”. *Bioinformatics*. 34(3): 530–532.
- Szklarczyk, D., A. L. Gable, D. Lyon, A. Junge, S. Wyder, J. Huerta-Cepas, M. Simonovic, N. T. Doncheva, J. H. Morris, P. Bork, *et al.* 2018. “STRING v11: protein–protein association networks with increased coverage, supporting functional discovery in genome-wide experimental datasets”. *Nucleic Acids Research*. 47(D1): D607–D613.
- Tan, P.-N., M. Steinbach, A. Karpatne, and V. Kumar. 2019. *Introduction to Data Mining*. 2nd ed. London, United Kingdom: Pearson.
- Todeschini, R. and V. Consonni. 2008. *Handbook of Molecular Descriptors*. Vol. 11. Weinheim, Germany: Wiley-VCH.
- Togninalli, M., E. Ghisu, F. Llinares-López, B. Rieck, and K. Borgwardt. 2019. “Wasserstein Weisfeiler–Lehman Graph Kernels”. *arXiv e-prints*. arXiv: [1906.01277 \[cs.LG\]](#).
- Trinajstić, N. 2018. *Chemical Graph Theory*. 2nd ed. Boca Raton, FL, USA: CRC Press.
- Tschiatschek, S., A. Singla, M. Gomez Rodriguez, A. Merchant, and A. Krause. 2018. “Fake News Detection in Social Networks via Crowd Signals”. In: *Companion Proceedings of the The Web Conference 2018*. 517–524.
- Vamathevan, J., D. Clark, P. Czodrowski, I. Dunham, E. Ferran, G. Lee, B. Li, A. Madabhushi, P. Shah, M. Spitzer, *et al.* 2019. “Applications of machine learning in drug discovery and development”. *Nature Reviews Drug Discovery*. 18: 463–477.
- Vega-Pons, S. and P. Avesani. 2013. “Brain Decoding via Graph Kernels”. In: *Proceedings of the 2013 International Workshop on Pattern Recognition in Neuroimaging*. PRNI ’13. IEEE Computer Society. 136–139.
- Vert, J.-P. 2008. “The optimal assignment kernel is not positive definite”. *arXiv e-prints*. arXiv: [0801.4061 \[cs.LG\]](#).
- Vert, J.-P., K. Tsuda, and B. Schölkopf. 2004. “A primer on kernel methods”. In: *Kernel Methods in Computational Biology*. Ed. by B. Schölkopf, K. Tsuda, and J.-P. Vert. Cambridge, MA, USA: MIT Press. 35–70.
- Villani, C. 2008. *Optimal Transport: Old and New*. Heidelberg, Germany: Springer.

- Vishwanathan, S. V. N., K. M. Borgwardt, and N. N. Schraudolph. 2006. "Fast Computation of Graph Kernels". In: *Advances in Neural Information Processing Systems* 19. 1449–1456.
- Wang, J., X. Zuo, and Y. He. 2010. "Graph-based network analysis of resting-state functional MRI". *Frontiers in Systems Neuroscience*. 4: 16:1–16:14.
- Warshall, S. 1962. "A Theorem on Boolean Matrices". *Journal of the ACM*. 9(1): 11–12.
- Wasserman, S. and K. Faust. 1994. *Social Network Analysis: Methods and Applications*. Cambridge, UK: Cambridge University Press.
- Weisfeiler, B. and A. A. Lehman. 1968. "A reduction of a graph to a canonical form and an algebra arising during this reduction". *Nauchno-Tekhnicheskaya Informatsia*. 2(9): 12–16.
- Wiener, H. 1947. "Structural Determination of Paraffin Boiling Points". *Journal of the American Chemical Society*. 69(1): 17–20. ISSN: 0002-7863.
- Williams, C. K. I. and M. Seeger. 2001. "Using the Nyström Method to Speed Up Kernel Machines". In: *Advances in Neural Information Processing Systems* 13. Ed. by T. K. Leen, T. G. Dietterich, and V. Tresp. MIT Press. 682–688.
- Wilson, R. C. and P. Zhu. 2008. "A study of graph spectra for comparing graphs and trees". *Pattern Recognition*. 41(9): 2833–2841.
- Wu, Z., B. Ramsundar, E. N. Feinberg, J. Gomes, C. Geniesse, A. S. Pappu, K. Leswing, and V. Pande. 2018. "MoleculeNet: a benchmark for molecular machine learning". *Chemical Science*. 9(2): 513–530.
- Wu, Z., S. Pan, F. Chen, G. Long, C. Zhang, and P. S. Yu. 2019. "A Comprehensive Survey on Graph Neural Networks". *arXiv e-prints*. arXiv: [1901.00596](https://arxiv.org/abs/1901.00596) [cs.LG].
- Xu, K., W. Hu, J. Leskovec, and S. Jegelka. 2019. "How Powerful are Graph Neural Networks?" In: *International Conference on Learning Representations (ICLR)*.
- Yanardag, P. and S. Vishwanathan. 2015. "Deep Graph Kernels". In: *Proceedings of the 21th ACM SIGKDD International Conference on Knowledge Discovery and Data Mining*. New York, NY, USA: ACM. 1365–1374.
- Yang, Y. 1999. "An Evaluation of Statistical Approaches to Text Categorization". *Information Retrieval*. 1(1): 69–90.
- Ying, R., J. You, C. Morris, X. Ren, W. L. Hamilton, and J. Leskovec. 2018. "Hierarchical Graph Representation Learning with Differentiable Pooling". In: *Advances in Neural Information Processing Systems* 32. 4805–4815.
- Zhang, B. and S. Horvath. 2005. "A General Framework for Weighted Gene Co-expression Network Analysis". *Statistical Applications in Genetics and Molecular Biology*. 4(1): 17:1–17:43.
- Zhang, Z., M. Wang, Y. Xiang, Y. Huang, and A. Nehorai. 2018. "RetGK: Graph kernels based on return probabilities of random walks". In: *Advances in Neural Information Processing Systems* 32. 3964–3974.

- Zhao, Q. and Y. Wang. 2019. “Learning metrics for persistence-based summaries and applications for graph classification”. In: *Advances in Neural Information Processing Systems 32 (NeurIPS)*. Ed. by H. Wallach, H. Larochelle, A. Beygelzimer, F. d’Alché-Buc, E. Fox, and R. Garnett. Curran Associates, Inc. 9855–9866.
- Zhou, J., G. Cui, Z. Zhang, C. Yang, Z. Liu, L. Wang, C. Li, and M. Sun. 2018. “Graph Neural Networks: A Review of Methods and Applications”. *arXiv e-prints*. arXiv: [1812.08434](#) [cs.LG].